

**MODIS Team Member - Semi-annual Report
Marine Optical Characterizations
December 1999**

**Dennis K Clark
NOAA/NESDIS**

SUMMARY

The Marine Optical Characterization Experiment (MOCE) Team started its second year of providing the SeaWiFS Project continuous observations for their initialization and calibration tasks. In support of the United States' Earth Observing System (EOS), the Moderate Resolution Imaging Spectrometer (MODIS) Algorithm Development/Process Experiment (MOCE-5) was conducted by the National Aeronautic and Space Administration (NASA) and the National Oceanic and Atmospheric Administration (NOAA). The launch of the first of NASA's EOS satellites, Terra, was delayed until December 18, 1999. This launch delay required that the experimental focus during MOCE-5 shift from validation/calibration of MODIS to utilizing the observations acquired by the Sea-viewing Wide Field-of-View Sensor (SeaWiFS) as a surrogate data set to test and enhance MODIS product algorithms. The data acquired during this experiment supported bio-optical process studies and validated SeaWiFS sensor calibration and products. Additionally, the team conducted two MOBY recovery and replacement cruises (MOBY-L48, MOBY-L51), and three MOBY calibration excursions at the Lanai mooring site (MOBY-L49, L50, L52). Team activities during the reporting period are shown in Figure 1.

FIELD OPERATIONS

MOBY-L48

The MOBY-L48/M214SO recovery and replacement cruise took place July 29 - August 1, 1999 aboard the Research Vessel (R/V) Ka'imikai-O-Kanaloa. The following personnel participated:

NOAA - Dennis Clark, Edwin Fisher, Ed King, Yong Sung Kim, Mike Ondrusek

MLML - Mark Yarbrough, Mike Feinholz, Darryl Peters, John Heine

HRA - Steve Juarez, Rob Wheeler

The tenth Marine Optical Buoy, MOBY210, was successfully deployed at the Lanai mooring site on July 29, 1999. MOBY209 and MOBY210 made several sets of side-by-side cross-over measurements on July 30 before MOBY209 was recovered. Diver calibrations of the new MOBY were performed with the assistance of Hawaiian Rafting Adventures. Satlantic Profiler Multichannel Radiometer (SPMR) profiles and Wide Angle Radiance System (WARS) scans

were performed on July 31. Routine maintenance on the weather station mooring buoy were carried out. MOBY209 was disassembled, cleaned, and calibrated after the cruise.

MOCE-5

The equipment was packed into large Matson shipping containers in Snug Harbor, Hawaii and sent to the Nimitz Marine Facility at Scripps Institution of Oceanography in San Diego, CA in late August. Calibrated radiometers were shipped FedEx freight in September. NOAA and MLML personnel began arriving in San Diego on September 14 and loading the ship on September 24. MOCE-5 occurred October 1-21, 1999 along the coast of Baja California and in the Sea of Cortez aboard the Scripps Institution of Oceanography (SIO) Research Vessel (R/V) Melville (Figure 2). The science party personnel and affiliations for MOCE-5 are listed in Figure 3.

The primary cruise objective was to provide radiometric characterizations and spatial variability of water-leaving radiances and atmospheric transmittances concurrent with SeaWiFS observations. The secondary objective was to acquire pertinent bio-optical and thermal measurements for SeaWiFS bio-optical and NOAA's Geostationary Operational Environmental Satellite (GOES-10) sea surface temperature (SST) derived products. A list of the observations focused on the primary objective are listed in Figure 4.

During this experiment, extensive measurements were conducted at locations along the coast of Baja California and within the Sea of Cortez. Operating areas and associated ship tracks are depicted in Figure 5. A complete suite of measurements, designed to characterize the bio-optical state, up to depth of 150 meters, were performed at stations within these sites during satellite overpasses. During the ship transits, an abbreviated set of observations documenting the surface waters and atmospheric state were conducted in order to address spatial variability uncertainties. The observations acquired provided a variety of marine optical, atmospheric, and biological signals for algorithm development, calibration and validation purposes. Throughout the entire cruise, rotating shadow band radiometer measurements were obtained with the Portable Radiation Package (PRP) and spectral radiance between 3 -18 um were measured with the Marine Atmosphere Emitted Radiance Interferometer (MAERI) on a continuous basis. MAERI measurements were used to compute air and ocean skin temperatures, and along with PRP measurements and hard hat thermistor observations, collected while on station, formed the backbone for SST retrieval validation.

The first week of the cruise proceeded exceptionally well. All systems were fully functional with the exception of the High Performance Liquid Chromatography (HPLC) system, which encountered an unresolvable white noise problem. The R/V Melville transited the west coast of Baja California, across the Gulf of California to Mazatlan and then south to Boca de Chila. Daily stations involved the deployment of up to eleven instrument packages coincident with SeaWiFS/Sea Star, NOAA-14, and NOAA-15 satellite overpasses. A nominal daily operational schedule for satellite overpasses is detailed in Figure 6 and some of the operations are shown in Figures 7 and 8. Continuous along-track surface measurements (i.e. inherent optical properties, reflected infrared energy, phytoplankton fluorescence, nitrate, and incident spectral irradiance)

were acquired during transits. Phytoplankton pigment concentrations ranged between 0.3 to 4 ug/l on station and high concentrations of colored dissolved organic matter in the Teacapan/San Blas area were observed.

During the second week of the cruise, the R/V Melville proceeded north into the Gulf of California along the west coast of Mexico until tropical storm Irwin formed, causing the R/V Melville to reposition off of Cabo San Lucas on October 9th. On the 10th, the ship returned to the Gulf and transited along the east coast of Baja into high concentration waters near the mid-rift islands. Weather conditions were perfect for marine and atmospheric optical measurements. All measurement systems continued to function properly and an excellent data set was acquired along approximately 1,800 nm of track line.

During the third, and final, week of the cruise, the R/V Melville proceeded south from the mid-rift islands to the southern tip of Baja California. A full along-track data set was collected during the mid-Gulf transit October 15th and 16th. The last station before the R/V Melville turned north and transited back to American waters occurred on October 17th at Bahia de San Lucas. All instrumentation systems functioned properly and the final cruise station took place on the 20th at Bahia de San Quintin, just south of US waters.

Preliminarily processed SeaWiFS (ocean color) and Advanced Very-High Resolution Radiometer (AVHRR - sea surface temperature) imagery were transmitted to the R/V Melville via INTERNET on a sporadic basis. Over 50 images were received in support of this experiment and when these images were available, they proved to be invaluable in determining station locations. This cruise was a very successful one and has produced the most comprehensive bio-optical, atmospheric optical, physical and chemical suite of measurements to date.

During MOCE-5, 24 SeaBird CTD casts were conducted, 7 of which were 1000 m casts (see Appendix 1). CTD casts and a long-track water pumping yielded 245 TSM/POC/PON samples which were filtered during the cruise (Figures 9 and 10) and are being processed at MLML. Additionally, 122 oxygen samples were collected and processed during the cruise to validate the CTD oxygen sensor data. TSM/POC/PON samples replicates will allow Craig Hunter to duplicate the Baker method used during the CZCS cruises to measure TSM/OM/IM. Ultimately, this will help determine the difference between the TSM data collected during the CZCS era and current data. A C-Star 25 cm path length, red LED transmissometer replaced the Martek 1 meter path length, blue LED transmissometer. The ship's flow-through water pump system and a Hewlett Packard 8452 Diode Array Spectrophotometer were used to examine the along-track changes in nitrate, a key nutrient in primary productivity. The MOCE-5 CTD and TSM/POC/PON data cruise report will be finished in January 2000.

The spectrophotometer-nitrate system was borrowed from the MLML Chemical Oceanography department for use during this cruise. The spectrophotometer collected data at two minute intervals for approximately 12 hours each day. The ultraviolet absorption spectra of the samples were used in a multiple regression model to determine surface nitrate concentrations. Additionally, discrete water samples were collected from the CTD casts. These will be analyzed colorimetrically and with the spectrophotometer to both verify the spectrophotometer method and

determine a vertical profile for nitrate.

During this cruise, 403 pigment samples were collected and analyzed using the standard fluorometric method. The fluorometric data are tabulated in Appendix 2. The HPLC system was installed on the ship and 304 samples were collected for shipboard processing. During the calibration of the system, several things were noticed related to problems associated with shipboard vibrations and electrical power. Baseline noise for the two absorption detectors had increased as compared to that measured at CHORS just before the cruise. The UV 2000 had increased by a factor of two (Figure 11), as where the more sensitive UV 3000 Diode Array detector showed a 100 fold increase in noise (Figure 12). We attributed this “white” noise to ship vibration and tried to dampen it by placing the detectors on foam pads. This did little to correct the problem. It was also observed that the UV 2000 was sensitive to some type of electrical or electromagnetic interference, which caused negative peaks to occur randomly throughout an HPLC run (Figure 13). During the analysis of 30 pigment standards, it was found that the interference occurred at 33% of the time. Based on these problems, which were specific to the operating the system on this ship, it was decided to keep the HPLC samples frozen for later analysis at CHORS.

Water samples were collected for cyanobacterial analysis and phycobiliprotein extraction methods. Samples were taken from surface and near chlorophyll maximum, and filtered through 0.22 um Nuclepore filters. These samples will be used in cyanobacterial pigment separation and quantification method development on the HPCE (Prince 310 High Performance Capillary Electrophoresis) system. In addition, samples were collected and analyzed shipboard using Wyman’s method, to investigate relative spacial differences in phycoerythrin (PE) fluorescence. The results were inconclusive, possibly showing variability in this method when analyzing whole-cell PE fluorescence.

During MOCE-5, 24 MOS/SIS optical profiles were conducted. Appendix 3 lists details of MOS data acquisition for the reporting period.

Hand Held Contrast Reduction Meter (HRCRM) measurements, to derive the spectral transmittances, specifically bracketed each overpass. Water vapor column, ozone column and aerosol optical depth during each overpass were measured using MICROTOPS. HRCRM and MICROTOPS calibrations were performed throughout the cruise using a Langley calibration procedure.

At the conclusion of the trip, all of the equipment was shipped back to Hawaii with everyone departing San Diego on October 28. All of the equipment had returned to Snug Harbor by late November.

MOBY-L51

The MOBY-L51/M215SO recovery and replacement cruise took place November 15 - 18, 1999. The following personnel participated:

NOAA - Dennis Clark, Ed Fisher, Yong Sung Kim, Mike Ondrusek, Ed King, Eric Stengel

MLML/QSS/Hawaii - Mike Feinholz, Darryl Peters, Mark Yarbrough

Hawaiian Rafting Adventures - Steve Juarez

The eleventh Marine Optical Buoy, MOBY211, was successfully deployed at the Lanai mooring site on November 15, 1999 during the MOBY-L51/M215SO oceanographic cruise aboard the R/V Ka'imikai-O-Kanaloa. Intercomparison measurements were obtained by SIS, SPMR, and the two MOBYs before MOBY210 was recovered on November 18. Diver calibrations of MOBY211 were performed on November 17.

INSTRUMENT CALIBRATIONS

MOBY

During this reporting period, MLML personnel and professional divers conducted three calibration excursions via Hawaiian Rafting Adventures (HRA) chartered dive boat to perform the diver calibrations. The first two trips (MOBY-L49 and MOBY-L50) in September and October were undertaken by HRA personnel while MOCE team members were engaged with the MOCE-5 cruise. A routine systems checkup was performed.

The MOBY-L52 service cruise was a three day operation conducted in December 1999. The top MOBY arm was found broken off but still attached to MOBY by the WARS cable. The arm was retrieved, but it doesn't look like it can be recycled. Dirty diver calibrations were performed on December 16 and clean ones on December 17. Meteorological data were downloaded and a new anchor was attached to MOBY.

RADIOMETRIC STANDARDS & RADIOMETERS

Team personnel stationed at the NOAA operations facility at Snug Harbor, Hawaii continued to maintain NIST-traceability of our radiometric standards and perform calibrations of our radiometers. We purchased a backup stability lamp from Gamma Scientific for use during long periods at sea, in particular, for the MOCE-5 cruise. Our two radiance sphere standards, the OL420 and OL425, were serviced by Optronic Laboratories, and the Single Channel Multi-Purpose Radiometers (SCAMPS) were returned to the National Institute of Standards and Technology (NIST) for service and recalibration. Detailed listing of calibrations and maintenance for each standard and instrument are provided in Appendix 4.

CIMEL SERVICE

The Lanai CIMEL site was serviced at approximately 2-weeks intervals, as time permitted during regular HRA charters to the area. CIMEL received a more thorough service during the scheduled

diver calibration trips. At the request of GSFC, CIMEL #93 was removed from Lanai on June 2, 1999 and replaced with the calibrated unit #106. CIMEL #93 was returned to GSFC on June 16 for recalibration. The decision has been made to deploy an additional CIMEL system on windward Oahu at Coconut Island. We will install the new site when we receive another instrument from NASA.

DATA PROCESSING

HPLC and fluorometric pigment data from MOBY-L38 and L43 are finally processed. The delay was caused by peak integration problems associated with the new HPLC software. In addition to these glitches, a poor separation of carotenoids was observed during the analyses. The carotenoid peaks had preceding shoulders making separation and quantification difficult. The MOBY-L38 and L43 pigment samples were analyzed anyway at these higher methodological and instrumental uncertainties. Fortunately, those peaks associated with chlorophylls *a*, *b* and *c* did not suffer these problems and concentrations were accurately calculated (3-5%).

Data processing of MOBY-L45 (May 1-6, 1999) pigment samples was delayed, in hopes of correcting the carotenoid separation problem. We continued to investigate possible causes for this poor separation. This included purchasing new solvents, chemicals and columns. We also sent example chromatograms to ThermoQuest Service Support Center for their review and possible explanation. During the analysis of standards prior to the MOCE-5 cruise, it was noticed that the mixing tube for sample preparation had numerous bubbles. According to ThermoQuest Service Support Center experts, this was not typical and there must be an air leak. Various components of the system were tested with the final diagnosis being that the 6-way solvent valve was probably not operating properly. A ThermoQuest service engineer came to CHORS to replace this valve, as well as perform general maintenance. Replacement of this solvent valve did not remove the air bubbles. Then other components related to sample pickup, water addition, mixing and injection were checked. The final culprit was a clogged 0.2 um stainless steel frit in the HPLC water bottle. Replacing this frit removed the bubbles in the mixing tube. The service engineer then checked the 6-way injection valve and found that it was corroded. After replacing these last two components, the separation problem was finally corrected and the HPLC system was back to normal operation. The HPLC system was calibrated using 15 pigment standards purchased from Carbon 14 Centralen, Denmark. The calibration curves for these standards are shown in Appendix 5 and represent the lowest uncertainties ever achieved with this system. MOBY-L45 pigment samples were then analyzed prior to departure on the MOCE-5 cruise.

In November, the MOCE-5 pigment samples were processed through the HPLC system. Fluorometric chlorophylls were determined for these samples taking an aliquot of the pigment extract and measuring it in a Turner-10 fluorometer. The results from these analyses will be completed in January 2000. In the middle of the MOCE-5 HPLC analyses, the scanning fluorometer (UV3000) quit working. This instrument is used to quantify phaeopigments, which occur at very low concentrations in natural samples. The instrument will be shipped back to the

manufacturer for repair, maintenance and calibration.

The MOCE-5 data workshop has been scheduled for February 23-25, 2000 and will be held in Honolulu, Hawaii. MOCE-5 participants and MODIS team members have been invited to participate in this workshop. During the workshop, participants will present the results of their data sets collected during MOCE-5.

INSTRUMENT DEVELOPMENT

The new MOBY tether systems have been delivered and successfully tested. The units incorporate a fiberglass rod stiffener and PMI flexible strain relief to keep the tether supported and tending away from the MOBY surface float. We have not observed the tether wrapped around the MOBY since the addition of the stiffener. The new units also have a stronger strain relief design than the older units to prevent cracking of the neoprene boot at the base of the strain relief. Two spare tethers have been delivered. We believe each tether will last for one year if we continue to swap tethers each deployment to allow cleaning of the entire line and servicing of the MOBY termination segment.

PUBLICATIONS

The paper titled “Chlorophyll *a* versus accessory pigment concentrations within the euphotic zone: An ubiquitous relationship” was submitted in November. The manuscript is presented in Appendix 6.

MOCE Team Activities

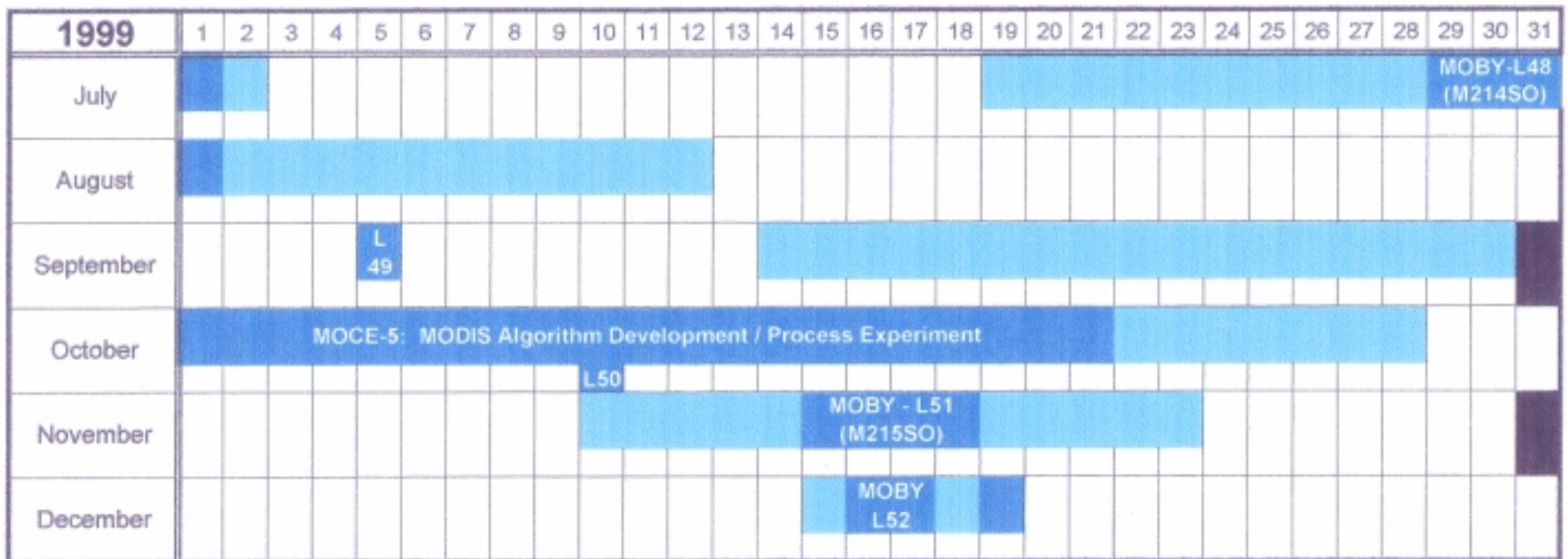


FIGURE 1.

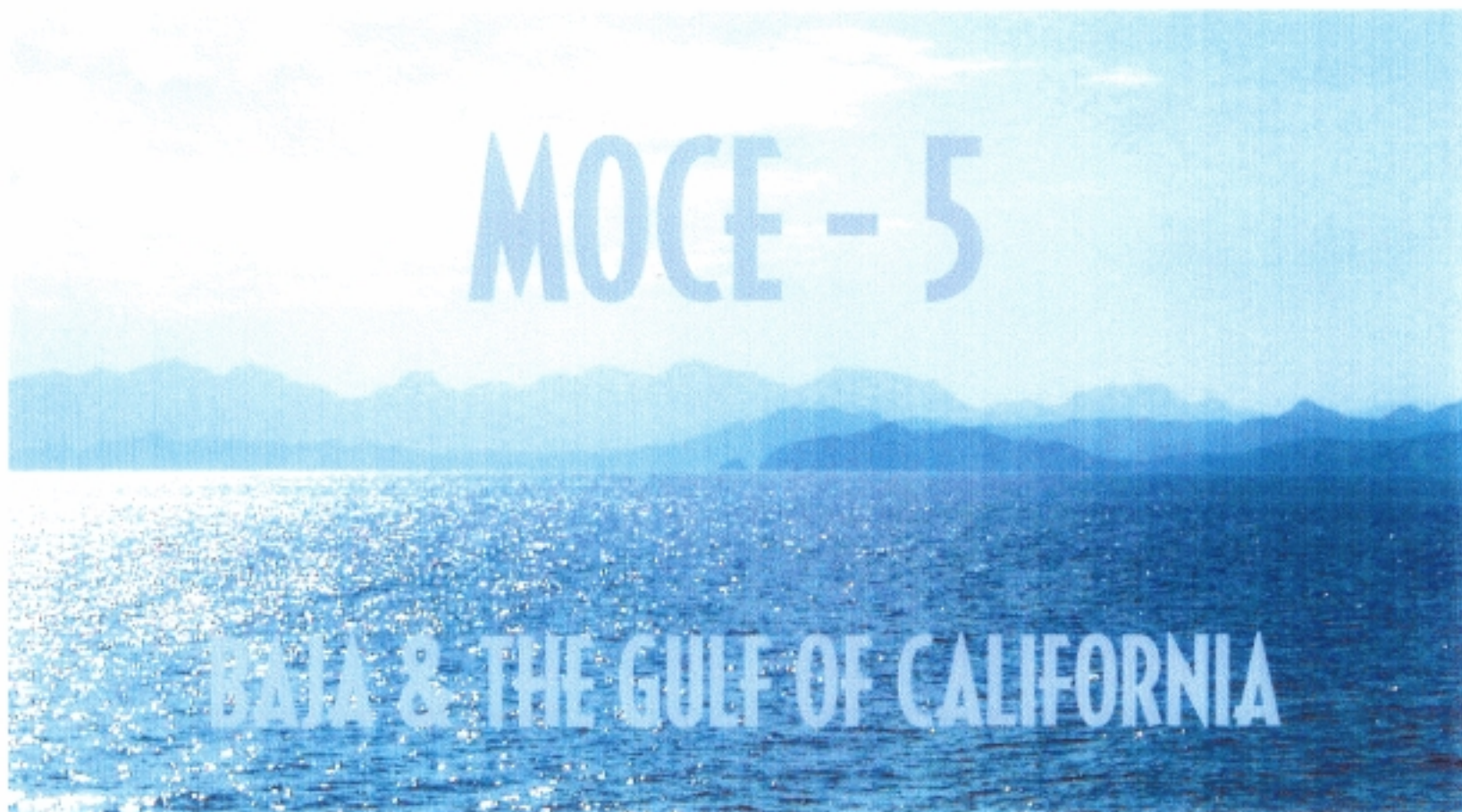


FIGURE 2.

PERSONNEL	TITLE
NOAA/NESDIS	Marine Optics Team
Dennis Clark	Senior Scientist
Marilyn Yuen	Research Associate
Edward King	Research Technician
Eric Stengel	Research Technician
Ed Fisher	Research Technician
Larisa Koval	Research Associate
Mike Ondrusek	Research Associate
San Jose State University	Moss Landing Marine Laboratories
Mark Yarbrough	Senior Research Associate
Mike Feinholz	Research Associate
Stephanie Flora	Research Technician-Student
Rachel Kay	Research Technician-Student
Darryl Peters	Research Technician-Student
San Diego State University	Center for Hydro-Optics & Remote Sensing
Chuck Trees	Research Professor
Chris Kinkade	Post-Doc
University of Miami	Physics Department
Ken Voss	Professor
Robert Evans	Research Associate Professor
Edward Kearns	Research Associate
Brian Ward	Post Doc. (Nansen Center, Norway)
Albert Chapin	Research Technician
Oregon State University	College of Oceanic and Atmospheric Science
Ricardo Letelier	Research Associate Professor
Andrew Barnard	Faculty Research Associate
Sarah Searson	Research Technician
Claudia Mengelt	Graduate Research Assistant
University of South Florida	Department of Marine Sciences
Zhong Ping Lee	Research Associate
CICESE - Mexico	Ecology Department
Saul Alvarez-Barrego	Professor
Eduardo Millan-Nunez	Research Associate
Eduardo Santamaria del Angel	Research Associate
Alma Giles-Guzman	Research Associate

FIGURE 3.

Optical Observations - Ocean	Responsible
Incident Spectral Irradiance	NOAA
Downwelled Spectral Irradiance	NOAA
Upwelled Spectral Radiance	NOAA
Upwelled Spectral Radiance Distributions	Miami
Whitecap Spectral Reflectance	Miami
Spectral Beam Attenuation	NOAA
Sea Surface Thermal Infrared	Miami
Attenuation Coefficients Upwelled Radiance	NOAA
Optical Observations - Atmosphere	
Sky Radiance Distributions	Miami
Sky Polarization Distributions	Miami
Solar Transmittance	NOAA
Solar Aureole	Miami
Meteorological Observations	
Surface Atmospheric Pressure	NOAA
Surface Humidity	NOAA & Miami
Surface Temperature	NOAA & Miami
Wind Speed & Direction	NOAA
Sky Video	NOAA
Physical Observations - Ocean	
Sea Surface Temperature	Miami
Salinity Profiles & Trackline	NOAA
Temperature Profiles & Trackline	NOAA

Measurements associated with the secondary product validation objective are:

Optical - TSRB Natural Fluorescence, FRR Fluorescence, Spectral Scattering, Spectral Beam Transmission, Spectral Absorption Surface Spectral Reflectance, Secchi Disk Depth and Munsell Color.

Biological - Particle Size Distribution, Particle Absorption, Colored Dissolved Organic Matter Absorption, Dissolved Oxygen, HPLC Phytoplankton Pigment Concentrations, Fluorometric Chlorophyll *a* Concentration, Total Suspended Matter, Nitrate and ¹⁴C PvsI

FIGURE 4.

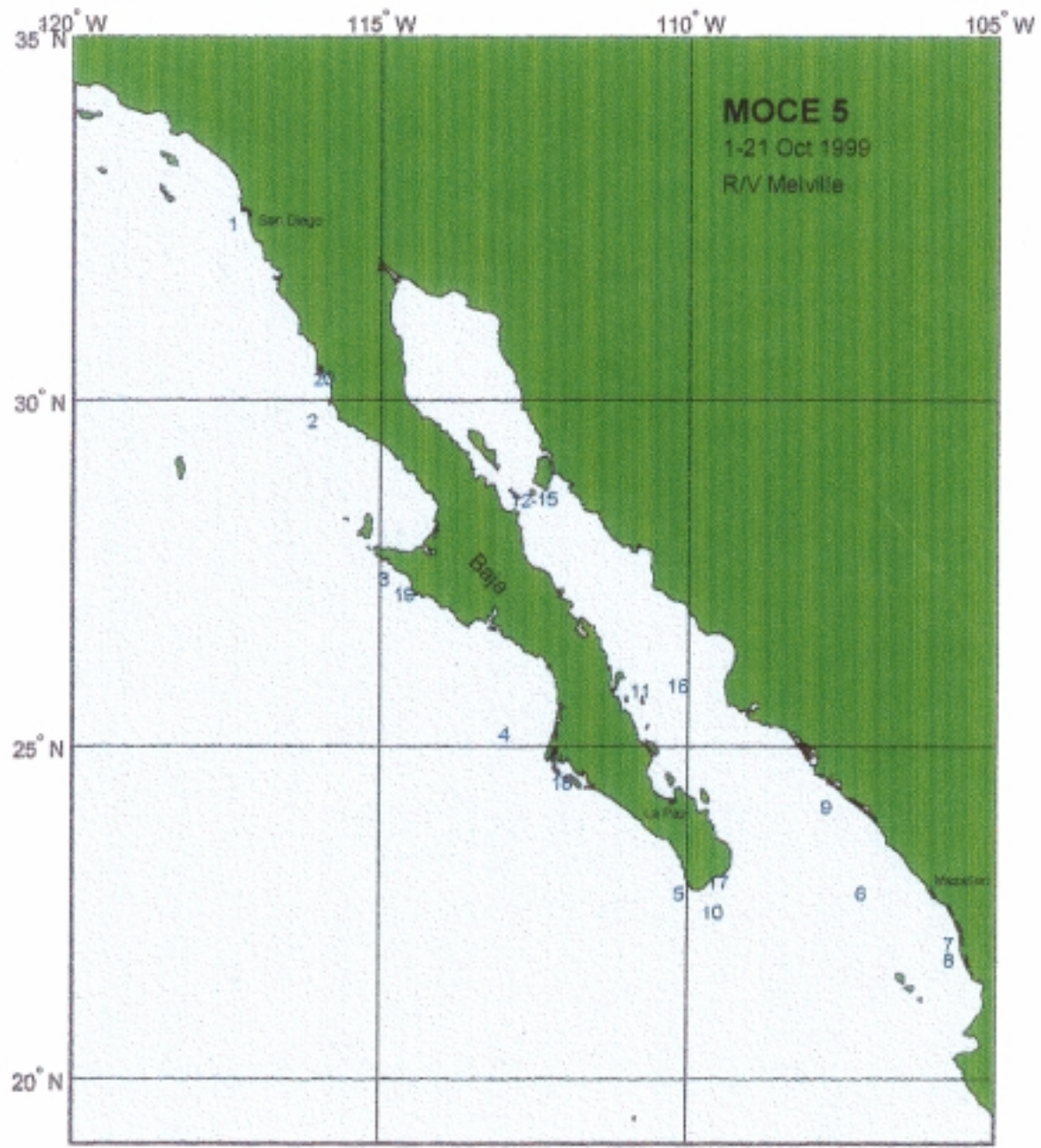


FIGURE 5.

MOCE - 5
Station 1: Islas Coronados

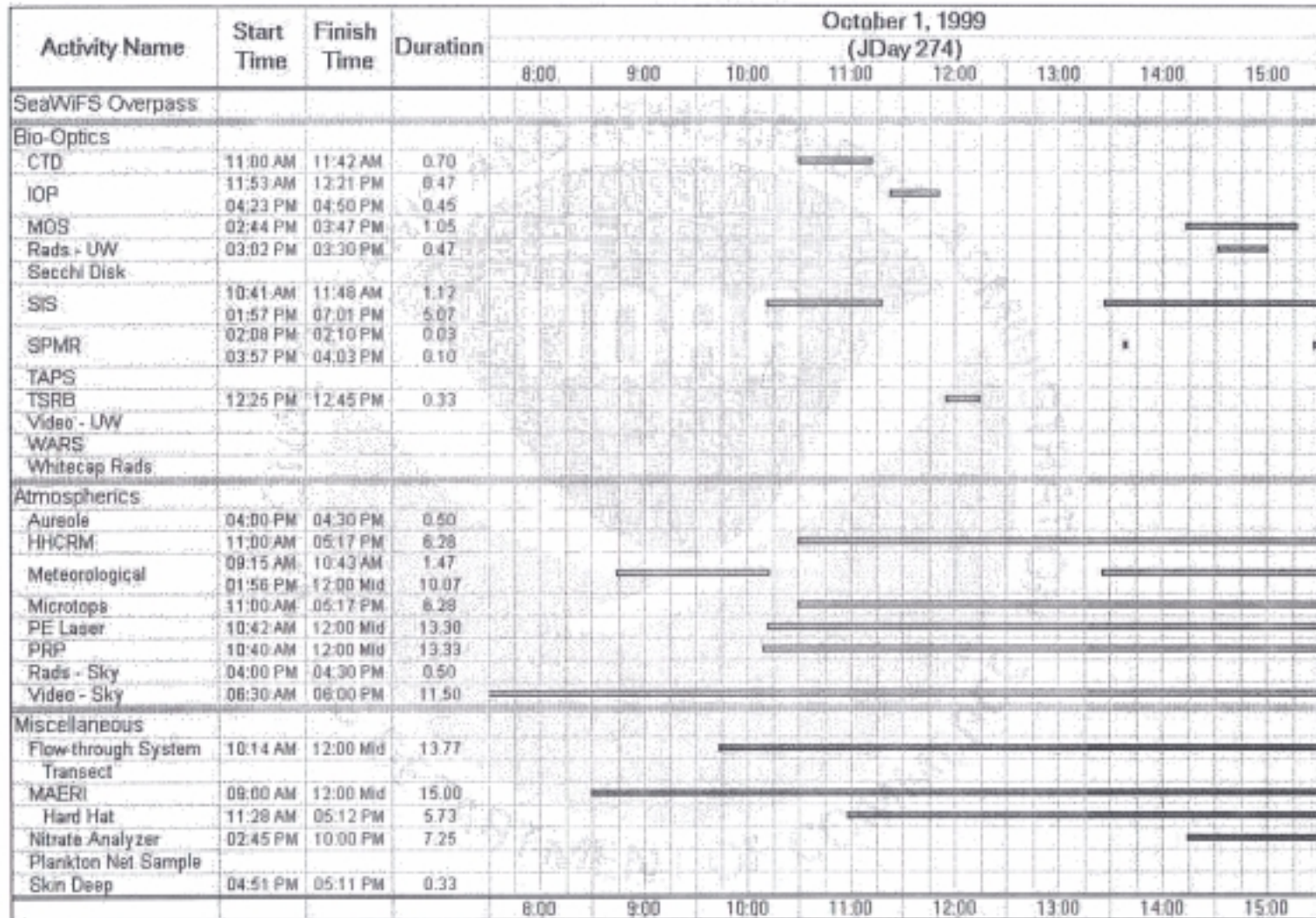


FIGURE 6.

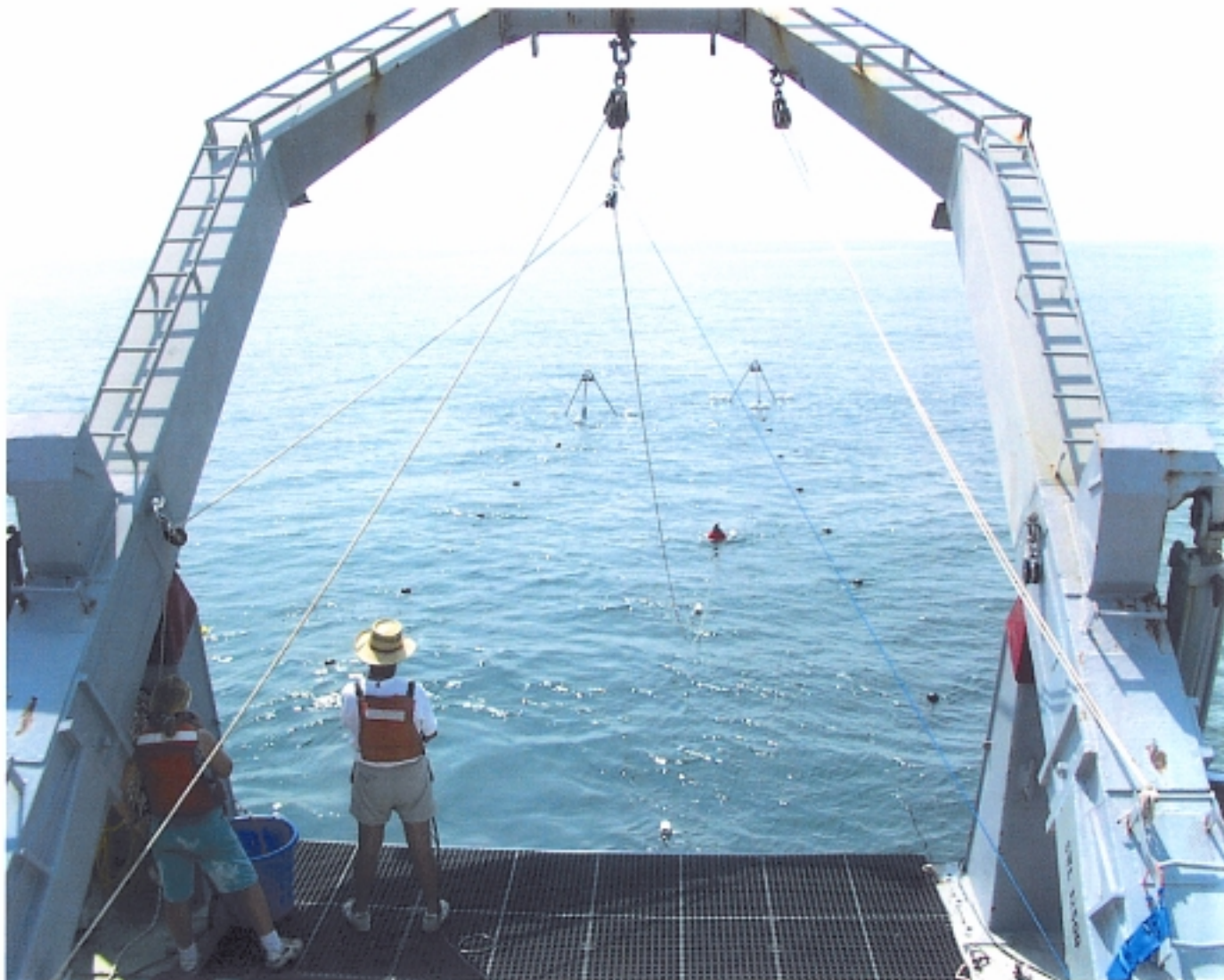


FIGURE 7.



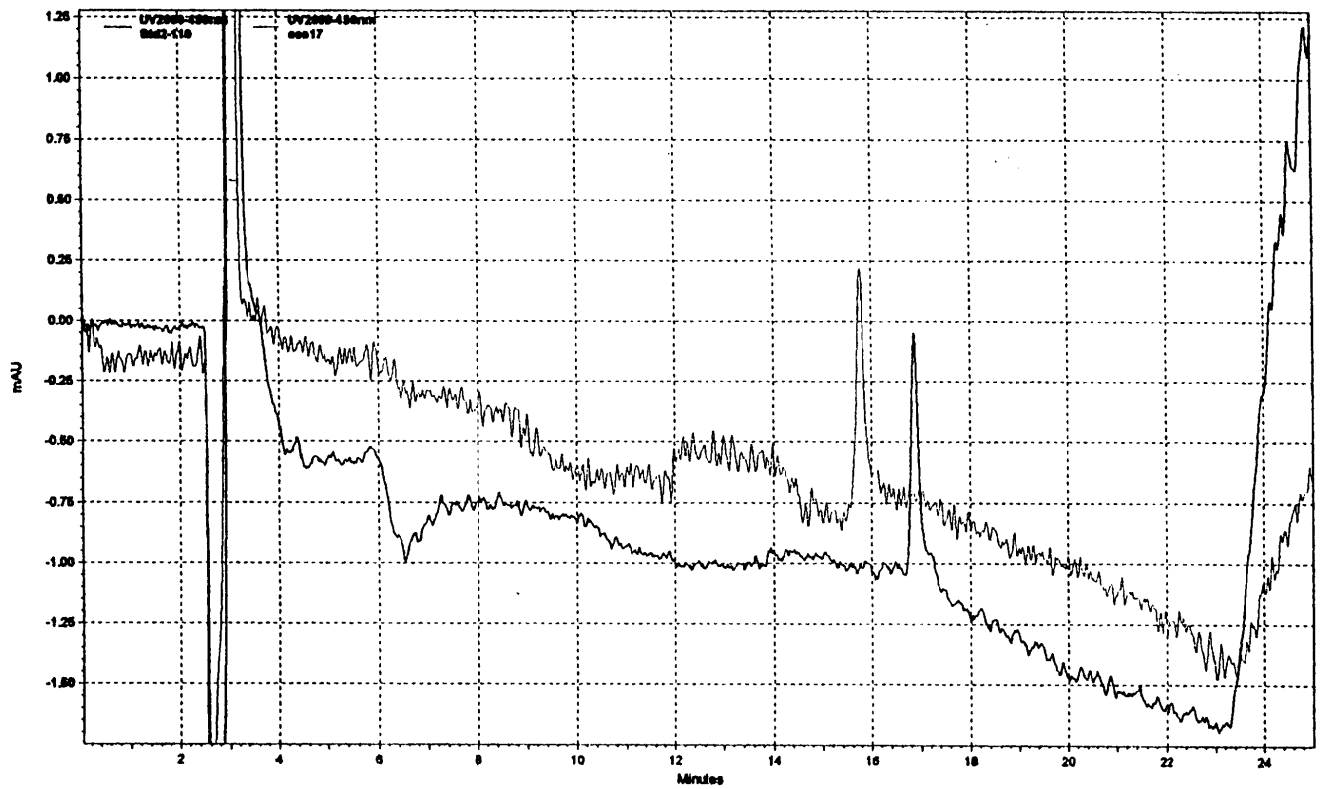
FIGURE 8.



FIGURE 9.



FIGURE 10.



—— D:\ChromQuest\DATA\Stds MOCE5\Std2-110.dat, UV2000-450nm
 —— D:\ChromQuest\DATA\Stds MOCE5\sss17.dat, UV2000-450nm

FIGURE 11. HPLC chromatograms for the internal standard canthaxanthin using the UV absorption detector (450 nm). The upper trace was run on the ship whereas the lower one was processed at CIORS.

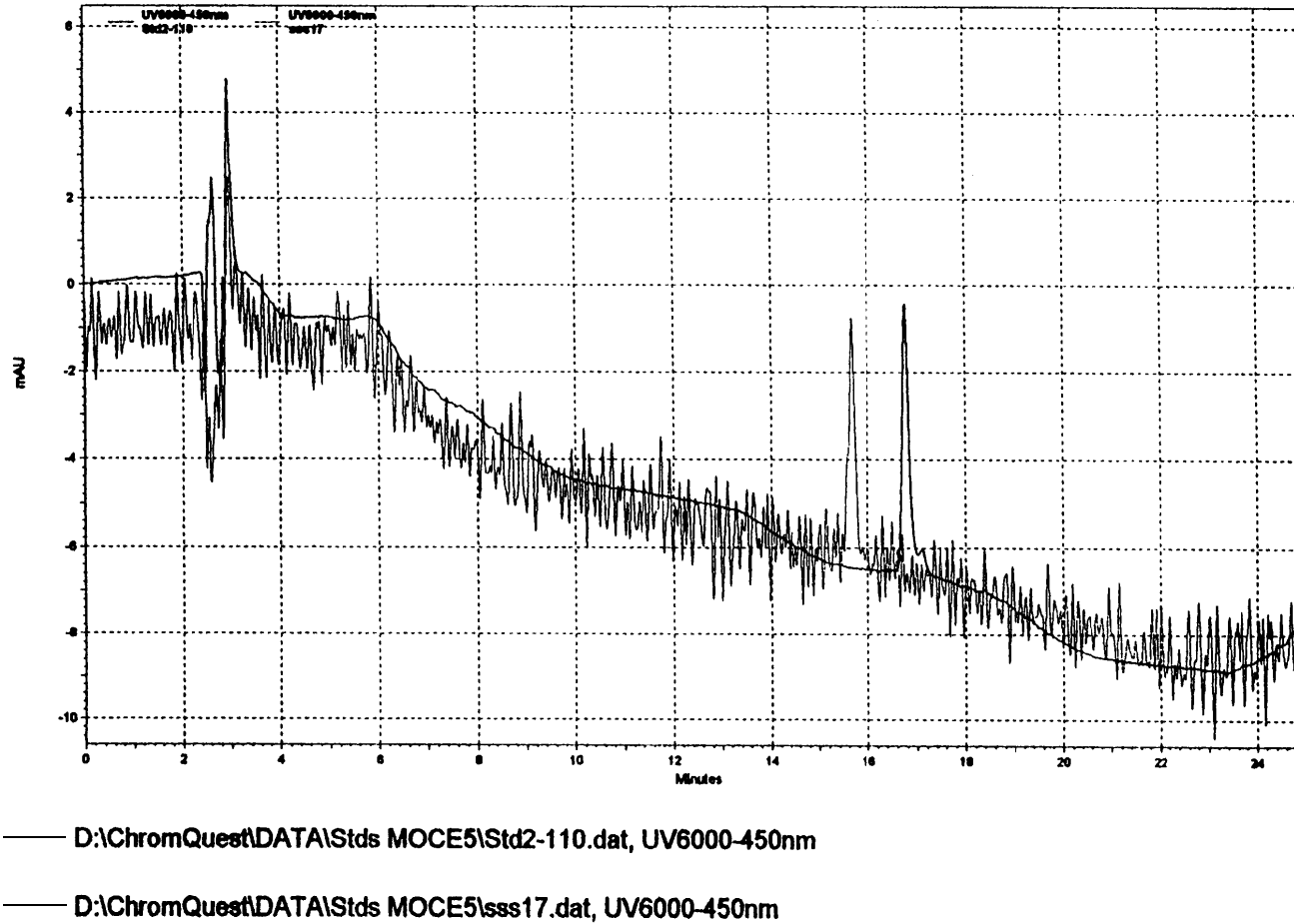
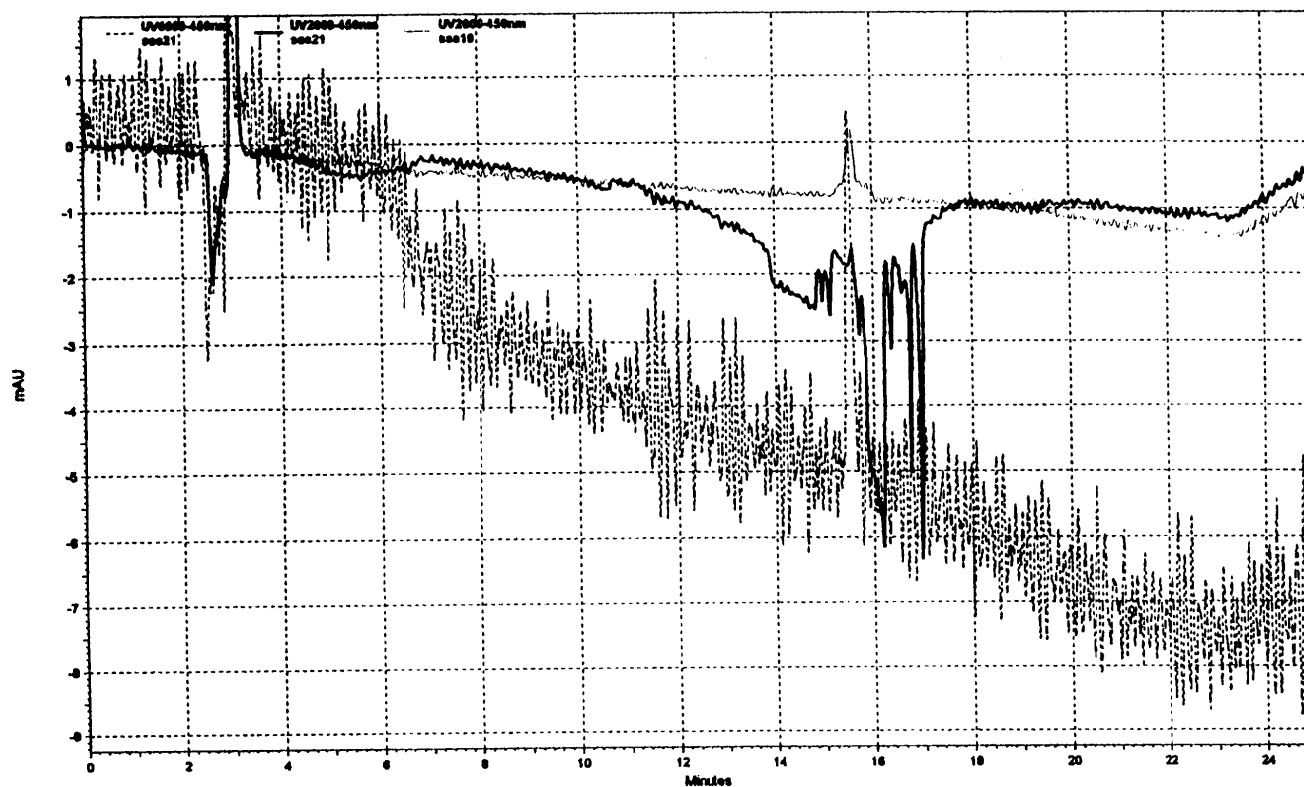


FIGURE 12. HPLC chromatograms for the internal standard, canthaxanthin, using the UV 6000 (450 nm). The noisy trace was processed on the ship.



..... D:\ChromQuest\DATA\Stds MOCE5\sss21.dat, UV6000-450nm
 —— D:\ChromQuest\DATA\Stds MOCE5\sss21.dat, UV2000-450nm
 —— D:\ChromQuest\DATA\Stds MOCE5\sss19.dat, UV2000-450nm

FIGURE 13. HPLC chromatograms showing the negative peaks for the UV 2000. The upper and lower traces are from the UV 2000 and 6000, showing the location of the canthaxanthin peak.

APPENDIX 1 MOCE-5 SeaBird CTD Stations

Station	Position	Date (GMT)	Filename	Max. Depth
01, Coronados	32° 26.77'N 117° 24.40'W	18:05 (GMT) 01 Oct 1999	sbe0106p.mld	205
02, Pta San Antonia	29° 41.68'N 116° 66.70'W	16:47 (GMT) 02 Oct 1999	sbe0107p.mld	205
02, Pta San Antonia	29° 42.51'N 116° 69.30'W	21:52 (GMT) 02 Oct 1999	sbe0108p.mld	1053
03, Bay of San Cristobal	27° 25.46'N 114° 56.99'W	17:50 (GMT) 03 Oct 1999	sbe0109p.mld	205
03, 'Bay of San Cristobal'	26° 47.73'N 114° 21.75'W	02:14 (GMT) 04 Oct 1999	sbe0110p.mld	1023
04, Magdalena Pta	25° 09.85'N 112° 59.90'W	16:46 (GMT) 04 Oct 1999	sbe0111p.mld	1022
05, Cabo San Lucas	22° 47.73'N 110° 07.42'W	16:50 (GMT) 05 Oct 1999	sbe0112p.mld	1015
05, 'Cabo San Lucas'	22° 46.97'N 107° 59.96'W	09:38 (GMT) 06 Oct 1999	sbe0113p.mld	1019
06, Eastern Rif	22° 47.85'N 107° 10.95'W	16:45 (GMT) 06 Oct 1999	sbe0114p.mld	1011
07, Teacapan	22° 02.27'N 105° 46.10'W	15:44 (GMT) 07 Oct 1999	sbe0115p.mld	22
08, Los Corchos	21° 47.51'N 105° 45.31'W	17:19 (GMT) 08 Oct 1999	sbe0116p.mld	26
09, Bahia de Altata	24° 04.91'N 107° 45.04'W	16:21 (GMT) 09 Oct 1999	sbe0117p.mld	72
10, Irwin	22° 30.55'N 109° 35.06'W	17:23 (GMT) 10 Oct 1999	sbe0118p.mld	206
11, Isla Carmen	25° 48.54'N 110° 45.90'W	18:31 (GMT) 11 Oct 1999	sbe0119p.mld	204
12, Mid Rif	28° 34.86'N 112° 25.63'W	17:43 (GMT) 12 Oct 1999	sbe0120p.mld	103
12, 'Mid Rif'	28° 22.79'N 112° 46.59'W	02:56 (GMT) 13 Oct 1999	sbe0121p.mld	197
13, Isla San Esteban	28° 34.76'N 112° 30.82'W	17:43 (GMT) 13 Oct 1999	sbe0122p.mld	203
14, Isla San Esteban 2	28° 34.64'N 112° 32.80'W	16:12 (GMT) 14 Oct 1999	sbe0123p.mld	201
15, Isla San Esteban 3	28° 34.98'N 112° 31.60'W	16:07 (GMT) 15 Oct 1999	sbe0124p.mld	200
16, Southern Gulf	25° 53.00'N 110° 09.70'W	20:34 (GMT) 16 Oct 1999	sbe0125p.mld	1011
17, Cabo San Lucas	22° 58.05'N 109° 29.33'W	15:49 (GMT) 17 Oct 1999	sbe0126p.mld	302
18, Santa Margarita Island	24° 26.50'N 112° 01.79'W	16:01 (GMT) 18 Oct 1999	sbe0127p.mld	89
19, San Cristobal	27° 12.67'N 114° 36.77'W	16:51 (GMT) 19 Oct 1999	sbe0128p.mld	89
20, San Quintin Bay	30° 17.50'N 115° 55.26'W	17:01 (GMT) 20 Oct 1999	sbe0129p.mld	48

APPENDIX 2

MOCE 5 Fluorometrically Determined Chlorophyll
and Phaeopigment

Sta	Date/Time	Lat	Long	z	Chl a	Phaeo
1	1999274180500	32.44617	-117.40333	0	0.452	0.133
1	1999274180500	32.44617	-117.40333	5	0.478	0.127
1	1999274180500	32.44617	-117.40333	8	0.774	0.437
1	1999274180500	32.44617	-117.40333	40	0.497	0.382
2	1999275164700	29.69466	-116.11117	0	0.177	0.064
2	1999275164700	29.69466	-116.11117	20	0.221	0.046
2	1999275164700	29.69466	-116.11117	40	0.332	0.154
2	1999275164700	29.69466	-116.11117	57	0.564	0.390
2	1999275164700	29.69466	-116.11117	75	0.329	0.305
2.1	1999275215200	29.70850	-116.10717	0	0.157	0.035
2.1	1999275215200	29.70850	-116.10717	50	0.555	0.301
2.1	1999275215200	29.70850	-116.10717	200	0.000	0.339
SC	1999276020700	29.29533	-116.00000	5	0.298	0.073
SC	1999276020700	29.29533	-116.00000	5	0.311	0.080
SC	1999276020700	29.29533	-116.00000	5	0.286	0.081
SC	1999276043700	28.81533	-115.85500	5	0.187	0.033
SC	1999276043700	28.81533	-115.85500	5	0.164	0.033
SC	1999276043700	28.81533	-115.85500	5	0.151	0.032
SC	1999276162600	27.40267	-114.92783	5	1.048	0.407
SC	1999276162600	27.40267	-114.92783	5	1.053	0.350
SC	1999276162600	27.40267	-114.92783	5	0.500	0.173
SC	1999276163200	27.40800	-114.94500	5	2.123	0.862
SC	1999276163200	27.40800	-114.94500	5	2.729	0.897
SC	1999276163200	27.40800	-114.94500	5	2.613	0.910
1	1999276175000	27.42433	-114.94983	12	1.520	0.645
3	1999276175000	27.42433	-114.94983	0	1.980	0.460
3	1999276175000	27.42433	-114.94983	5	2.210	0.547
3	1999276175000	27.42433	-114.94983	10	2.597	0.620
3	1999276175000	27.42433	-114.94983	50	0.296	0.267
SC	1999276194100	27.44283	-114.96250	5	4.261	1.218
SC	1999276194100	27.44283	-114.96250	5	4.480	-0.031
MOS	1999276194107	27.443	-114.963	5	4.134	1.501
SC	1999276212900	27.42483	-114.93267	5	3.453	1.245
SC	1999276212900	27.42483	-114.93267	5	4.045	0.718
SC	1999276212900	27.42483	-114.93267	5	3.328	1.270
SC	1999276234200	27.10567	-114.64817	5	0.822	0.274
SC	1999276234200	27.10567	-114.64817	5	0.656	0.181
3.1	1999277034000			0	0.265	0.070
3.1	1999277034000			50	0.603	0.346
3.1	1999277034600	26.796	-114.363	0	0.229	0.096
3.1	1999277034600	26.796	-114.363	50	0.628	0.459
3.1	1999277034600	26.796	-114.363	100	0.056	0.172
3.1	1999277034600	26.796	-114.363	175	0.010	0.088
3.1	1999277034600	26.796	-114.363	200	0.015	0.087
SC	1999277154700			5	0.193	0.052
AT	1999277154851	25.163	-112.994	5	0.129	0.041
4	1999277164900	25.165	-112.992	0	0.136	0.041
4	1999277164900	25.16417	-112.99167	0	0.155	0.033
4	1999277164900	25.165	-112.992	20	0.149	0.051

Sta	Date/Time	Lat	Long	z	Chl a	Phaeo
4	1999277164900	25.16417	-112.99167	20	0.169	0.038
4	1999277164900	25.165	-112.992	40	0.227	0.105
4	1999277164900	25.16417	-112.99167	40	0.222	0.096
4	1999277164900	25.165	-112.992	67	0.508	0.480
4	1999277164900	25.16417	-112.99167	67	0.526	0.362
4	1999277164900	25.165	-112.992	200	0.011	0.050
4	1999277164900	25.16417	-112.99167	200	0.037	0.103
AT	1999277 192822	25.164	-112.998	5	0.141	0.047
SC	1999277193400	25.16383	-112.99783	5	0.159	0.045
AT	1999277214959	25.148	-112.978	5	0.128	0.043
SC	1999277215000			5	0.122	0.037
AT	19992772333120	24.941	-112.711	5	0.162	0.043
SC	1999277233200	24.94067	-112.71067	5	0.162	0.029
AT	1999278011741	24.726	-112.430	5	0.286	0.075
SC	1999278011800	24.726 17	-112.42950	5	0.313	0.063
5.1	1999278105600	22.783	-107.999	0	0.152	0.057
5.1	1999278105600	22.783	-107.999	50	0.573	0.529
5.1	1999278105600	22.783	-107.999	75	0.094	0.131
A T	1999278152212	22.904	-110.144	5	0.246	0.068
AT	1999278 154807	22.828	-110.108	5	0.352	0.069
SC	1999278155200	22.82767	-110.10800	5	0.286	0.098
5	1999278165000	22.796	-110.124	0	0.445	0.331
5	1999278 165000	22.79550	-110.12367	0	0.245	0.067
5	1999278165000	22.796	-110.124	30	0.002	0.045
5	1999278 165000	22.79550	-110.12367	30	0.537	0.146
5	1999278165000	22.796	-110.124	45	0.265	0.125
5	1999278 165000	22.79550	-110.12367	45	0.302	0.116
5	1999278165000	22.796	-110.124	60	0.567	0.203
5	1999278165000	22.79550	-110.12367	60	0.502	0.301
5	1999278165000	22.796	-110.124	215	0.241	0.072
5	1999278165000	22.79550	-110.12367	215	0.015	0.039
MOS	1999278193131	22.812	-110.144	5	0.211	0.062
AT	1999278224722	22.840	-110.116	5	0.388	0.132
AT	1999279155716	22.790	-107.180	5	0.215	0.073
6	1999279164500	22.798	-107.183	0	0.219	0.056
6	1999279164500	22.798	-107.183	10	0.236	0.065
6	1999279164500	22.798	07.183	30	0.439	0.140
6	1999279164500	22.798	-07.183	45	0.768	0.725
6	1999279164500	22.798	07.183	117	0.010	0.262
MOS	1999279193601	22.838	-107.176	5	0.264	0.052
MOS	1999279193601	22.838	-107.176	5	0.248	0.061
MOS	1999279193601	22.838	-107.176	5	0.252	0.056
AT	1999279232454	22.862	-107.137	5	0.213	0.056
AT	1999280010102	22.815	-106.894	5	0.214	0.053
AT	1999280145943	22.039	-105.768	5	1.825	0.337
7	1999280161900	22.038	-105.768	0	1.875	0.324
7	1999280161900	22.038	-105.768	5	1.762	0.434
7	1999280161900	22.038	-105.768	10	1.214	0.417
7	1999280161900	22.038	-105.768	15	1.460	0.469

Sta	Date/Time	Lat	Long	z	Chl a	Phaeo
7	1999280161900	22.038	-105.768	20	0.707	0.282
SeaWiFS	1999280174653	22.040	-105.771	5	2.450	0.443
SeaWiFS	1999280174653	22.040	-105.771	5	2.663	0.466
SeaWiFS	1999280174653	22.040	-105.771	5	2.674	0.544
T-9	1999280234015	22.028	-105.744	5	2.492	0.540
T-9	1999280234015	22.028	-105.744	5	2.215	0.470
T-9	1999280234015	22.028	-105.744	5	2.278	0.519
T-9	1999280235226	21.991	-105.738	5	3.889	0.386
T-9	1999280235226	21.991	-105.738	5	3.511	0.466
T-9	1999280235226	21.991	-105.738	5	3.511	0.466
T-9	1999281000720	21.945	-105.729	5	3.253	0.509
T-9	1999281000720	21.945	-105.729	5	3.473	0.546
T-9	1999281000720	21.945	-105.729	5	3.423	0.722
T-9	1999281004248	21.840	-105.687	5	3.322	0.506
T-9	1999281004248	21.840	-105.687	5	3.052	0.633
T-9	1999281004248	21.840	-105.687	5	3.058	0.591
T-9	1999281005600	21.807	-105.659	5	3.958	0.668
T-9	1999281005600	21.807	-105.659	5	3.706	0.840
T-9	1999281005600	21.807	-105.659	5	3.574	0.619
T-9	1999281012322	21.735	-105.607	5	2.725	0.472
T-9	1999281012322	21.735	-105.607	5	2.567	0.652
T-9	1999281012322	21.735	-105.607	5	2.838	0.505
T-9	1999281020403	21.611	-105.598	5	3.329	0.564
T-9	1999281020403	21.611	-105.598	5	3.071	0.607
T-9	1999281020403	21.611	-105.598	5	3.115	0.657
T-9	1999281025648	21.538	-105.477	5	4.468	1.023
T-9	1999281025648	21.538	-105.477	5	4.694	0.904
T-9	1999281025648	21.538	-105.477	5	4.644	1.010
T-9	1999281163143	21.795	-105.747	5	6.399	0.175
8	1999281165900	21.792	-105.755	0	3.763	1.006
8	1999281165900	21.792	-105.755	6	3.020	1.069
8	1999281165900	21.792	-105.755	9	2.504	1.005
8	1999281165900	21.792	-105.755	12	0.755	0.467
8	1999281165900	21.792	-105.755	25	0.388	0.326
MOS	1999281191348	21.795	-105.775	5	5.122	0.861
MOS	1999281191348	21.795	-105.775	5	4.751	0.999
MOS	1999281191348	21.795	-105.775	5	4.770	0.817
MOS'	1999281201129	21.806	-105.783	5	4.549	0.567
MOS'	1999281201129	21.806	-105.783	5	4.442	0.649
MOS'	1999281201129	21.806	-105.783	5	4.593	1.115
T-10	1999281230754	21.832	-105.798	5	5.027	0.310
T-10	1999282023818	22.315	-106.209	5	0.634	0.136
T-10	1999282152202	24.067	-107.735	5	0.349	0.123
9	1999282165600	24.081	-107.751	0	0.329	0.092
9	1999282165600	24.081	-107.751	10	0.360	0.109
9	1999282165600	24.081	-107.751	20	0.365	0.110
9	1999282165600	24.081	-107.751	31	0.633	0.299
9	1999282165600	24.081	-107.751	45	0.841	0.779
SeaWiFS	1999282192201	24.099	-107.751	5	0.332	0.097

Sta	Date/Time	Lat	Long	z	Chl a	Phaeo
SeaWiFS	1999282192201	24.099	-107.751	5	0.337	0.092
SeaWiFS	1999282192201	24.099	-107.751	5	0.324	0.090
T11	1999282230618	24.767	-107.739	5	0.323	0.104
T11	1999282230618	24.767	-107.739	5	0.330	0.096
T11	1999282230618	24.767	-107.739	5	0.334	0.093
T11	1999283015521	23.841	-108.208	5	0.171	0.059
T11	1999283 134223	22.753	-109.882	5	0.168	0.062
T11	1999283163211	22.508	-109.580	5	0.172	0.057
10	1999283172400	22.509	-109.584	0	0.180	0.053
10	1999283172400	22.509	-109.584	10	0.173	0.048
10	1999283172400	22.509	-109.584	20	0.201	0.061
10	1999283172400	22.509	-109.584	30	0.628	0.327
10	1999283172400	22.509	-109.584	40	1.033	0.741
SeaWiFS	1999283200429	22.536	-109.599	5	0.156	0.047
SeaWiFS	1999283200429	22.536	-109.599	5	0.154	0.047
SeaWiFS	1999283200429	22.536	-109.599	5	0.159	0.053
T-12	1999283224758	22.527	-109.575	5	0.154	0.047
T-12	1999284020020	23.100	-109.373	5	0.145	0.052
T-13	1999284110555	28.188	-112.306	5	0.363	0.175
T-12	1999284134834	25.192	-110.321	5	0.201	0.086
T-12	1999284172856	25.810	-110.752	5	0.279	0.090
11	1999284183100	25.809	-110.765	0	0.319	0.077
11	1999284183100	25.809	-110.765	15	0.359	0.12
11	1999284183100	25.809	-110.765	30	0.453	0.130
11	1999284183100	25.809	-110.765	45	1.101	0.963
11	1999284183100	25.809	-110.765	60	0.353	0.329
MOS	1999284200204	25.819	-110.792	5	0.258	0.087
T-13	1999284210439	25.838	-110.816	5	0.286	0.094
T - 13	1999285114145	28.283	-112.386	5	3.656	1.591
T-13	1999285114145	28.283	-112.386	5	3.594	1.521
T-13	1999285114145	28.283	-112.386	5	3.533	1.710
T-13	1999285121755	28.394	-112.420	5	4.167	2.025
T-13	1999285121755	28.394	-112.420	5	4.634	1.743
T-13	1999285121755	28.394	-112.420	5	4.946	1.928
T-13	1999285124734	28.489	-112.426	5	10.219	1.190
T-13	1999285124734	28.489	-112.426	5	10.483	1.733
T-13	1999285124734	28.489	-112.426	5	11.805	2.948
T-13	1999285133246	28.591	-112.448	5	7.382	0.961
T-13	1999285 133246	28.591	-112.448	5	7.418	1.286
T-13	1999285 133246	28.591	-112.448	5	7.206	1.231
T-13	1999285140555	28.644	-112.496	5	8.034	1.587
T-13	1999285140555	28.644	-112.496	5	7.937	1.392
T-13	1999285140555	28.644	-112.496	5	7.796	1.588
T-13	1999285143727	28.645	-112.411	Bucket	4.365	1.522
T-13	1999285150319	28.644	-112.339	5	4.650	0.569
T-13	1999285150319	28.644	-112.339	5	4.285	0.908
T-13	1999285150319	28.644	-112.339	5	4.386	1.124
T-13	1999285152625	28.649	-112.281	5	3.102	1.040
T-13	1999285152625	28.649	-112.281	5	3.354	1.010

Sta	Date/Time	Lat	Long	z	Chl a	Phaeo
T-13	1999285152625	28.649	-112.281	5	3.102	1.040
T-13	1999285160015	28.651	-112.286	5	4.140	0.926
T-13	1999285160015	28.651	-112.286	5	3.977	0.985
T-13	1999285160015	28.651	-112.286	5	3.895	1.014
T-13	1999285162630	28.643	-112.310	5	3.058	1.203
T-13	1999285162630	28.643	-112.310	5	3.222	1.145
T-13	1999285162630	28.643	-112.310	5	3.008	1.238
T-13	1999285165958	28.589	-112.408	5	6.796	1.194
T-13	1999285165958	28.589	-112.408	5	3.996	0.945
T-13	1999285165958	28.589	-112.408	5	6.733	1.326
T-13	1999285171011	28.579	-112.427	5	8.432	1.963
T-13	1999285171011	28.579	-112.427	5	8.369	1.953
T-13	1999285171011	28.579	-112.427	5	8.495	1.689
12	1999285180000	28.581	-112.427	0	11.326	1.801
12	1999285180000	28.581	-112.427	5	7.488	2.235
12	1999285180000	28.581	-112.427	7	5.273	1.541
12	1999285180000	28.581	-112.427	10	2.882	1.431
12	1999285180000	28.581	-112.427	15	1.970	1.116
T-13	1999285180731	28.583	-112.431	5	10.194	1.827
T-13	1999285180731	28.583	-112.431	5	9.565	2.293
T-13	1999285180731	28.583	-112.431	5	9.690	2.029
T-14	1999285183429	28.588	-112.438	5	9.627	1.947
T-14	1999285183429	28.588	-112.438	5	10.320	2.062
T-14	1999285183429	28.588	-112.438	5	9.627	2.161
T-14	1999285190325	28.598	-112.440	5	9.816	1.978
T-14	1999285190325	28.598	-112.440	5	10.257	2.550
T-14	1999285190325	28.598	-112.440	5	9.502	1.998
T-14	1999285193455	28.609	-112.440	5	10.257	2.336
T-14	1999285193455	28.609	-112.440	5	10.068	2.519
T-14	1999285193455	28.609	-112.440	5	10.131	2.030
T-14	1999285195505	28.617	-112.437	5	9.753	1.826
T-14	1999285195505	28.617	-112.437	5	9.124	2.006
T-14	1999285195505	28.617	-112.437	5	9.565	1.581
T-14	1999285202958	28.630	-112.432	5	8.872	1.751
T-14	1999285202958	28.630	-112.432	5	8.872	1.822
T-14	1999285202958	28.630	-112.432	5	8.684	2.361
T-14	1999285205614	28.637	-112.429	5	5.946	0.840
T-14	1999285205614	28.637	-112.429	5	5.751	1.534
T-14	1999285205614	28.637	-112.429	5	5.720	1.316
T-14	1999285210013	28.639	-112.428	5	8.684	1.506
T-14	1999285210013	28.639	-112.428	5	8.558	1.699
T-14	1999285210013	28.639	-112.428	5	8.306	1.942
T-14	1999285213609	28.648	-112.424	5	12.081	2.353
T-14	1999285213609	28.648	-112.424	5	12.081	2.780
T-14	1999285213609	28.648	-112.424	5	12.081	2.353
T-14	1999285220007	28.649	-112.421	5	10.194	1.827
T-14	1999285220007	28.649	-112.421	5	9.942	1.928
T-14	1999285220007	28.649	-112.421	5	9.879	1.846
T-14	1999285230057	28.647	-112.421	5	7.299	1.562

Sta	Date/Time	Lat	Long	z	Chla	Phaeo
T-14	1999285230057	28.647	-112.421	5	7.803	1.930
T-14	1999285230057	28.647	-112.421	5	7.551	1.248
T-14	1999286000034	28.635	-112.427	5	8.117	1.911
T-14	1999286000034	28.635	-112.427	5	8.243	1.790
T-14	1999286000034	28.635	-112.427	5	8.558	2.126
T-14	1999286011630	28.494	-112.615	5	6.481	1.427
T-14	1999286011630	28.494	-112.615	5	5.978	1.486
T-14	1999286011630	28.494	-112.615	5	6.481	1.570
T-14	1999286014957	28.430	-112.711	5	5.827	0.878
T-14	1999286014957	28.430	-112.711	5	5.399	0.850
T-14	1999286014957	28.430	-112.711	5	5.663	1.007
12.3	1999286025600	28.380	-112.777	0	4.782	0.790
12.3	1999286025600	28.380	-112.777	5	4.877	0.806
12.3	1999286025600	28.380	-112.777	10	4.738	0.954
12.3	1999286025600	28.380	-112.777	20	3.190	0.997
12.3	1999286025600	28.380	-112.777	50	0.799	0.574
	1999286165519	28.572	-112.510	5	10.634	1.615
13	1999286174300	28.579	-112.514	0	10.445	2.438
13	1999286174300	28.579	-112.514	5	6.450	0.781
13	1999286174300	28.579	-112.514	10	5.198	1.557
13	1999286174300	28.579	-112.514	30	2.322	1.359
13	1999286174300	28.579	-112.514	100	1.038	0.663
	1999286192457	28.610	-112.536	5	12.585	3.575
	1999286193045	28.613	-112.539	5	11.389	3.164
MOS	1999286194623	28.620	-112.543	5	11.704	2.575
MOS	1999286194623	28.620	-112.543	5	11.452	2.676
MOS	1999286194623	28.620	-112.543	5	10.949	2.522
MOS	1999286200654	28.629	-112.547	Bucket	6.230	1.101
MOS	1999286200654	28.629	-112.547	Bucket	6.041	1.283
MOS	1999286200654	28.629	-112.547	Bucket	6.104	1.294
MOS	1999286205854	28.640	-112.565	Bucket	9.816	1.978
MOS	1999286205854	28.640	-112.565	Bucket	9.502	2.282
MOS	1999286205854	28.640	-112.565	Bucket	9.627	1.876
T-16	1999287004042	28.565	-112.468	5	5.474	0.976
T-16	1999287004042	28.565	-112.468	5	6.078	1.204
T-16	1999287004042	28.565	-112.468	5	5.776	0.983
MOS	1999287152759	28.582	-112.538	5	7.425	0.657
MOS	1999287152759	28.582	-112.538	5	6.922	1.286
MOS	1999287152759	28.582	-112.538	5	6.859	1.418
MOS	1999287152759	28.582	-112.538	Bucket	6.733	0.899
MOS	1999287152759	28.582	-112.538	Bucket	6.985	1.012
MOS	1999287152759	28.582	-112.538	Bucket	6.796	1.123
14	1999287165758	28.572	-112.560	0	7.740	1.849
14	1999287165758	28.572	-112.560	8	8.998	1.487
14	1999287165758	28.572	-112.560	15	8.180	1.637
14	1999287165758	28.572	-112.560	40	3.511	1.250
14	1999287165758	28.572	-112.560	120	0.617	0.536
MOS	1999287165758	28.572	-112.560	5	7.803	1.147
MOS	1999287165758	28.572	-112.560	5	7.299	1.491

Sta	Date/Time	Lat	Long	z	Chl a	Phaeo
MOS	1999287165758	28.572	-112.560	5	7.551	1.319
MOS	1999287165758	28.572	-112.560	Bucket	7.551	0.892
MOS	1999287165758	28.572	-112.560	Bucket	8.369	1.312
MOS	1999287165758	28.572	-112.560	Bucket	7.740	1.706
MOS	1999287184422	28.596	-112.554	5	9.942	1.501
MOS	1999287184422	28.596	-112.554	5	8.998	1.843
MOS	1999287184422	28.596	-112.554	5	5.802	0.788
MOS	1999287 184422	28.596	-112.554	Bucket	5.865	0.513
MOS	1999287184422	28.596	-112.554	Bucket	5.393	1.148
MOS	1999287184422	28.596	-112.554	Bucket	8.054	1.758
MOS	1999287194540	28.617	-112.552	5	9.690	1.602
MOS	1999287194540	28.617	-112.552	5	7.991	1.677
MOS	1999287194540	28.617	-112.552	5	7.991	1.890
MOS	1999287 194540	28.617	-112.552	Bucket	8.746	1.446
MOS	1999287194540	28.617	-112.552	Bucket	8.998	1.772
MOS	1999287194540	28.617	-112.552	Bucket	8.935	1.975
Satlantic	1999287212020	28.609	-112.509	5	8.369	2.523
Satlantic	1999287212020	28.609	-112.509	5	8.243	2.146
Satlantic	1999287212020	28.609	-112.509	5	8.180	2.491
Satlantic	1999287212020	28.609	-112.509	Bucket	3.461	0.643
Satlantic	1999287212020	28.609	-112.509	Bucket	2.939	0.571
Satlantic	19992872 12020	28.609	-112.509	Bucket	3.411	0.678
	199928804 1750	28.591	-112.464	5	8.054	1.545
	1999288041750	28.591	-112.464	5	8.306	1.871
	1999288041750	28.591	-112.464	5	8.746	1.517
	1999288153120	28.584	-112.516	5	7.236	0.413
15	1999288160800	28.583	-112.527	0	6.796	1.266
15	1999288160800	28.583	-112.527	5	7.173	1.186
15	1999288160800	28.583	-112.527	10	8.369	1.383
15	1999288160800	28.583	-112.527	20	4.077	0.987
15	1999288 160800	28.583	-112.527	30	3.171	1.179
MOS	1999288191041	28.597	-112.579	5	8.054	1.901
MOS	1999288191041	28.597	-112.579	5	7.740	2.347
MOS	1999288191041	28.597	-112.579	5	7.425	1.654
MOS	1999288191041	28.597	-112.579	Buck	5.852	1.110
MOS	1999288191041	28.597	-112.579	Buck	6.368	0.525
MOS	1999288191041	28.597	-112.579	Bucket	6.041	0.713
MOS'	1999288202942	28.618	-112.577	5	6.418	1.203
MOS'	1999288202942	28.618	-112.577	5	6.230	1.386
MOS'	1999288202942	28.618	-112.577	5	6.922	1.358
MOS'	1999288202942	28.618	-112.577	Buck	3.549	0.814
MOS'	1999288202942	28.618	-112.577	Buck	3.517	0.809
MOS'	1999288202942	28.618	-112.577	Bucket	3.631	0.856
T-17	1999288233543	28.627	-112.554	5	9.124	1.437
T-17	1999288233543	28.627	-112.554	5	7.614	2.113
T-17	1999288233543	28.627	-112.554	5	7.803	2.358
T-17	1999289000000	28.573	-112.518	5	3.851	0.822
T-17	1999289000000	28.573	-112.518	5	4.033	0.937
T-17	1999289000000	28.573	-112.518	5	3.738	0.917

Sta	Date/Time	Lat	Long	z	Chl a	Phaeo
T-17	1999289001856	28.520	-112.488	5	8.054	2.257
T-17	1999289001856	28.520	-112.488	5	7.991	2.389
T-17	1999289001856	28.520	-112.488	5	8.180	1.922
T-17	1999289003001	28.487	-112.472	5	9.690	2.385
T-17	1999289003001	28.487	-112.472	5	9.753	2.253
T-17	1999289003001	28.487	-112.472	5	9.879	1.775
T-17	1999289010000	28.397	-112.428	5	5.040	1.032
T-17	1999289010000	28.397	-112.428	5	5.135	1.119
T-17	1999289010000	28.397	-112.428	5	5.078	1.096
T-17	1999289013001	28.314	-112.373	5	3.077	0.879
T-17	1999289013001	28.314	-112.373	5	3.020	0.998
T-17	1999289013001	28.314	-112.373	5	3.052	0.789
T-17	1999289020001	28.240	-112.300	5	1.705	0.688
T-17	1999289020001	28.240	-112.300	5	1.705	0.716
T-17	1999289020001	28.240	-112.300	5	1.812	0.627
T-17	1999289023000	28.163	-112.233	5	4.638	1.023
T-17	1999289023000	28.163	-112.233	5	4.638	1.023
T-17	1999289023000	28.163	-112.233	5	4.417	1.129
T-17	1999289030034	28.085	-112.157	5	2.567	0.873
T-17	1999289030034	28.085	-112.157	5	2.530	0.831
T-17	1999289030034	28.085	-112.157	5	2.435	0.887
T-17	1999289033002	28.006	-112.078	5	1.032	0.441
T-17	1999289033002	28.006	-112.078	5	0.994	0.456
T-17	1999289033002	28.006	-112.078	5	0.997	0.450
T-17	1999289040300	27.913	-111.995	5	0.531	0.247
T-17	1999289040300	27.913	-111.995	5	0.536	0.260
T-17	1999289040300	27.913	-111.995	5	0.529	0.250
T-17	1999289043001	27.839	-111.925	5	0.423	0.255
T-17	1999289043001	27.839	-111.925	5	0.420	0.263
T-17	1999289043001	27.839	-111.925	5	0.408	0.247
T-17	1999289153243	26.120	-110.315	5	0.247	0.122
T-17	1999289153243	26.120	-110.315	5	0.238	0.123
T-17	1999289153243	26.120	-110.315	5	0.240	0.132
T-17	1999289170213	25.907	-110.125	5	0.331	0.105
MOS	1999289193701	25.889	-110.155	5	0.289	0.105
MOS	1999289193701	25.889	-110.155	5	0.285	0.108
MOS	1999289193701	25.889	-110.155	5	0.289	0.105
16	1999289203400	25.883	-110.162	0	0.269	0.064
16	1999289203400	25.883	-110.162	10	0.260	0.071
16	1999289203400	25.883	-110.162	20	0.354	0.093
16	1999289203400	25.883	-110.162	30	0.571	0.447
16	1999289203400	25.883	-110.162	40	0.457	0.393
	1999289231925	25.821	-110.177	5	0.293	0.107
	1999290151557	22.967	-109.483	5	0.174	0.075
17	1999290154900	22.968	-109.489	0	0.167	0.053
17	1999290154900	22.968	-109.489	10	0.172	0.058
17	1999290154900	22.968	-109.489	20	0.680	0.447
17	1999290154900	22.968	-109.489	30	1.635	0.887
17	1999290154900	22.968	-109.489	40	0.395	0.336

Sta	Date/Time	Lat	Long	Z	Chl a	Phaeo
MOS	1999290180902	22.971	-109.505	5	0.175	0.077
MOS	1999290180902	22.971	-109.505	5	0.181	0.073
MOS	1999290180902	22.971	-109.505	5	0.174	0.063
T-19	1999290205348	22.954	-109.537	5	0.170	0.074
T-19	1999290205348	22.954	-109.537	5	0.141	0.055
T-19	1999290205348	22.954	-109.537	5	0.153	0.068
	1999291151606	24.444	-112.042	5	0.280	0.083
18	1999291160100	24.442	-112.030	0	0.234	0.052
18	1999291160100	24.442	-112.030	10	0.243	0.068
18	1999291160100	24.442	-112.030	20	0.324	0.089
18	1999291160100	24.442	-112.030	37	0.659	0.279
18	1999291160100	24.442	-112.030	45	0.836	0.620
	1999291164342	24.442	-112.026	5	0.221	0.099
MOS	1999291192600	24.456	-112.020	5	0.206	0.051
MOS	1999291192600	24.456	-112.020	5	0.199	0.064
MOS	1999291192600	24.456	-112.020	5	0.198	0.047
T-20	1999291201840	24.464	-112.018	5	0.235	0.068
T-20	1999292145039	27.203	-114.602	5	1.825	0.316
T-20	1999292145039	27.203	-114.602	5	1.749	0.489
T-20	1999292145039	27.203	-114.602	5	1.699	0.437
	1999292160351	27.225	-114.604	5	1.116	0.373
	1999292164820	27.211	-114.612	5	1.586	0.490
19	1999292165200	27.211	-114.613	0	1.951	0.579
19	1999292165200	27.211	-114.613	10	2.001	0.587
19	1999292165200	27.211	-114.613	20	2.026	0.762
19	1999292165200	27.211	-114.613	30	3.675	1.177
19	1999292165200	27.211	-114.613	40	1.410	0.974
MOS	1999292185516	27.235	-114.640	5	1.053	0.268
MOS	1999292185516	27.235	-114.640	5	1.133	0.287
MOS	1999292185516	27.235	-114.640	5	1.075	0.323
	1999292192426	27.242	-114.647	Bucket	1.118	0.253
MOS	1999292200901	27.255	-114.657	5	0.983	0.217
MOS	1999292200901	27.255	-114.657	5	0.972	0.240
MOS	1999292200901	27.255	-114.657	5	0.977	0.230
T-21	1999292221547	27.273	-114.675	5	0.930	0.384
T-21	1999292221547	27.273	-114.675	5	0.881	0.245
T-21	1999292221547	27.273	-114.675	5	0.931	0.225
T-21	1999293011730	27.709	-115.129	5	2.001	0.445
T-21	1999293011730	27.709	-115.129	5	2.039	0.508
T-21	1999293011730	27.709	-115.129	5	2.064	0.555
T-21	1999293162439	30.291	-115.921	5	0.724	0.269
20	1999293170200	30.291	-115.921	0	0.882	0.314
20	1999293170200	30.291	-115.921	5	1.334	0.605
20	1999293170200	30.291	-115.921	7	1.422	0.634
20	1999293170200	30.291	-115.921	10	1.976	0.953
20	1999293170200	30.291	-115.921	18	1.913	1.014
MOS	1999293191849	30.302	-115.936	5	0.916	0.300
MOS	1999293191849	30.302	-115.936	5	0.910	0.284
MOS	1999293191849	30.302	-115.936	5	0.886	0.292

Sta	Date/Time	Lat	Long	z	Chl a	Phaeo
MOS	1999293 193526	30.303	-115.938	Bucket	1.183	0.395
MOS	1999293193526	30.303	-115.938	Bucket	1.208	0.413
MOS	1999293193526	30.303	-115.938	Bucket	1.196	0.369
MOS	1999293195526	30.305	-115.940	5	1.447	0.553
MOS	1999293195526	30.305	-115.940	5	I .472	0.471
MOS	1999293195526	30.305	-115.940	5	1.435	0.579
MOS	1999293204547	30.3 13	-115.948	5	1.900	0.684
MOS	1999293204547	30.313	-115.948	5	I .850	0.633
MOS	1999293204547	30.313	• 115.948	5	1.863	0.678
MOS	1999293204547	30.313	-115.948	Bucket	2.177	0.759
T-22	1999293224743	30.318	-115.947	5	1.498	0.646
T-22	1999294130400	32.111	-117.054	5	0.274	0.048
T-22	1999294130400	32.111	-117.054	5	• 0.274	0.105

APPENDIX 3 History of NOAA/MLML Marine Optical System (MOS) Observations

MOBY-L47: 29-June to 01-July-1999 aboard the HRA Manta Raiv

Station (# - Name)	Date (GMT)	Time	Latitude (+North)	Longitude (+East)	Depths (dbar)
01 - Lanai Mooring	29-Jun- 1999		20.8	-157.2	NO MOS
02- Lanai Mooring	30-Jun-1999		20.8	-157.2	NO MOS
03- Lanai Mooring	01-Jul-1999		20.8	-157.2	NO MOS

MOBY-L48: 29-July to 01-August- 1999 aboard the R/V Ka'imikai-0-Kanaloa

Station (# - Name)	Date (GMT)	Time	Latitude (+North)	Longitude (+East)	Depths (dbar)
01- Lanai Mooring	29-Jul- 1999		20.8	-157.2	N O MOS
02- Lanai Mooring	30-Jul- 1999		20.8	-157.2	N O MOS
03- Lanai Mooring	01-Aug-1999		20.8	-157.2	N O MOS

MOBY-L49: 05-September-1999 aboard the HRA Manta Raiv

Station (# - Name)	Date (GMT)	Time	Latitude (+North)	Longitude (+East)	Depths (dbar)
01- Lanai Mooring	05-Sep- 1999		20.8	-157.2	NO MOS

MOBY -L50: 10-October- 1999 aboard the HRA Manta Raiv

Station (# - Name)	Date (GMT)	Time	Latitude (+North)	Longitude (+East)	Depths (dbar)
01- Lanai Mooring	10-Oct- 1999		20.8	-157.2	NO MOS

MOCE-5: 01 to 21 -October- 1999 aboard the RN Melville

Station (# - Name)	Date (GMT)	Time	Latitude (+North)	Longitude (+East)	Depths (dbar)
01 - Islas Coronados	01-Oct-1999	22:16	32.449	-117.357	1,6
02 - Punta San Anotnio	02-Oct-1999		29.697	-116.123	NO MOS
03 - Bahia de San Cristobal	03-Oct-1999	19:17	27.433	-114.959	0,1,11,16
04 - Punta Magdalena	04-Oct-1999	19:09	25.158	-112.997	0,1,5,10,15
05 - Cabo San Lucas	05-Oct-1999	19:24	22.800	-110.145	1,6,16
06 - Mazatlan	06-Oct-1999	19:06	22.820	-107.178	0,1,3,5,7,9,11,13,15
07 - Teacapan	07-Oct-1999	17:48	22.042	-105.770	0,1,2,3,5,8
08 - Los Corchos	08-Oct-1999	18:53	21.790	-105.766	0,1,2,3,4,5,6
09 - Bahia De Altata	09-Oct-1999	19:22	24.099	-107.751	1,3,5,6,11,16
10 - TS Irwin	10-Oct-1999	19:57	22.520	-109.589	10,20,30,35
11 - Isla Carmen	11-Oct-1999	19:57	25.814	-110.781	1,6,11
12a- Mid Rift	12-Oct-1999	19:12	28.617	-112.437	0,1,2,3,5
12b- Mid Rift	12-Oct-1999	19:55	28.617	-112.437	0,1,2,3,5
13a- Isla San Esteban I	13-Oct-1999	19:45	28.596	-112.528	0,1,2,3,5
13b- Isla San Esteban I	13-Oct-1999	20:06	28.596	-112.528	0,1,2,3,5
14 - Isla San Esteban II	14-Oct-1999	19:45	28.617	-112.552	0,1,2,3,5
15-a Isla San Esteban III	15-Oct-1999	19:12	28.618	-112.577	0,1,2,3,5,8,11
15b- Isla San Esteban III	15-Oct-1999	20:49	28.618	-112.577	0,1,2,3,5,8,11
16 - Southern Gulf	16-Oct-1999	19:36	25.889	-110.155	1,6,11,16
17 - Bahia San Lucas	17-Oct-1999	18:54	22.972	-109.498	1,2,6,11,16
18 - Isla Santa Margarita	18-Oct-1999	19:26	24.456	-112.020	1,2,6,11,16
19 - Bahia de San Cristobal	19-Oct-1999	20:08	27.256	-114.657	1,2,3,6,11
20a- Bahia de San Quintin	20-Oct-1999	19:44	30.294	-115.924	0,1,2,6,11
20b- Bahia de San Quintin	20-Oct-1999	20:30	30.294	-115.924	0,1,2,6,11
20c- Bahia de San Quintin	20-Oct-1999	21:15	30.294	-115.924	0,1,2,6,11

MOBY -L51: 15 to 18-November- 1999 aboard the R/V Ka'imikai-0-Kanaloa

Station (# - Name)	Date (GMT)	Time	Latitude (+North)	Longitude (+East)	Depths (dbar)
01- Lanai Mooring	15-Nov-1999		20.8	-157.2	NO MOS
02- Lanai Mooring	16-Nov-1999		20.8	-157.2	NO MOS
03- Lanai Mooring	17-Nov-1999		20.8	-157.2	NO MOS
04- Lanai Mooring	18-Nov-1999		20.8	-157.2	NO MOS

APPENDIX 4 Calibrations and maintenance schedules for MLML standards and instruments

• Radiometric Calibration Standards

- 25 June: purchased new **RS-10BU irradiance** head and spare lamp from Gamma Scientific
- 28 September: **OL425** pre-calibration, re-lamp and re-calibration # 2 via Optronic Laboratories
- 29 November: SCAMPS sent to NIST for re-calibration # 3
- 23 December: **OL420** to Optronic Laboratories for re-calibration # 6

. SCAMPS

- 24 to 29 July **Pre-L48**: with **MOBY210**
- 10 to 12 August **Pos-L48**: with **MOBY209**
- 11 September **Pos-L48**: with **MOS205**
- 17 August to 09 September **Pre-MOCE-5**: with **MOS202**, **SIS 101**
- 10 November **Pos-MOCE-5**: with **SIS 101**
- 11 to 13 November **Pre-L51**: with **MOS205**, **DWAIN**, **MOBY211**, **SIS101**
- 24 to 25 November **Pos-L51**: with **MOBY210**, **SIS101**
- 29 November: sent to NIST for re-calibration

. SIS 101

- 17 to 18 August **Pre-MOCE-5**: RS 10 stability, Es
- 29 September **Pre-MOCE-5**: RS 10 stability aboard RN Melville
- 21 October **Pos-MOCE-5**: RS 10 stability aboard RN Melville
- 10 November **Pos-MOCE-5**: RS 10 stability, Es
- 13 November **Pre-L5 1**: Es
- 25 November **Pos-L5 1**: Es

• MOS20 1

- 10 September **Pre-MOCE-5**: re-assembled and tested as backup during **MOCE-5**

• MOS202

- 03 September Cfg07: red CCD # 5 replaced with #7, red shutter replaced
- 08 to 10 September **Pre-MOCE-5**: Ed, Lu, Wavelength, Integration Time
- 30 September **Pre-MOCE-5**: RS 10 stability aboard RN Melville
- 02 October **MOCE-5**: **LEDs**
- 22 October **Pos-MOCE-5**: RS 10 stability aboard RN Melville

• MOS204

- 20 July **Pre-L48**: installed in **MOBY210**
- 27 July Cfg03: blue shutter replaced
- 28 July **Pre-L48**: Lu, Bin Factor
- 29 July to 18 November deployed in **MOBY2 10**
- 2 1 December **Pos-L5 1**: Lu, Wavelength, Integration Time

- MOS205

01 May to 31 July deployed in MOBY209

11 September **Pos-L48**: Lu, Wavelength, Integration Time

10 November **Cfg05**: CCD heads pumped, dual D/A board solder joints modified

11 November **Pre-L5 1**: Lu, Wavelength, Integration Time, Bin Factor

15 November deployed in **MOBY2 11**

- MOBY209

30 July **L48**: cross-over profiles with **MOBY210**

31 July **L48**: recovered via RN Ka'imikai-0-Kanaloa

10 to 12 August **Pos-L48**: Ed, Lu Top,Mid,Bot

- MOBY210

24 to 29 July **Pre-L48**:Ed, Lu Top,Mid,Bot

29 July **L48**: deployed via R/V Ka'imikai-0-Kanaloa

30 July **L48**: cross-over profiles with MOBY209

31 July **L48**: diver calibrations via HRA

05 September **L49**: inspection and cleaning via HRA

10 October **L50**: inspection and cleaning via HRA

16 to 17 November **L5 1**:cross-over profiles with MOBY2 11, SIS 101, Satlantic

18 November **L5 1**: recovered via RN Ka'imikai-0-Kanaloa

24 to 25 November **Pos-L5 1**: Ed, Lu Top,Mid,Bot

- MOBY211

12 to 14 November **Pre-L5 1**: Ed, Lu Top,Mid,Bot

15 November **L5 1**: deployed via R/V Ka'imikai-0-Kanaloa

16 November **L5 1**: cross-over profiles with MOBY2 10, SIS 10 1, Satlantic

16 November **L5 1**: diver calibrations via HRA

17 November **L5 1**: cross-over profiles with MOBY210, SIS 101, Satlantic

17 November **L5 1**:diver calibrations via HRA

16 December **L52**: "dirty" diver calibrations via HRA, broken top arm removed

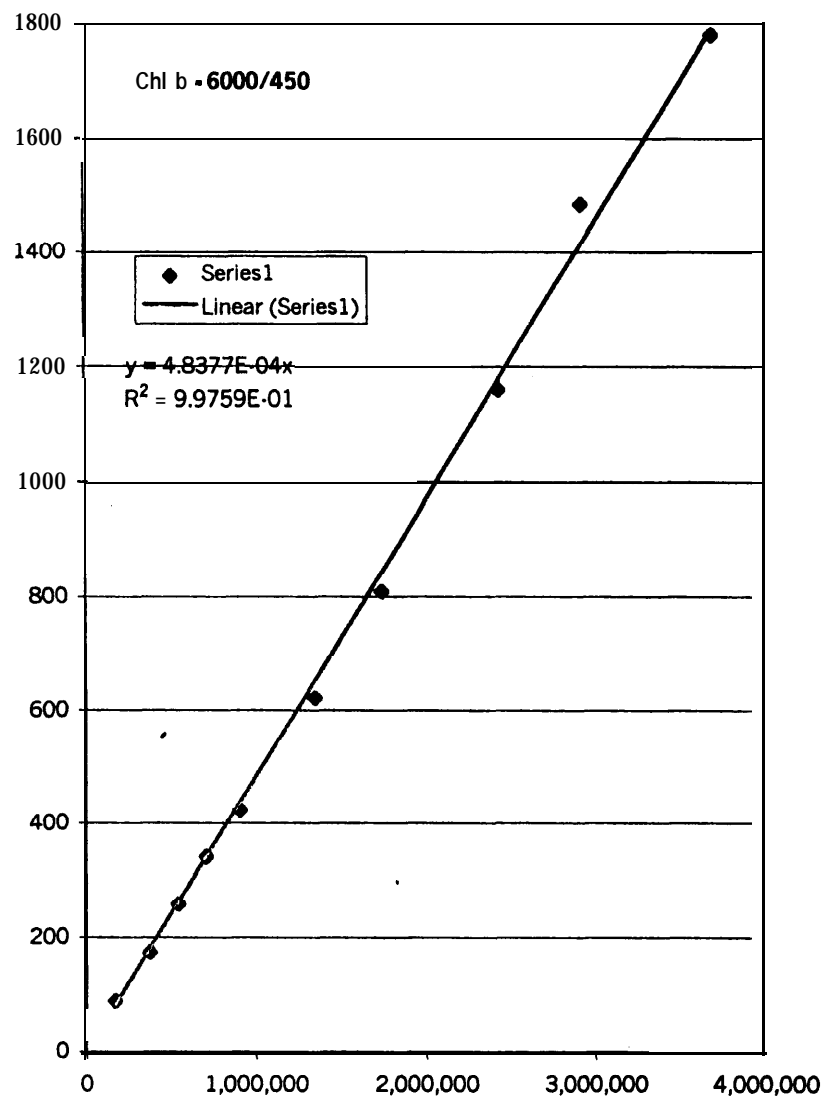
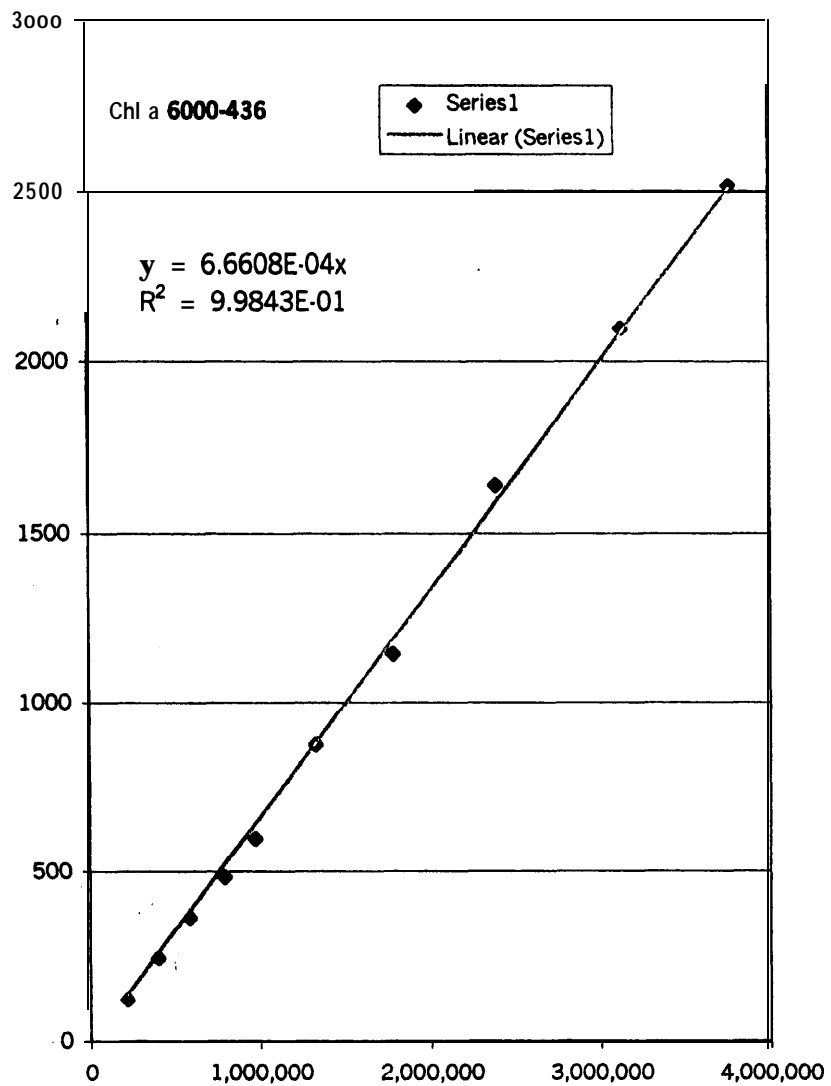
17 December **L52**: collector cleaning, "clean" diver calibrations via HRA

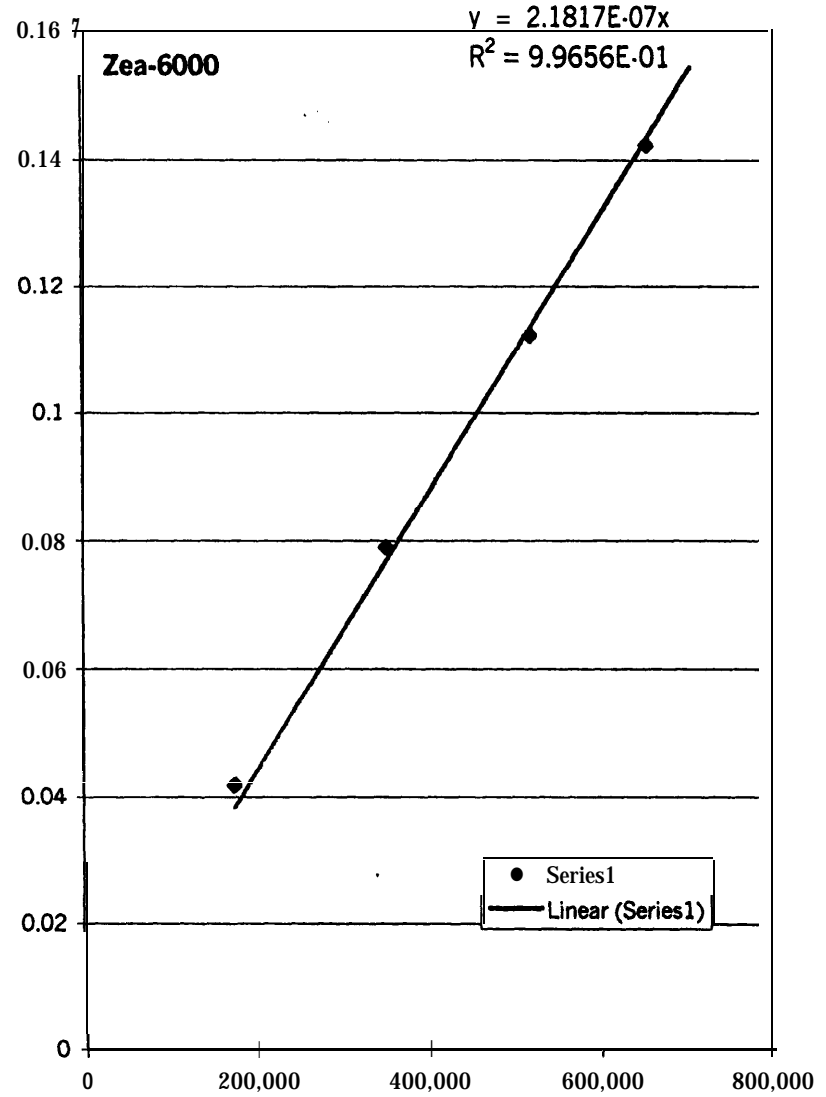
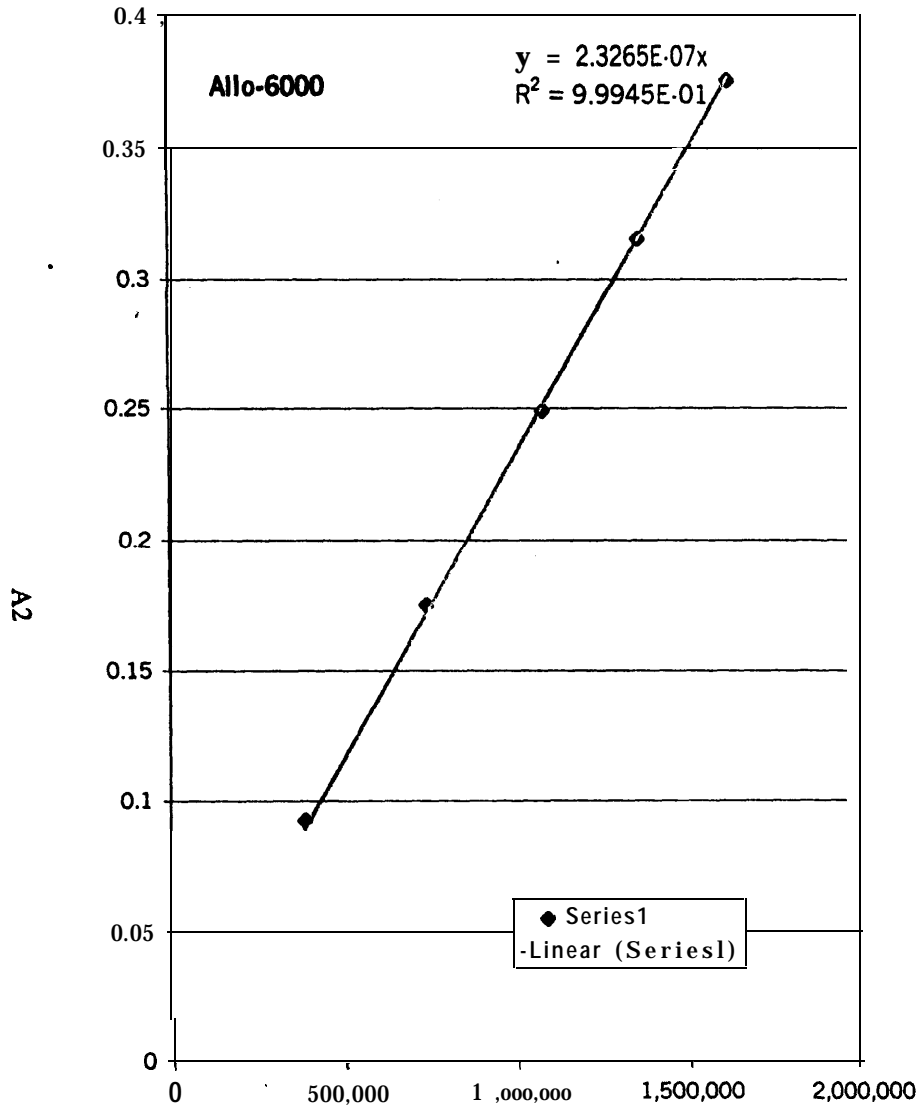
APPENDIX 5

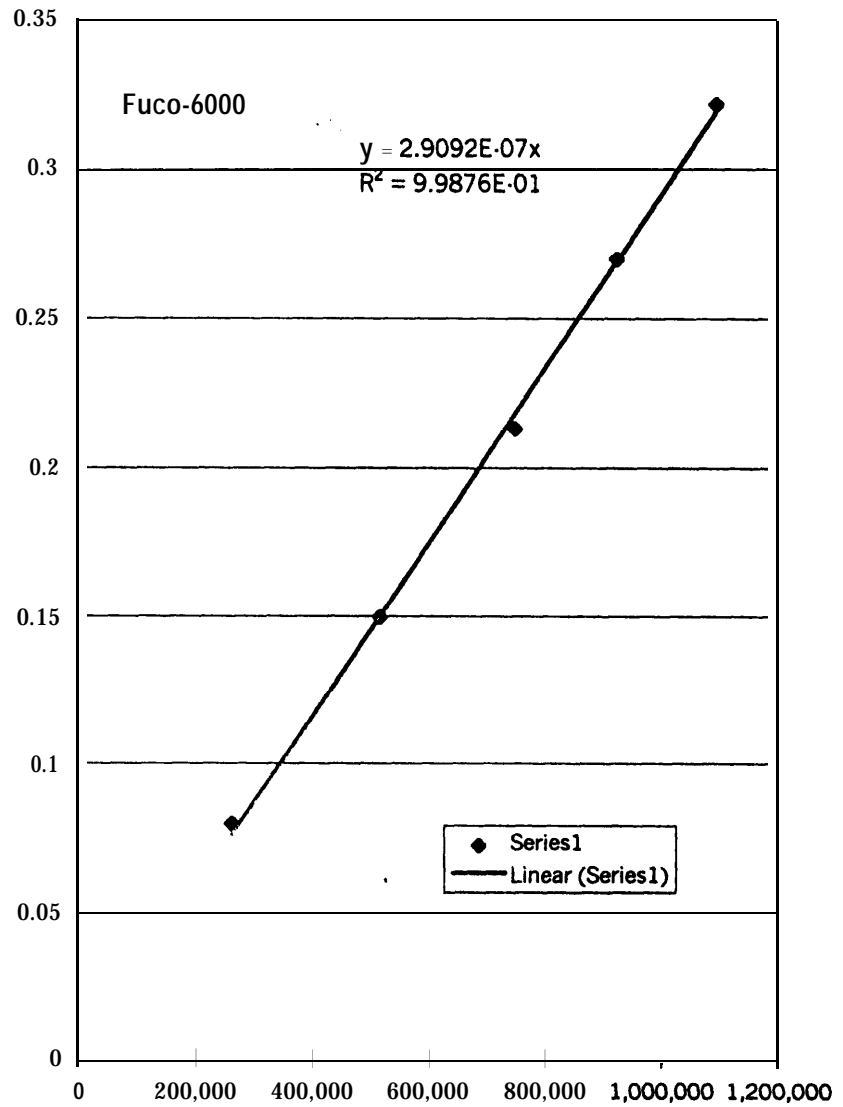
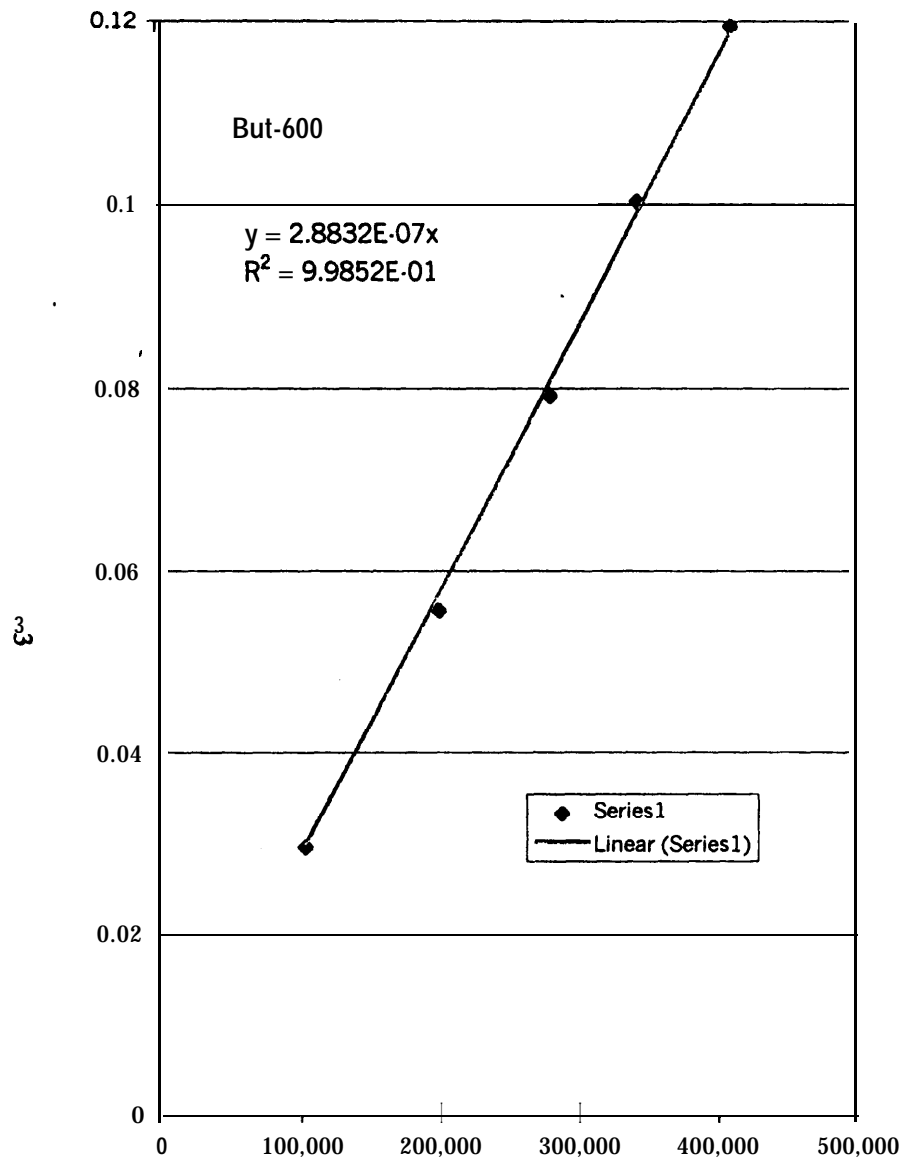
HPLC Calibration Curves for Pigment Standards

/

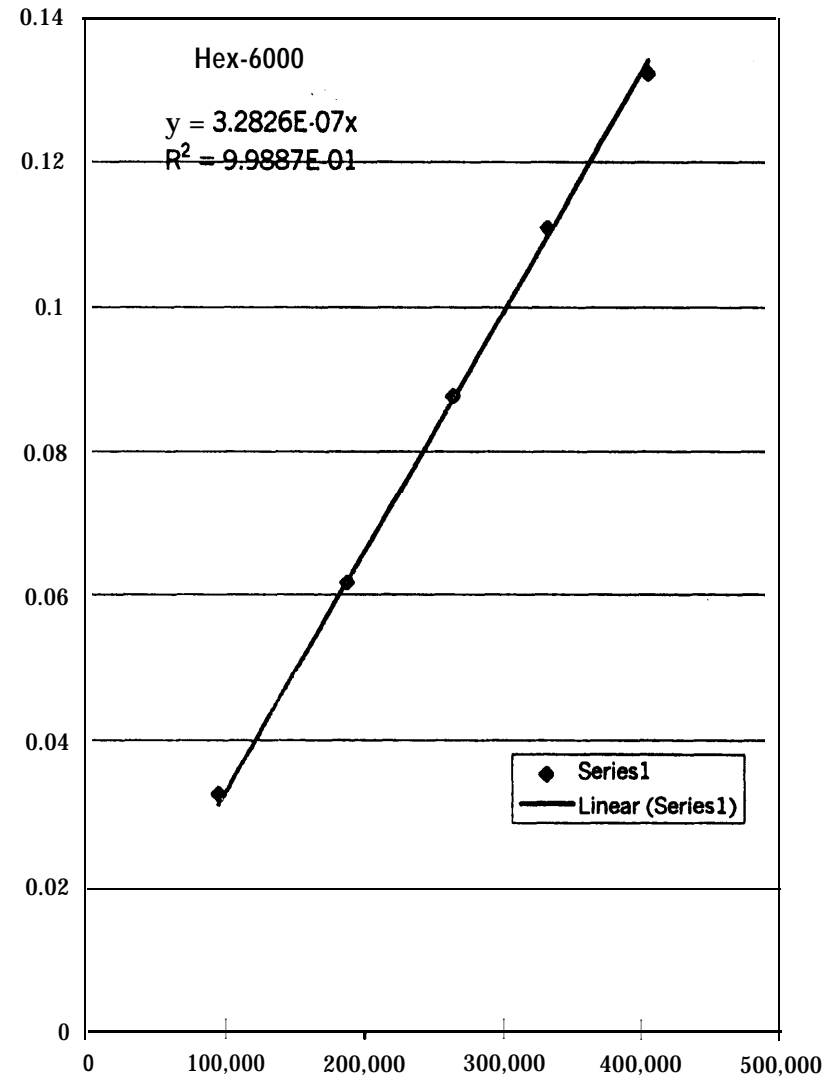
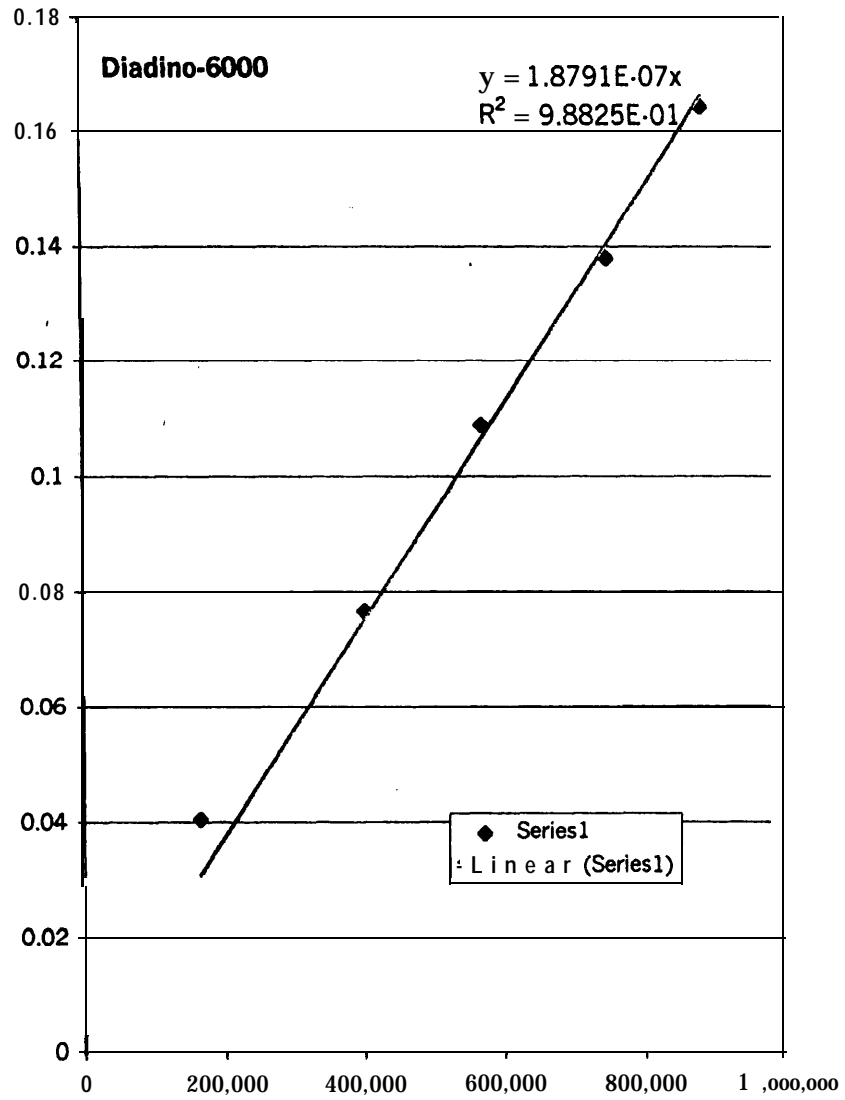
AI



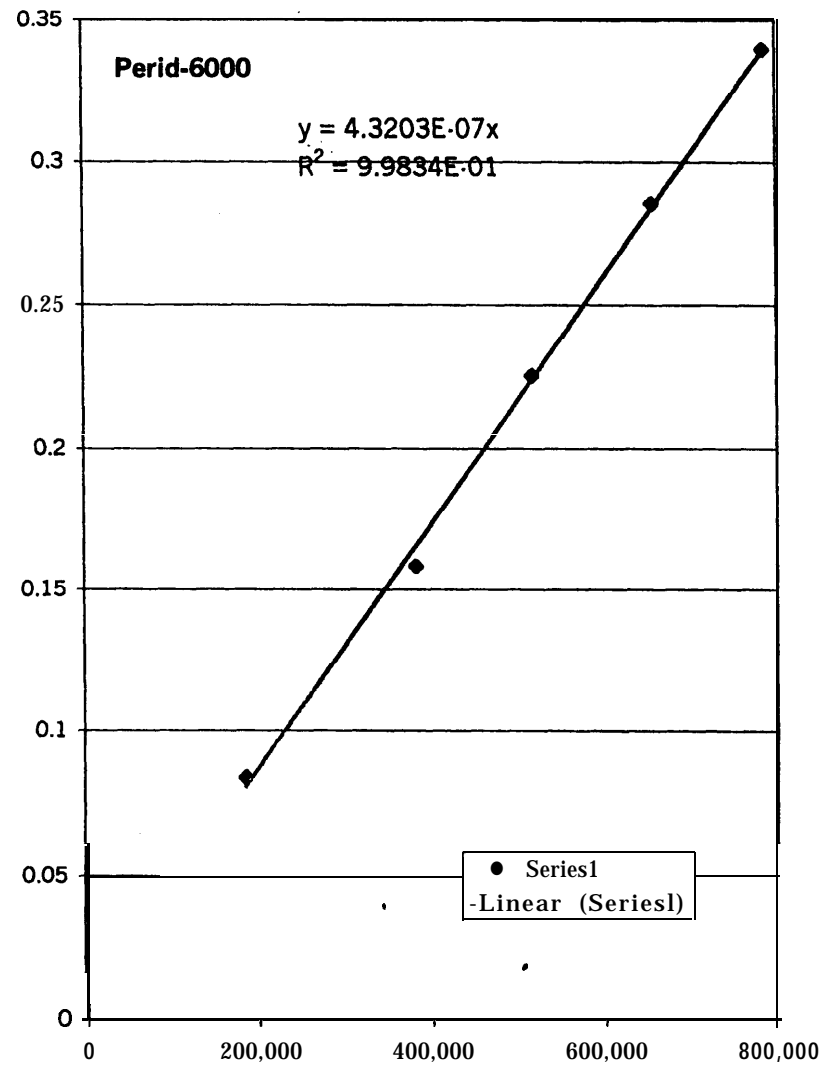
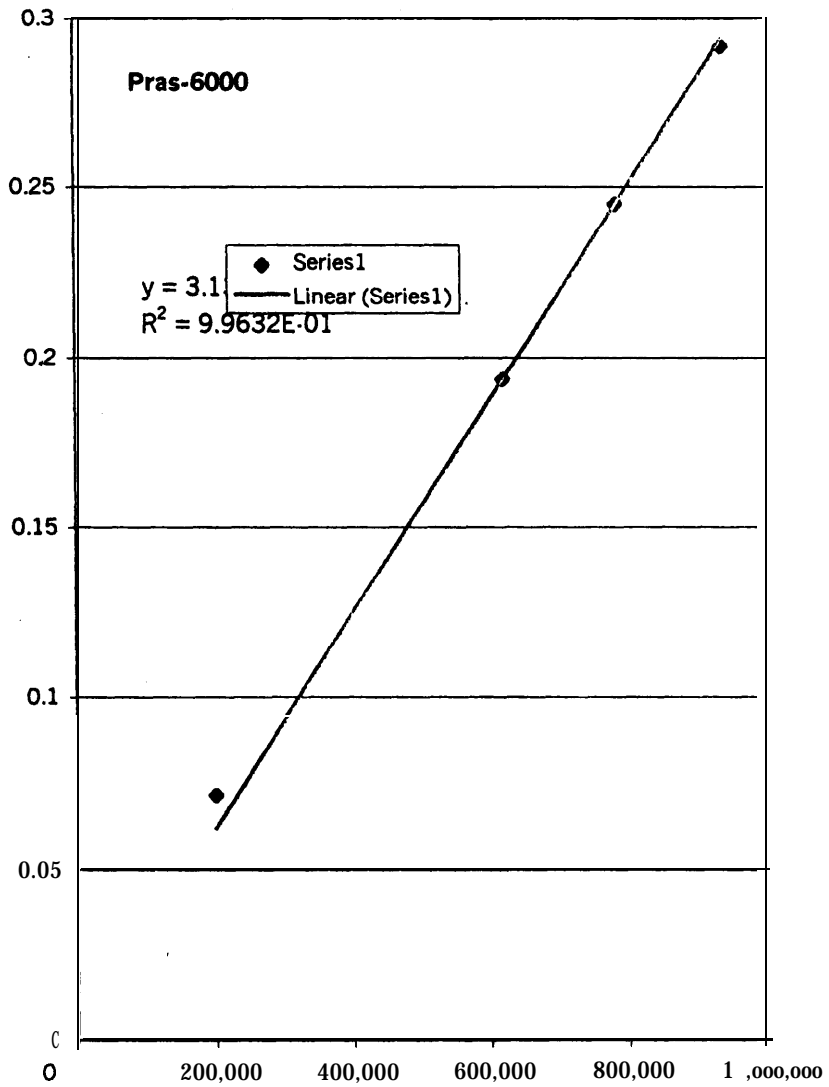


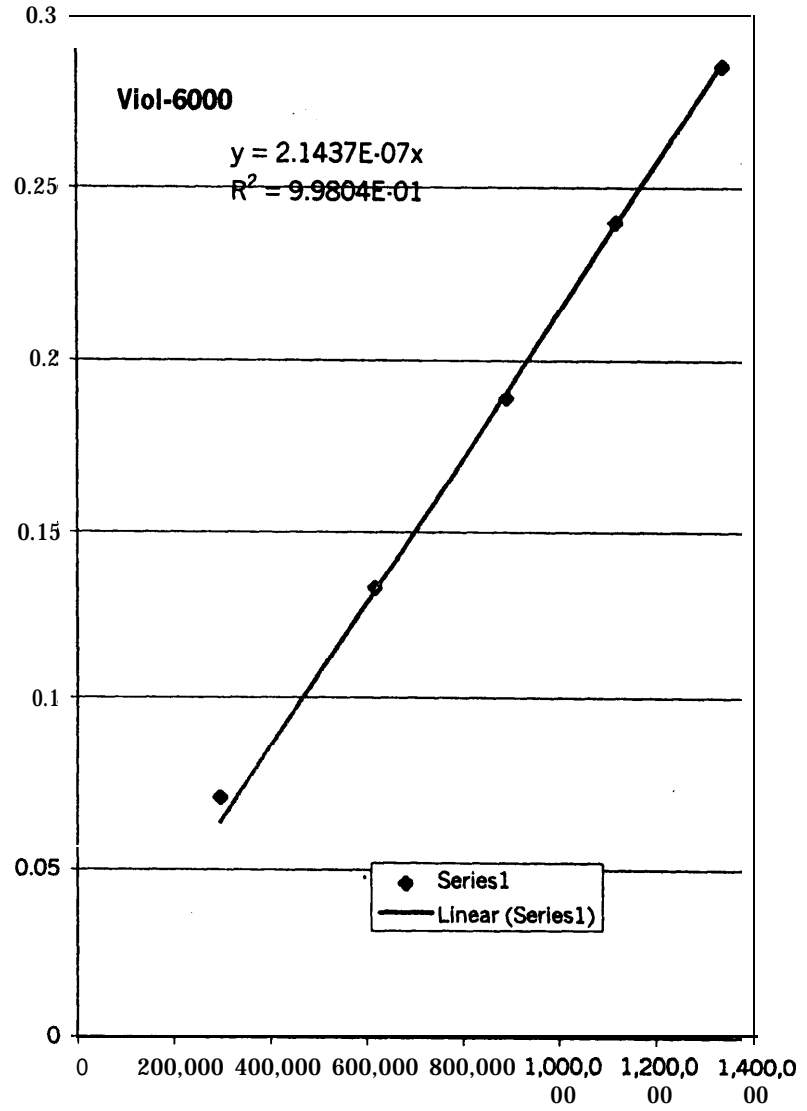
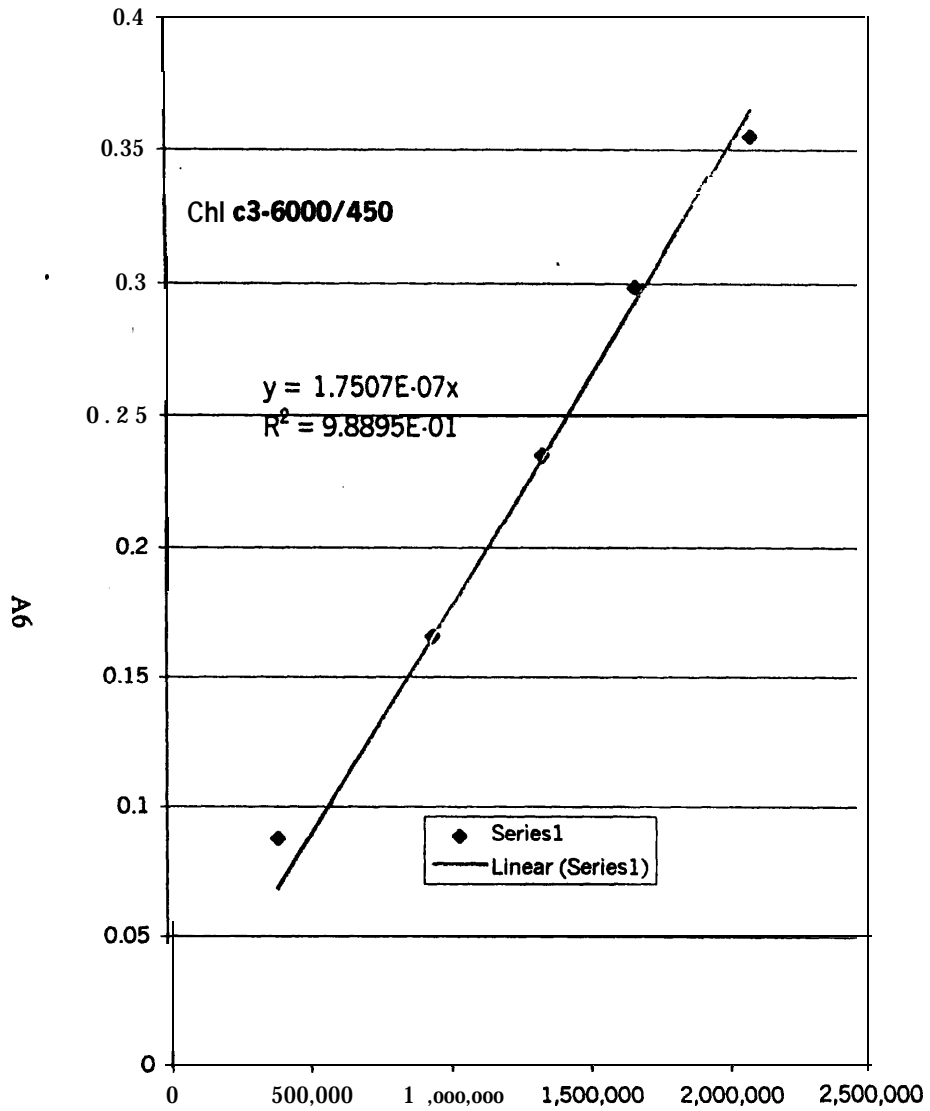


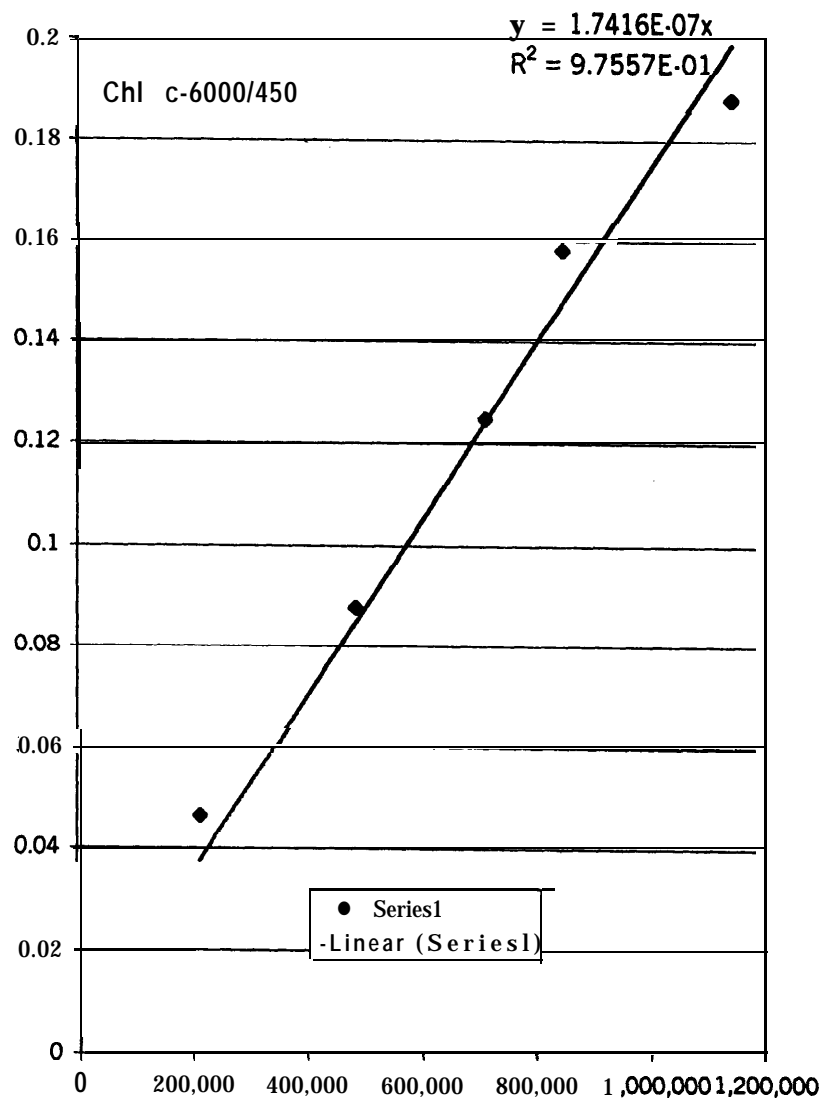
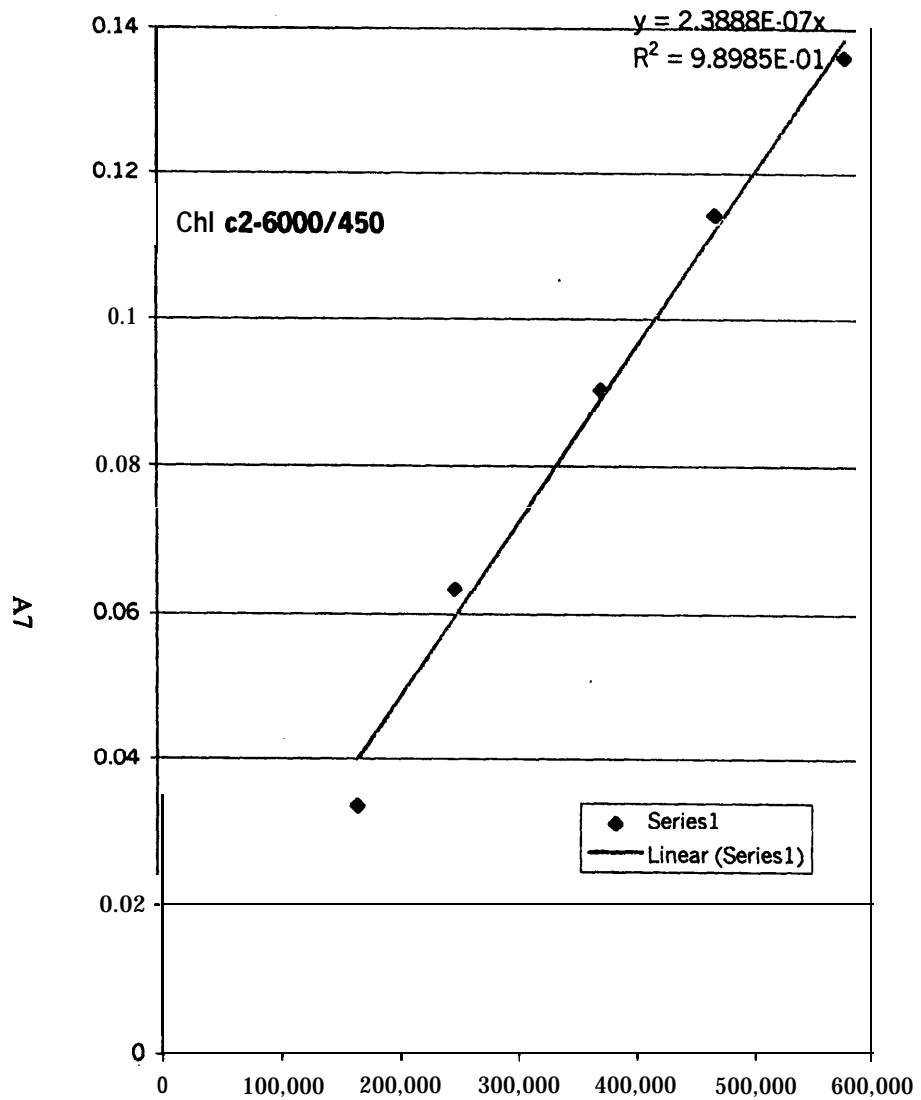
A4

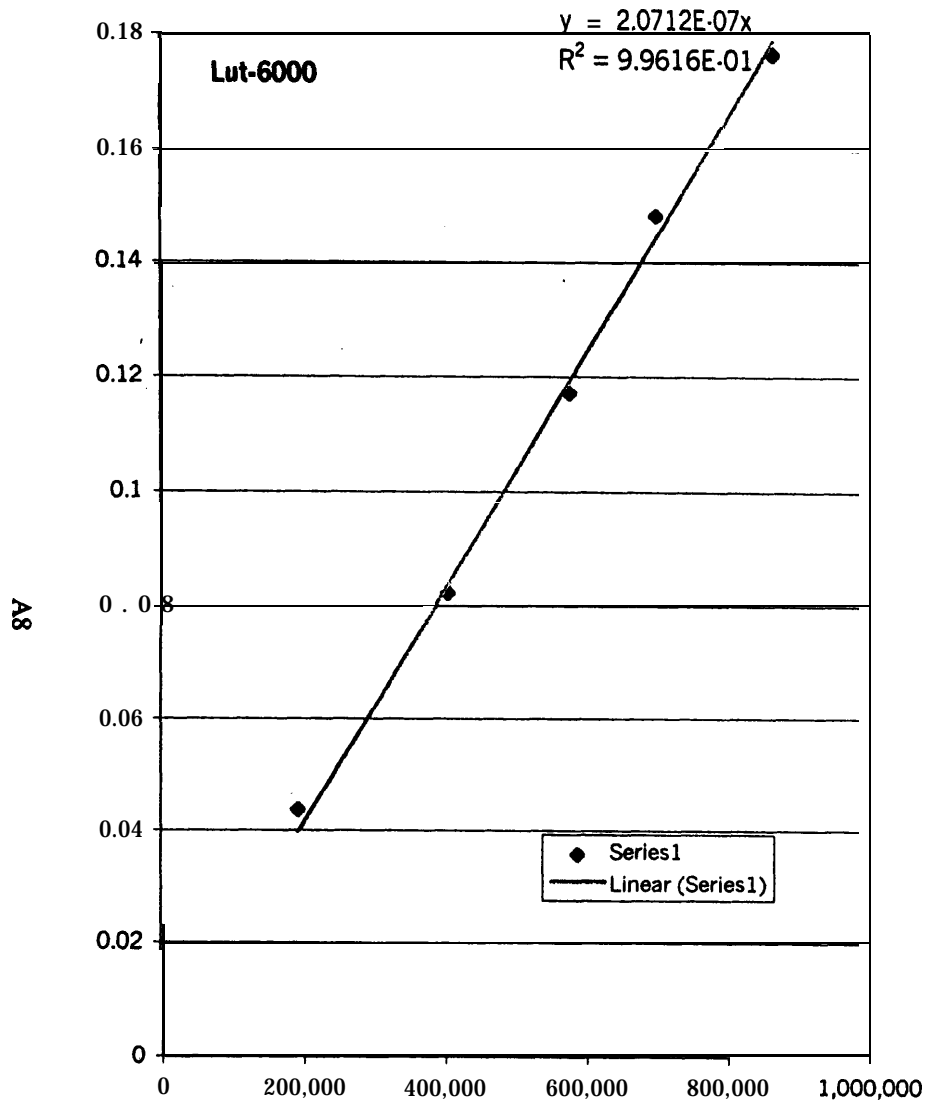


AS









APPENDIX 6

Chlorophyll *a* versus accessory pigment concentrations within the euphotic zone: A ubiquitous relationship?

Charles C. Trees

Center for Hydro-Optics and Remote Sensing, San Diego State University, San Diego, CA 92 120

Dennis K. Clark

National Oceanic and Administration/National Environmental Satellite Data and Information Service, Camp Springs, MD 20746

Robert R. Bidigare and Michael E. Ondrusek¹

Department of Oceanography, University of Hawaii, Honolulu, HI 96822

¹Present address: National Oceanic and Administration/National Environmental Satellite Data and Information Service, Camp Springs, MD 20746

ABSTRACT

Remote sensing of chlorophyll *a* has proven to be a powerful tool in assessing phytoplankton population dynamics, modeling primary production and global carbon budgets. Quantification of chlorophyll *a* is primarily based on *in situ* absorption and scattering properties of phytoplankton cells, that are strongly influenced by chlorophyll *a*, as well as accessory pigments (chlorophylls *b* and *c* and carotenoids). Specifically, remotely sensed chlorophyll *a* concentrations are determined by the ratio of upwelled radiances within the Soret band of chlorophyll *a* (443 nm) and at 550 nm. Absorption at wavelengths outside the Soret band (>460 nm) is dominated by accessory pigments and for the successful measurement of chlorophyll *a* (e.g. 520:550) early Coastal Zone Color Scanner (CZCS) investigators speculated that these accessory pigments must co-vary with chlorophyll *a*, although a routine method to measure these pigments had not yet been developed. Nearly 7,000 HPLC pigment samples were measured since 1985 to test the consistency of the relationship between accessory pigments and chlorophyll *a*. Despite the various sampling periods and numerous geographic locations, consistent patterns have emerged in the ratios of accessory pigments:TCHLA (chlorophyll *a* allomer, chlorophyll *a* epimer and chlorophyllide *a*). There were strong linear relationships within cruises for these ratios with an average r^2 of 0.946. An even more impressive relationship was observed on a global scale when all the data were combined. Despite a wide range of environments sampled, the over all slope of accessory pigments:TCHLA was found to be 1 with an r^2 of 0.963. This explains the success in remotely sensing chlorophyll *a* concentrations on a global scale, even though phytoplankton populations vary in composition and photoadaptive states.

Marine phytoplankton utilize chlorophyll *a* as their major light harvesting pigment for photosynthesis. **Other** pigment compounds such as chlorophylls *b* and *c*, carotenoids and cryptomonad phycobiliproteins, termed accessory pigments [cyanobacteria phycobiliproteins are not accessory pigments, but are their major light harvesting pigments (Johnson and Sieburth, 1979 and Waterbury et *al.* 1979)], also play a significant role in photosynthesis by **extending** the organism's optical collection window, thereby improving absorption efficiencies and adaptation capabilities. The unique optical properties of chlorophyll *a* have been used to develop spectrophotometric (Jeffrey and Humphrey, 1975) and fluorometric (Holm-Hansen et al., 1965) measurement techniques. With the commercial availability of fluorometers for routine measurements of chlorophyll *a*, this single pigment compound became a universal parameter in biological oceanography for estimating phytoplankton biomass and productivity.

Absorption properties of chlorophyll *a*, especially in the **Soret** band with its *in vivo* maximum near 440 nm, were found to be a major factor contributing to ocean color. This led to the development of remote sensing techniques, which culminated with the successful measurement of ocean color from space using the Coastal Zone Color Scanner (CZCS; Hovis et *al.*, 1980). Empirical relationships were developed relating water-leaving radiance ratios at four wavelengths (**443:550 nm**, **520:550 nm** and **520:670 nm**; Clark, 1981 and Gordon et *al.*, 1983) and diffuse attenuation **coefficients** at two wavelengths (490 nm and 520 **nm**, Austin and Petzold, 1981) to chloropigments (chlorophyll *a* plus phaeopigments as determined by the fluorometric method). Although most of these relationships were at wavelengths outside the **Soret** band of chlorophyll *a* and did not include accessory pigments, they were still able to account for most of the variance ($r^2 > 0.90$) in chloropigment concentrations. Based on these results, it was assumed that the absorption contributed by accessory pigments must be small, or highly covariant with chlorophyll *a*.

It was only towards the end of the life of the CZCS that new methods were developed (e.g. Mantoura and **Llewellyn, 1983**), using high performance liquid chromatography (HPLC), to measure phytoplankton pigment concentrations. The application of HPLC to phytoplankton pigment analysis has lowered the uncertainty for measuring chlorophyll *a* and phaeopigments, as well as, the accessory pigments, since compounds are physically separated and individually quantified. HPLC has provided oceanographers with a powerful tool for studying the processes affecting the phytoplankton pigment pool. HPLC methods have revealed that divinyl chlorophylls *a* and *b* are only present in prochlorophytes (Goericke and **Repeta, 1992**), the photoprotective carotenoid pool is dynamic in nature (Bidigare et *al.*, **1987**), phaeopigments (fluorometrically determined) are overestimated in the presence of

chlorophyll *b* (Vemet and Lorenzen, **1987**), and the uncertainty in fluorometrically determined chlorophyll *a* concentration is variable in space and time (Trees et *al.*, 1985; Smith et al., 1987; Hoepffner and **Sathyendranath**, 1992; Bianchi et *al.*, 1995; Tester et *al.*, **1995**).

Laboratory and field studies have shown that the concentration ratios of individual accessory pigments to chlorophyll *a* can vary as a function of taxonomic composition and physiological state, as modulated by nutrients, temperature, light intensity and spectral composition, and photoperiod (Bidigare et *al.*, 1990; Millie et al., 1993; Morel et *al.*, 1993; Bricaud et *al.*, 1995;. **Rucker et al.**, 1995; etc). Bidigare et *al.* (1987) collected samples in the Sargasso Sea and showed that non-photosynthetic carotenoids comprised a highly dynamic pigment pool. During a drift station for sunny and overcast days (5 and 7 April **1985**), the photosynthetic carotenoid:chlorophyll *a* ratios were found to be relatively constant with respect to depth and irradiance, where as the photoprotective carotenoid:chlorophyll *a* ratios varied by a factor of 3.2 in the upper 15 meters. This showed that, besides individual accessory pigments, select groups of pigment compounds can also have a high degree of variability, relative to chlorophyll *a*. Accessory pigments have also been used as diagnostic markers for specific phytoplankton groups, such as peridinin for dinoflagellates, chlorophyll *b* for green algae, zeaxanthin for cyanobacteria, fucoxanthin for diatoms, etc. (**Mackey et al.**, **1996**), indicating changes both horizontally and vertically in phytoplankton community structure.

In preparation for a new generation of ocean color sensors (**SeaWiFS** and MODIS), advanced technology has been used to develop new bio-optical instrumentation. These developmental efforts were undertaken to reduce the uncertainties in bio-optical algorithms that generate satellite derived products. As a result of this effort, NASA has adopted the U.S. JGOFS recommendation that HPLC is the preferred method for measuring phytoplankton pigments and should be used for ocean color pigment product development and validation (Mueller and Austin, 1995).

We have assembled an extensive HPLC pigment database in order to gain a better understanding of the variability in the phytoplankton pigment pool. This data extends over a decade of sampling and analyses, and includes a variety of environments ranging from freshwater to marine, oligotrophic to eutrophic, and tropical to polar. The central purpose of this study and the question we address herein is, “What is the concentration of accessory pigments relative to chlorophyll *a* and are these accessory pigments varying individually or in concert with chlorophyll *a*, as hypothesized from results inferred from remote sensing applications?”

METHODS

Study sites---From 1985 to 1995, we participated in 31 cruises and deployments collecting samples for **HPLC** analysis. An additional cruise (**MOCE 4**) in 1998 was added to this data base, since this was a major **SeaWiFS** calibration and validation effort. These 32 cruises and deployments are listed in Table 1 by cruise, date, geographical area and average sampling depth. A total of 6,985 samples were collected and analyzed in two different laboratories (C. Trees at San Diego State University and R. Bidigare at University of Hawaii) using a variety of instruments and methods as HPLC methodology evolved over the decade in study.

Sampling---Nominally, samples were collected in Niskin or polycarbonate bottles and filtered through either 0.4 μm polyester Nuclepore filters or 0.7 μm **GF/F** glass fiber filters. The volumes ranged **from** 0.125 liters for turbid waters and up to 2.2 liters for oceanic areas. Samples were analyzed on the ship or stored in liquid nitrogen for ashore laboratory analysis. The filtered samples were extracted in either 90% acetone or a 40:60 mixture of **DMSO:90%** acetone for 24 to 48 hours, following sonication in some cases. Nuclepore filters and **DMSO** extractions were limited to the early cruises before JGOFS pigment protocols were developed and adopted.

Pigment concentrations--The following published methods were used for the HPLC analyses: Mantoura and Llewellyn (**1983**), Hooks et *al.* (**1988**), Bidigare et *al.* (**1989**), Wright *et al.* (1991) and Goericke and **Repeta** (1993). During this period the following columns and flow rates were used to separate the pigment compounds: a **Radial-Pak C18** column (0.8 x 10 cm; 5 or 10 μm particle size, Waters Associates) at a flow rate of 6 or 10 ml min^{-1} , a Spherisorb ODS-2 stainless steel column (0.046 x 25 cm; 5 μm particle size, **Alltech** Associates) and a C8 column (10 cm; 3 μm particle size), both at a flow rate of 1 ml min^{-1} . To facilitate separation of the dephytolated pigments, all methods used an ion-pairing solution (Mantoura and Llewellyn, 1983) or distilled water (Wright et *al.*, **1991**), which was mixed with the sample immediately prior to the injection on the column. Techniques for injecting the samples have progressed from manual 'hand injections' to autosampler injections, which are temperature controlled with automated sample preparation and mixing.

A number of absorption and fluorescence detectors were used to identify **and** quantify the various pigment compounds as they were eluted off the columns. These detectors included a Waters Associates (Model 440) Absorbance Detector (436 nm), and progressed through a Waters Associates (Model **420-AC**) Fluorometer (**Ex** 400-460 nm, **Em** > 600 nm), a **Kratos** (Model FS950) Fluorometer (**Ex** 400-460 nm, **Em** > 600 nm), a **Thermo**

Separations Products (Model **UV2000**) Dual Wavelength UVMS Programmable Absorbance Detector (436 and 450 nm), and a Linear Model LC 304 **Fluorometer** (**Ex** 404 nm, **Em** 680 nm). The fluorescence detectors were primarily used to assist in the identification and quantification of phaeopigments, which typically occur in **low** concentrations.

Peak identifications and purity were confirmed 'on-line' using either a Hewlett Packard (Model 845 **1A**) Diode Array Spectrophotometer, or a **Thermo** Separations Products (Model **SpectraFOCUS**) 32 Channel Forward Optical Scanning Detector. Measurements of spectral absorbance were important, since the HPLC methods employed prior to 1996 did not separate zeaxanthin from **lutein** or monovinyl chlorophylls **a** and **b** from divinyl chlorophylls **a** and **b**. **In** most of the samples it has been assumed that the **zeaxanthin/lutein** peak is dominated by zeaxanthin, as inferred **from** the absorbance spectra and published data.

For the divinyl chlorophylls **a** and **b**, which are found in prochlorophytes, it has only been recognized in the past few years that they can contribute significantly to phytoplankton biomass (Goericke and **Repeta**, 1993). The separation of these compounds requires calibration procedures and pigment standards, which account for the **divinyl** forms. Since most of the cruises and analyses in this data base were performed prior to the development of these methodologies, divinyl chlorophylls **a** and **b** *were* included in the concentration estimates for "chlorophylls" **a** and **b**.

Calibration standards were either obtained from Sigma Chemical Co., purified from cultures by thin-layer chromatography (Jeffrey, 198 **1**), or obtained from other sources listed in Latasa et *al.* (1996). Pigment standards were exchanged between the two laboratories on numerous occasions during this ten-year period to assure the generation of an internally consistent pigment data base. System calibrations were performed **using pigment** standards, which were injected onto the HPLC columns and peak areas calculated to generate individual standard response factors for each compound. Concentration of the standards was determined spectrophotometrically using published extinction coefficients (see Table 2, Latasa et *al.*, 1996).

Statistical analysis---**To** compare accessory pigments to chlorophyll **a**, Model I regressions were performed. Model I regressions were selected because accessory pigment concentrations were to be predicted from chlorophyll **a** concentrations [Model I regressions are appropriate for both predictions and determining functional relationships, where as Model II regressions should not be used to predict values of y given x, (page 543, Sokal and Rohlf, **1995**)].

RESULTS

Vertical sample distribution---The final HPLC pigment data base consisted of 6,580 measurements with samples limited to the euphotic zone (1% light level) at depths ranging from surface to as deep as **130** meters (5.8 % of the original 6,985 samples were excluded because of this depth criteria). Samples collected below the **euphotic** zone depth had abnormally high accessory pigment to chlorophyll *a* ratios, indicating a resistance, as compared to chlorophyll *a*, to degradation of accessory pigments as particles are removed from the euphotic zone. A histogram of the number of observations in one-meter depth bins is shown in Fig. 1. The data were skewed to near surface samples, since 23% of the data were collected in the upper 4 meters. Many of these near surface samples (40%) were collected from five cruises (TEW, Icecolors, BOFS, and MOCE 3 and **4**), using alongtrack sampling **from** the ships' scientific "sea chest". Also apparent in Fig. 1, is the increased numbers of samples at 10 meter intervals, a characteristic of following standard hydrocast depth intervals (e.g. SLC 86 and 87, BOFS, Optical Closure, **Solars** 17 and 19, and **EqPac** Spring and **EqPac** Fall).

Total chlorophyll *a*---Chlorophyll *a* derivatives, such as epimers and allomers, as well as chlorophyllide *a* were summed together to calculate total chlorophyll *a* concentrations (TCHLA). The average contribution to the chlorophyll *a* pool for these three pigment compounds was 0.7 %, 0.4 % and 2.6 %, respectively. Chlorophyllide *a* is the precursor molecule for chlorophyll *a*, as well as a degradation product of chlorophyll *a* in senescent cells. It can also be formed when the enzyme chlorophyllase is not inactivated during the solvent extraction process. Generally, chlorophyllide *a* is found in low concentrations (2-5% of chlorophyll *a*) in most pigment samples. Concentrations of this pigment exceeding 15 to 20% of the total chlorophyll *a* pool are regarded as a consequence associated with collection of chlorophyllase-containing senescent diatoms and the extraction process (Jeffrey and Hallegraeff, 1987; Latasa and Bidigare, 1998). High chlorophyllide *a* levels were detected in some samples collected during Biowatt 85, **TransPac 47N**, GSP, SLC 86 and 87, **Solars** 19, and MOCE 1 and 2 cruises.

Total chlorophyll *a* versus accessory pigments---TCHLA and accessory pigment concentrations and ratios for each cruise are shown in Table 2. All pigments including phaeopigments (**phaeophytin *a*** and phaeophorbide *a*), **carotenoids**, and chlorophylls *b* and *c*, were summed to get the total accessory pigment concentrations by weight. Phaeopigments were added to the accessory pigment pool, because these degradation compounds contribute to ocean color and affect the vertical distribution of spectral irradiance in the water column. The average contribution

of phaeophytin *a* and phaeophorbide *a* to TCHLA **was** only 0.2% (see Table 2). Accessory pigment concentrations generally exceeded TCHLA concentrations. Photosynthetic carotenoids (**PSC**; peridinin, **fucoxanthin**, 19' hexanoyloxyfucoxanthin, 19' butanoyloxyfucoxanthin, and prasinoxanthin) and photoprotective carotenoids (**PPC**; diadinoxanthin, alloxanthin, diatoxanthin, zeaxanthin, **a**, p-carotene, and violoxanthin) were also summed to examine regional differences. Photosynthetic carotenoids (**PSC**) to TCHLA ratios were about twice the ratio of **PPC** to **TCHLA**. Pigment concentrations were not converted to molar equivalents, because these conversions did not improve accessory pigment pool predictability.

Plots of accessory pigments versus TCHLA for each cruise are shown in Fig. 2, with slopes, intercepts, correlation coefficients (*r*) and numbers of observations. Within each cruise, the relationships are quite linear even though the samples represent different depths and water masses.

DISCUSSION

Selective transmission of light in the sea results in a wide range of variability in spectral irradiance in the water column. In response, phytoplankton have developed numerous accessory pigment systems, enabling them to utilize a number of habitats. By varying the mixture of accessory pigments, a phytoplankton population may change its overall absorption spectrum to better match the spectrum of light available in its habitat. This photoadaptive ability may give select phytoplankton groups competitive advantage in the various spectral environments encountered in the sea. Different accessory pigments have different physiological functions, yet the ratio of total accessory pigments to TCHLA is remarkably constant at a value of 1. This is shown in Fig. 3, which is a plot of the entire data set from 0 to 130 meters. This relationship did not change, or improve, if data were limited to the first optical depth (37% light level), the depth at which 90% of the remote sensed ocean color signal originates. The insert in Fig. 3 shows data plotted in log space, so that the scatter at low concentrations can be viewed. There is a slight downward curvature for the insert in Fig. 3 at TCHLA concentrations below 0.1 mg m^{-3} , which is attributed to accessory **pigments being** present, but below detection limits at these low TCHLA concentrations.

In neritic waters, phytoplankton composition tends to shift towards larger organisms with different pigment signatures (Malone, 1980). During the **TransPac 24N** cruise (Ondrusek *et al.*, 1991), the dominant phytoplankton accessory pigment changed from zeaxanthin and chlorophyll *b* in the stratified open-ocean waters to fucoxanthin

and **19'-hexanoyloxy-fucoanthin** in the upwelling regions off the coast of California, indicating a shift from cyanobacteria dominated waters offshore to diatoms and prymnesiophytes near shore. Barlow *et al.* (1999) found a similar distributional pattern in the Arabian Sea in that inshore fucoxanthin and **19'-hexanoyloxy-fucoanthin** were the dominated pigments, whereas offshore in the oligotrophic areas zeaxanthin became important, indicating a shift to **cyanobacteria** (*Synechococcus* and *Prochlorococcus*). Most of the high TCHLA regions listed in Table 1 also have high fucoxanthin to TCHLA ratios.

Pigment ratios---The averages listed in Table 1 can be misleading, since they depend on the number of samples collected at each depth. The low TCHLA regions are mainly located in open ocean, oligotrophic waters and have high **zeaxanthin** to TCHLA ratios near the surface, and high chlorophyll *b* to TCHLA ratios at depth. A few sites, such as Mill Creek, have extremely high TCHLA concentrations and low fucoxanthin to TCHLA ratios. This is indicative of a phytoplankton bloom of a group other than diatoms. Despite the wide range of **TCHLA** concentrations and the variation in phytoplankton composition, however, the accessory pigment to **TCHLA** ratios remain fairly constant near a value of 1.

Differences in the ratios of certain accessory pigments to TCHLA shown in Table 2 can be used to infer changes in the phytoplankton community structure. For example, during the BOFS cruise off Iceland in 1991, samples were collected within a major coccolithophore bloom (Holligan *et al.*, 1993; Balch *et al.*, 1996). This cruise recorded the highest average ratio of **19'-hexanoyloxyfucoxanthin** to TCHLA (0.436). Other high latitude cruises such as SLC 86 and 87, and Icecolors measured similarly elevated ratios, indicating the presence of prymnesiophytes.

The linear regression plots in fig. 2 show that there are significant differences in the relationship between total accessory pigments and TCHLA as a function of cruises and deployments. Since these data cover a 13 year period, in which methods, instruments and pigment standards have been changed and improved, these differences may be methodological and not caused by photoadaptation of the pigment pools to changes in the ambient conditions. These relationships were very linear with little scatter within a cruise indicating that, again, the variability in slopes might be caused by cruise-specific methodological differences.

Statistical analysis of slope differences---Two approaches were used to examine the cause of these slope differences. One was to perform an error analysis on the data assuming interlaboratory uncertainties and the other

was to search for other pigment data, which were collected in the same geographic area over a relatively short period of time and processed by a single laboratory. An interlaboratory comparison was performed as part of the US JGOFS intercalibration exercise (Latasa *et al.*, 1996). Latasa *et al.* (1996) compared HPLC-pigment results between eight national and international laboratories using pigment standards and found that 90% of the chlorophyll **a** determinations and 85% of the pooled pigments fell within 20% of the interlaboratory medians. This equates to standard deviations of 0.12 and 0.14 for chlorophyll **a** and total accessory pigments, respectively. To estimate the uncertainty in the slopes when plotting total accessory pigments as a function of TCHLA, the quadrature sums were used in the form of

$$\text{Std. Dev. of the Slope} = \text{Sqrt} [0.12^2 + 0.14^2] = 0.184.$$

New 95% confidence limits were calculated for each cruise and are shown in Fig 4. Besides the 0.184 standard deviation of the slope, a lower value (0.092 = 0.18412) was also plotted in Fig. 4. Selection of a lower uncertainty value than that estimated by Latasa *et al.* (1996) could be justified, considering that only two laboratories performed the analyses and pigment standards were exchanged. On the other hand, this data compares HPLC pigment results spanning 13 years (1985-98) and uncertainties due to method changes over this time period could be as large as those found for eight laboratories which performed the intercomparison over a much smaller time interval. Applying an uncertainty value of 0.184, as determined by Latasa *et al.* (1996), 30 cruises were found to have statistically similar slopes (**94%**), where as using half of this value, 69% were still similar.

To investigate whether the differences between accessory pigments:TCHLA ratios are the result of changes in phytoplankton community structure and photoadaptation of the pigment pool to surrounding environmental conditions, pigment data sets were analyzed which met the following criteria: (1) collected from one geographic location, covering several seasons and (2) processed in a relatively short period of time, using the same method and analyst. Three pigment data bases were found; **EqPac** Spring and Fall Cruises (R. Bidigare and is part of this analysis), US JGOFS Arabian Sea Process Cruises 045,050 and 053 (R. Bidigare; Mar, Aug and Nov 1995) and Atlantic Meridional Transect Cruises 2 and 3 (C. Trees; Apr and Sep 96). All of these cruises, except for two of the Arabian Sea Cruises (045 and **050**), showed statistically different slopes at the 95% confidence level, but they were centered near 1.1. The first two Arabian Sea cruises had slopes of 1.4, possibly indicating the dynamic nature of the monsoon seasons. These results seem to indicate that the phytoplankton pigment pool does respond to ambient

conditions, although the changes are relatively small. Differences in slopes may be the result of the presence of *Synechococcus* in these waters and not including phycobiliproteins in the analysis.

"Photoadaptive effect"---The consistent linear relationship between accessory pigments and **TCHLA** could be termed a 'photoadaptive effect' in that as one pigment (or photoreceptor) or group of pigments decrease in the water column in response to the light field or environmental conditions, other others increase to fill in the void and visa versa [e.g. as photoprotective carotenoids decrease with depth, photosynthetic carotenoids increase (see Fig. 5, Bidigare et al., 1987), latitudinal changes in surface waters from high photosynthetic carotenoids in the polar regions to lower values towards the tropics (Aiken et al., 1995; Gibb et al. 1999), and an increase in chlorophyll *b* with depth as chlorophyll *c* decreases (Trees et al. 1986; Bidigare et al., 1990)]. This 'photoadaptive effect' is maintained throughout the water column as can be seen in Fig. 5, which is a log plot of accessory pigment:TCHLA ratios as a function of depth for the entire data set.

The energetic advantage of maintaining a relatively relative constant accessory pigment ratio can be rationalized in relation to the different functions of the accessory pigments (i.e. photosynthetic antennae vs. photoprotective). Composition of accessory pigments is controlled by a dynamic balance of energy, in which the cost of maintaining essential physiological functions are "balanced" against that of utilizing the energy for light capture and carbon assimilation. Ideally, the most efficient balance would be maintained. In high light, less energy is required for the light harvesting apparatus and more energy is required to protect the organism from too much light via energy dissipation (heat or fluorescence) or "screening". This is true for UV as well as visible light (Bidigare, 1989). Under light limiting conditions, more energy is required for capturing the low amount of available light . At depth, most of the available light occurs at wavelengths where absorption by chlorophyll *a* is small. Specific accessory pigments, such as chlorophyll *b*, enable deep living phytoplankton to capture enough light to drive photosynthesis. The present results suggest that for transitions between high and low light environments, a constant accessory pigment to TCHLA ratio near 1 may be optimal to maintain the most **efficient** energy trade-off between photosynthetic and photoprotective functions.

The photoadaptive strategy described about above is reflected between groups of organisms as well as within a group. Under oligotrophic conditions, near surface waters are dominated by photosynthetic prokaryotes, including *Synechococcus* and *Prochlorococcus* (Glover 1991). In *Synechococcus*, the main acetone extractable accessory

pigment is zeaxanthin, a photoprotective pigment. *Prochlorococcus* has zeaxanthin as a dominant accessory pigment, but also contains high concentrations of divinyl chlorophyll *b*, a photosynthetic antenna pigment (Jeffrey, 1997). Concentrations of *Synechococcus* decrease with depth while concentrations of *Prochlorococcus* are most abundant deep in stratified water columns (Chisholm et al., 1988; Li and Wood, 1988; Olson et al., 1990). Within the *Prochlorococcus* population, the ratio of chlorophyll *b* to zeaxanthin increases with depth where light becomes limiting (Moore et al., 1995). Below the compensation depth, the ratio of chlorophyll *b*:chlorophyll *a* becomes greater than unity and zeaxanthin drops below the limit of detection. This is an example of community pigment composition changing with ambient light levels as well as pigment ratios changing within a group (zeaxanthin:chlorophyll *b* in *Prochlorococcus*) in oligotrophic conditions. Under these conditions photoautotrophs are small and “pigment packaging” effects are small.

Another example of this ‘photoadaptive effect’ can be found in Bidigare et al. (1990) in which over a two week period, at the same location, a diatom bloom was replaced by a more diverse assemblage of prymnesiophytes, cyanobacteria, dinoflagellates, green algae and diatoms. Chlorophyll *a* decreased by a factor of two and the accessory pigment to chlorophyll *a* ratios for individual compounds showed significant changes (e.g. fuco:chlorophyll *a*, 0.64 to 0.23; chlorophyll *b*:chlorophyll *a*, 0.08 to 0.22 and hex:chlorophyll *a*, 0.11 to 0.38; see Table 1, Bidigare et al., 1990). These pigment data been included in our pigment data base as Biowatt 1985 (see Table 1). A comparison was made between accessory to TCHLA ratios for the bloom and post bloom conditions. It was found that there was no statistical significant difference in this ratio. This showed that even though the phytoplankton community changed drastically as far as the composition of the accessory pigments and that the euphotic zone deepened some 30%, the total accessory pigment concentration per TCHLA within the euphotic zone photoadapted to the ambient conditions.

Using data again from the Biowatt 1985 cruise, the relationship of accessory pigments to TCHLA between sunny and overcast days can be compared. Bidigare et al. (1987) showed that the ratios of photosynthetic carotenoids to chlorophyll *a* was relative constant throughout the water column, where as the ratios of photoprotective carotenoids to chlorophyll *a* exhibited large changes both vertically and temporally as a function of the incident solar flux. Plotting total accessory pigments as a function of TCHLA for these 11 pigment samples, a linear relationship was found with a slope of 0.865 and an $r^2 = 0.916$. Phytoplankton seem to be maintaining a

relative constant ratio of accessory pigments to TCHLA, even though they are cycling between photosynthetic and photoprotective carotenoids in response to irradiance fluctuations.

Effects of divinyl chlorophyll *a*---As stated previously, this pigment data base has not been corrected for the presence of divinyl chlorophyll *a* or *b* which can cause errors if not separated either physically on the column, or by a channels ratio method (Latasa *et al.*, 1996). Latasa *et al.* (1996) showed that the use of a single response factor (i.e. that determined only for monovinyl chlorophyll *a*) could result in a **15-25%** overestimation of total chlorophyll *a* concentration if divinyl chlorophyll *a* was present in significant concentrations (ratios from 0.2 to 0.4; divinyl chlorophyll *a*:total chlorophyll *a*). Elevated concentrations of divinyl chlorophyll *a* and *b* can be found in tropical and subtropical oceans where *Prochlorococcus* is found to be ubiquitous throughout the **euphotic** zone Goericke and Repetta, 1993; Goericke and Welschmeyer, 1993; Zubkov *et al.*, 1998; Gibb *et al.*, 1999). Therefore, some of the variability in the ratio of chlorophyll *a* to accessory pigments maybe attributed to the presence of divinyl chlorophyll *a*.

Phaeopigments---The ratios of chlorophyll *a* degradation products (phaeophytin *a* and phaeophorbide *a*) to TCHLA (chlorophyll *a* allomer, chlorophyll *a* epimer and chlorophyllide *a*) were generally low to below detection limits (ranging from 0.000 to 0.052 with a mean of 0.002; see Table 2). This average ratio is significantly lower than values measured using the standard fluorometric method. Smith and Baker (1978) and others have found **phaeopigment** concentrations to be approximately 25% of the total chlorophyll *a* concentration when using this technique. Even if chlorophyllide *a* concentrations are included in phaeopigment estimates, the average phaeopigment to chlorophyll *a* ratio is only 0.037. This low contribution of phaeopigments to the total chlorophyll *a* pool as measured by HPLC has also been found by Everitt *et al.*, (1990), Bricaud *et al.* (1995) and others and highlights on a global scale some of the problems associated with estimating phaeopigments using the standard fluorometric method.

CONCLUSIONS

It can be shown that variations in light intensity and quality, as well as nutrients, can change the ratio of accessory pigments:TCHLA in a given phytoplankton specie. Secondly, phytoplankton community structure and

hence pigment ratios adjust in response to changing environmental conditions. Yet, over a decade of data from environments ranging from freshwater to marine, oligotrophic to eutrophic, and tropical to polar show that **the ratio** of accessory **pigments:TCHLA** remains relatively constant (1). This is important for remote sensing purposes, since it provides the ability for estimating chlorophyll *a* and total accessory pigment concentrations at wavelengths **which** minimizes interferences caused by other in-water constituents (e.g. dissolved organic material absorption has little affect on pigment estimates from remotely sensed ocean color, if wavelengths above 470 nm are used) .

Linear relationships were found between accessory pigments and TCHLA concentrations within the euphotic zone for a variety of oceanic and freshwater environments. Claustre (1994), Tester *et al.* (1990) and Gieskes *et al.* (1988) also found linear relationships between chlorophyll *a* and selected accessory pigments, although they used multiple regression analyses and limited the data base to a single cruise. Many published articles have also shown this relationship, indirectly, in the form of tabulated accessory concentrations, which one can then be plotted as a function of chlorophyll *a* (e.g. Table 1, Hoepffner and Sathyendranath, 1992 and Table 2, **McManus *et al.*, 1992**). Statistically significant differences were found between cruises/areas and this variability may be a combination of methodological uncertainties, as well as natural changes occurring as phytoplankton assemblages adjust to differing light and nutrient conditions. On a basin to global scale, this relationship is still linear and provides a means for estimating the total pigment concentration **from** chlorophyll *a* within the euphotic zone. As mentioned previously, this pigment data base has not been corrected for errors caused by divinyl chlorophyll *a*, which, if present, would cause the slopes of these relationship to increase slightly. In addition, many of these relationships would likely change if phycobiliprotein concentrations were routinely measured and included in the analysis. The success of relating optical properties to chlorophyll *a* concentrations at wavelengths far removed from the chlorophyll *a* absorption maximum is based on the linear relationship of accessory pigments to TCHLA and the associated 'photoadaptive effect'.

REFERENCES

- Aiken, J., G.F. Moore, C.C. Trees, S.B. Hooker and D.K. Clark. 1995. The **SeaWiFS** CZCS-type pigment algorithm. *NASA Tech. Memo. 104566, Vol. 29*, S.B. Hooker and E.R. Firestone (eds.), NASA Goddard Space Flight Center, Greenbelt, MD, 34 pp.

- Austin, R.W. and T.J. Petzold. 1981. The determination of the diffuse attenuation coefficient of sea water using the Coastal Zone Color Scanner, pp. 239-256. **In** J.F.R. Gower [ed.], Oceanography from space. Plenum Press.
- Balch**, W.M., K.A. Kilpatrick, and C.C. Trees. 1996. The 1991 coccolithophore bloom in the central North Atlantic. 1. Optical properties and factors affecting their distribution. *Limnol. Oceanogr.* 41: 1669-1683.
- Barlow, R.G., R.F.C. Mantoura, and D.G. Cummings. 1999. Monsoonal influence on the distribution of phytoplankton pigments in the Arabian Sea. *Deep-Sea Res. II* 46: 677-699.
- Bianchi, T.S., C. **Lambert** and D.C. Biggs. 1995. Distribution of chlorophyll **a** and phaeopigments in the northwestern Gulf of Mexico: a comparison between fluorometric and high-performance liquid chromatography measurements. *Bull. Mar. Science* 56: 25-32.
- Bidigare, RR. 1989. Potential effects of W-B radiation on marine organisms of the Southern Ocean: distributions of phytoplankton and krill during austral spring. *Photochem. Photobiol.* **50**: 469-477.
- Bidigare, R.R., R.C. Smith, K.S. Baker, and J. Marra. 1987. Oceanic primary production estimates from measurements of spectral irradiance and pigment concentrations. *Global Biogeochem. Cycles* 1: 171-186.
- Bidigare, R.R., J. Marra, T.D. Dickey, R. Iturriaga, **K.S.** Baker, R.C. Smith, and H. Pak. 1990. Evidence for phytoplankton succession and chromatic adaptation in the Sargasso Sea during spring 1985. *Mar. Ecol. Prog. Ser.* 60: 113-122.
- Bidigare, R.R., O. Schofield, and B.B. Prezelin. 1989. Influence of zeaxanthin on quantum yield of photosynthesis of *Synechococcus* clone WH7803 (**DC2**). *Mar. Ecol. Prog. Ser.* 56: 177-188.
- Bricaud, A., M. Babin, A. Morel, and H. Claustre. 1995. Variability in the chlorophyll-specific absorption coefficients of natural phytoplankton: Analysis and **parameterization**. *J. Geophys. Res.*, 100: **13,321-13,332**.
- Chisholm, S.W., R.J. Olson, E.R. **Zettler**, R. Goericke, J.B. Waterbury, and N.A. Welschmeyer. 1988. A novel free-living prochlorophyte abundant in the oceanic **euphotic** zone. *Nature*, 334: **340-343**.
- Clark, D.K. 1981. Phytoplankton pigment algorithms for the Nimbus-7 **CZCS**, pp. 227-238. **In** J.F.R. Gower [ed.], Oceanography from space. Plenum Press.
- Claustre, H. 1994. The **trophic** status of various oceanic provinces as revealed by phytoplankton pigment signatures. *Limnol. Oceanogr.*, 39: **1206-1210**.

- Everitt, D.A., S.W. Wright, J.K. Volkman, D.P. Thomas, and E.J. Lindstrom. 1990. Phytoplankton community compositions in the western Pacific determined from chlorophyll and carotenoid pigment distributions. *Deep-Sea Res.* 37: 975-997.
- Gibb, S.W. R.G. Barlow, D.G. Cummings, N.W. Rees, C.C. Trees, P. Holligan, and D. Suggett. (1999). Surface phytoplankton pigment distributions in the Atlantic: an assessment of basin scale variability between **50°N** and **50°S**. *Mar. Ecol. Prog. Ser.* (accepted).
- Gieskes, W.W.C., G.W. Kraay, A. Nontji, D. Setiapermana, and Sutomo. 1988. Monsoonal alternation of a mixed and a layered structure in the phytoplankton of the **euphotic** zone of the **Banda** Sea (Indonesia): a mathematical analysis of algal pigment fingerprints. *Netherlands J. of Sea Res.*, 22: 123-137.
- Glover, H.E. 1991. Oceanic phytoplankton communities: our changing perception. *Rev. Aquatic Sci.* 5: 307-331.
- Goericke, R., and D.J. Repeta. 1992. The pigments of *Prochlorococcus marinum*: The presence of divinyl chlorophyll **a** and **b** in a marine prokaryote. *Limnol. Oceanogr.*, 37: 425-433.
- Goericke, R., and D.J. Repeta. 1993. Chlorophylls **a** and **b** and divinyl chlorophylls **a** and **b** in the open subtropical North Atlantic Ocean. *Mar. Ecol. Prog. Ser.* 101: 307-313
- Goericke, R., and N.A. Welschmeyer. 1993. The marine prochlorophyte *Prochlorococcus* contributes significantly to phytoplankton biomass and primary productivity in the Sargasso Sea. *Deep-Sea Res. A* 40: 2283-2294.
- Gordon, H.R., D.K. Clark, J.W. Brown, O.B. Brown, R.H. Evans, and W.W. Broenkow. 1983. Phytoplankton pigment concentrations in the Middle Atlantic Bight: comparison of ship determinations and CZCS estimates. *Appl. Opt.* 22: 20-36.
- Hoepffner, N., and S. Sathyendranath. 1992. Bio-optical characteristics of coastal waters: Absorption spectra of phytoplankton and pigment distribution in the western North Atlantic. *Limnol. Oceanogr.*, 37: 1660-1679.
- Holligan, P.M., E. Fernandez, J. Aiken, W.M. Balch, P. Boyd, P.H. Burkill, M. Finch, S.B. Groom, G. Malin, K. Muller, D.A. Purdie, C. Robinson, C.C. Trees, S.M. Turner, and P. van der Wal. 1993. A biogeochemical study of the **coccolithophore, *Emiliana huxleyi***, in the North Atlantic. *Global Biogeochemical Cycles*, 7: 879-900.
- Holm-Hansen, O., C.J. Lorenzen, R.W. Holmes, and J.D.H. Strickland. 1965. Fluorometric determination of chlorophyll. *J. Cons. perm. int. Explor. Mer.* 30: 3-15.

- Hooks, C.E., R.R. Bidigare, M.D. Keller, and R.L. Guillard. 1988. Coccoid eukaryotic marine **ultraplankters with** four different HPLC pigment signatures. *J. Phycol.* **24:57** 1-580.
- Hovis, W.A., D.K. Clark, F. Anderson, R.W. Austin, W.H. Wilson, E.T. Baker, D. Ball, H.R. Gordon, **J.L. Mueller**, S.Z. El-Sayed, B. Strum, R.C. Wrigley, and C.S. **Yentsch**. 1980. Nimbus-7 Coastal **Zone** Color Scanner: system description and initial imagery. *Science* 210: 60-63.
- Jeffrey, S.W. 1997. Application of pigment methods to oceanography, pp. 127-166. *In* J.W. Jeffrey, R.F.C. Mantoura and S.W. Wright [**eds.**], *Phytoplankton pigments in oceanography: guidelines to modern methods*, UNESCO Publishing.
- Jeffrey, S.W., and G.F. Humphrey. 1975. New spectrophotometric equations for determining chlorophylls **a**, **b**, **c**¹ and **c**² in higher plants, algae and natural populations. *Biochem Physiol. Pflanzen* 167: **191-194**.
- Jeffrey, S.W., and H.G. Hallegraeff. 1987. Chlorophyllase distribution in ten classes of phytoplankton: a problem for chlorophyll analysis. *Mar. Ecol. Prog. Ser.* 35: 293-304.
- Jeffrey, S.W. 1981. An improved thin-layer chromatographic technique for marine phytoplankton pigments. *Limnol. Oceanogr.* 16: 191-197.
- Johnson, P.W., and **J.McN.** Sieburth. 1979 Chroococcoid cyanobacteria in the sea: an ubiquitous and diverse phototrophic biomass. *Limnol. Oceanogr.* 24: 928-935.
- Latasa, M., and R.R. Bidigare. 1998. A comparison of phytoplankton populations of the Arabian Sea during the Spring Inter-monsoon and Southwest Monsoon of 1995 as described by HPLC-analyzed pigments. *Deep-Sea Res.* 45: 2133-2170.
- Latasa, M., R.R. Bidigare, M.E. Ondrusek, and M.C. Kennicutt. 1996. HPLC analysis of algal pigments: a comparison exercise among laboratories and recommendations for improved analytical performance. *Mar. Chem.* 5 1: 3 15-324.
- Li, W.K.W., and A.M. Wood. 1988. Vertical distribution of North Atlantic ultraphytoplankton: analysis by flow cytometry and epifluorescence microscopy. *Deep-Sea Res.* 35: 1615-1638.

- Mackey, M.D., D.J. Mackey, H.W. Higgins and S.W. Wright. 1996. **CHEMTAX** - a program for estimating class abundances from chemical markers: application to **HPLC** measurements of phytoplankton. Mar. **Ecol. Prog. Ser.** 144: 265-283.
- Malone, T.C. 1980. Algal size, pp. 433-464. *In* I. Morris [ed.], The physiological ecology of phytoplankton. University California Press.
- Mantoura**, R.F.C., and C.A. Llewellyn. 1983. The rapid determination of algal chlorophyll and carotenoid pigments and their breakdown products in liquid chromatography. *Analytica Chimica Acta.* 15 1: 297-314.
- McManus**, G.B., and M.C. Ederington-Cantrell. 1992. Phytoplankton pigments and growth rates, and **microzooplankton** grazing in a large temperate estuary. Mar. Ecol. Prog. Ser., 77: 77-85.
- Millie, D.F., H.W. Paerl, and J.P. Hurley. 1993. Microalgal pigment assessments using high-performance liquid chromatography: a synopsis of organismal and ecological applications. Can. J. Fish. Aquat. Sci. 50: 2513-2527.
- Moore, L.R., R. Goericke, and S.W. Chisholm. 1995. Comparative physiology of *Synechococcus* and *Prochlorococcus*: influence of light and temperature on growth, pigments, fluorescence and absorptive properties. Mar. Ecol. Prog. Ser. 116: 259-275.
- Morel, A., Y.-H. Ahn, F. Partensky, D. Vaulot, and H. Claustre. 1993. *Prochlorococcus* and *Synechococcus*: A comparative study of their optical properties in relation to their size and pigmentation. J. Mar. Res., 5 1: 617-649.
- Mueller, J.L., and R.W. Austin, 1995. Ocean optics protocols for **SeaWiFS** validation, revision 1. NASA TM 104566, **Vol 25**, NASA, GSFC, Greenbelt, MD.
- Olson, R.J., S.W. Chisholm, E.R. **Zettler**, M.A. Altabet, and J.A. **Dusenberry**, 1990. Spatial and temporal distributions of prochlorophyte picoplankton in the North Atlantic Ocean. **Deep-Sea Research**, 37: 1033-1051.
- Ondrusek, M.E., R.R. Bidigare, S.T. Sweet, D.A. **Defreitas**, and J.M. Brooks. 1991. Distribution of phytoplankton pigments in the North Pacific Ocean in relation to physical and optical variability. *Deep-Sea Res.*, 38: 243-266.

- Rucker**, J., J.-G. Kohl, and K Kaiser. 1995. Responses of carotenoids and chlorophylls to variations of **growth-** limiting factors in three filamentous blue-green algae. *Algological Studies*. 77: 51-65.
- Smith, R.C., and K.S. Baker. 1978. The bio-optical state of ocean waters and remote sensing. *Limnol. Oceanogr.* 23: 247-259.
- Smith, R.C., R.R. Bidigare, B.B. Prezelin, K.S. Baker, and J.M. Brooks. 1987. Optical characterization of primary productivity across a coastal front. *Mar. Biol.* 96: 575-591.
- Sokal, R.R. and F.J. Rohlf 1995. *Biometry, the principles and practice of statistics in biological research.* **W.H.** Freeman and Company.
- Tester, P.A., M.E. Geesey, C. Guo, H.W. Paerl, and D.F. Millie. 1995. Evaluating phytoplankton dynamics in the Newport River estuary (North Carolina, USA) by HPLC-derived pigment profiles. *Mar. Ecol. Prog. Ser.* 124: 237-245.
- Trees, C.C., M.C. Kennicutt, II and J.M. Brooks, 1985. Errors associated with the standard fluorometric determination of chlorophylls and phaeopigments. *Marine Chemistry*. 17: 1-12.
- Trees, C.C. R.R. Bidigare, and J.M. Brooks. 1986. Distribution of chlorophylls and phaeopigments in the Northwestern Atlantic Ocean. *J. Plk. Res.* 8: 447-458.
- Vemet, M., and C.J. Lorenzen., 1987. The presence of chlorophyll b and the estimation of phaeopigments in marine phytoplankton. *J. of Plank. Res.* 9: 255-265.
- Waterbury, J.B., SW. Watson, R.R. Guillard, and L.E. Brand. 1979. Widespread occurrence of a unicellular, marine, planktonic cyanobacterium. *Nature* **277:293-294.**
- Wright, S.W., S.W. Jeffrey, R.F.C. Mantoura, C.A. Llewellyn, T. Bjornland, D. **Repeta**, and N. Welschmeyer. 1991. An improved HPLC method for the analysis of chlorophylls and carotenoids from marine phytoplankton. *Mar. Ecol. Prog. Ser.* 77: 183-196.
- Zubkov, M.V., M.A. Sleigh, G.A. **Tarran**, P.H. Burkill, and R.J.G. **Leakey**. 1998. Picoplankton community structure on an Atlantic transect from **50°N** to **50°S**. *Deep-Sea Res. I*, 45: 1339-1355.

Acknowledgements. The collection and processing of these **HPLC** samples over the 14 year period were sponsored by numerous grants and contracts from NSF, NASA, DOE, ONR, NOAA and various Navy agencies. The authors are grateful for support for the synthesis of this data **from** NOAA under grant **NA77EC0131** (C. Trees), from **the** NASA Headquarters, Ocean Biology Program under grants NAGW-2154 (C. Trees) and **NAG5-7 17 1** (R. **Bidigare**), and from the NASA Goddard Space Flight Center, under contract S-19864 (D. Clark, the **EOS/MODIS** Project).

Figure Captions

Fig. 1. A histogram of the number of HPLC samples in 1-meter bins as a function of depth (m).

Fig. 2. Regression equations for accessory pigments (y) versus TCHLA (x; chlorophyll **a** allomer, chlorophyll **a** epimer and chlorophyllide a) by cruise/deployment, including slope, intercept, correlation coefficient (r) and number of samples (n).

Fig. 3. Regression equation for accessory pigments versus TCHLA (chlorophyll a allomer, chlorophyll a epimer and chlorophyllide a) for the entire HPLC pigment data base. This includes slope, intercept, correlation coefficient (r) and number of samples (n). The insert is a log log transformation-of the data to highlight the trend at lower concentrations.

Fig. 4. Mean slopes for accessory pigments:TCHLA by cruise (x). Included are the 95% confidence limits for standard deviations of the slope using 0.184 (wider errors bars) and 0.092, as calculated from the **interlaboratory** HPLC comparison of Latasa et al. (1996). The dashed line represents the average slope for the entire data base.

Fig. 5. A plot of accessory pigment:TCHLA ratios as a function of depth. The gray line represents the data base average.

Cruises	Date	Area	Ave Depth
Biowatt 85	Apr 85	Northwestern Atlantic	53.0
Transpacific 24N	Apr-May 85	North Pacific along 24 N	57.0
Transpacific 47N	Aug-Sep 85	North Pacific along 47N	49.0
SLC 86	Aug 86	Greenland, Norwegian and Barents Seas	28.0
Biowatt 87-1	Mar 87	sargasso sea	48.0
Biowatt 87-2	May 87	sargasso sea	59.0
GSP	May-Jun 87	Greenland Sea - Arctic and Polar Fronts	18.0
TEW	Jun-Jul87	Equatorial Pacific	54.0
SLC 87	Jul-Aug 87	Greenland, Norwegian & Iceland Seas	27.0
Biowatt 87-3	Aug 87	sargasso sea	65.0
AVIFUS	Oct 87	San Francisco Bay	0.7
Biowatt 874	Nov 87	sargasso sea	58.0
Solars 17	Apr 88	Caribbean Sea and off the Orinoco River	52.0
Solars 19	Sep 88	Caribbean Sea and off the Orinoco River	45.0
CaBS 11	Jan-Feb 90	Northeastern Pacific/Santa Monica Basin	42.0
CaBS 12	Jul 90	Northeastern Pacific/Santa Monica Basin	42.0
Icecolors	Ott-Nov 90	Bellingshausen Sea/Antarctic	30.0
MLML 91	May 91	North Atlantic/Southwest of Iceland	38.0
BOFS	Jun-Jul 91	North Atlantic/South of Iceland	13.0
Moss Landing	Oct 91	Moss Landing South Harbor, California	0.1
EqPac Spring	Feb-Mar 92	Equatorial Pacific	65.0
Optical Closure	Apr-May 92	Lake Pend Chielle, Idaho	39.0
EqPac Fall	Aug-Sep 92	Equatorial Pacific	65.0
MOCE 1	Aug-Sep 92	Northeastern Pacific/Monterry Bay	12.0
MOCE 2	Mar-Apr 93	Northeastern Pacific and Gulf of California	19.0
IronEx I	Oct 93	Southeastern Pacific around the Galapagos Island	29.0
Arabesque 1	Aug-Sep 94	Gulf of Oman and Arabian Sea	19.0
MOCE 3	Ott-Nov 94	North Pacific/Hawaiian Island Arch Chain	30.0
Mill Creek	Jul-Aug 95	Mill Creek/Chesapeake Bay	0.3
Snug Harbor	Aug 95	Snug Harbor, Hawaii	0.2
Turbid 5	Sep-Ott 95	Mill Creek/Chesapeake Bay	0.6
MOCE 4	Jan-Feb 98	North Pacific/Hawaiian Islands	14.2

Table 1. HPLC pigment data base as a function of cruise/deployment, date, geographical area and average sampling depth.

Cruises	Total Chl a	Accessory	c:A	b:A	Ph a:A	Fuco:A	Hex:A	PSC:A	PPC:A
Biowatt 85	0.31±0.24	0.32±0.26	0.09	0.16	0.000	0.26	0.29	0.58	0.23
TransPac 24N	0.09±0.10	0.08±0.12	0.01	0.18	0.000	0.06	0.15	0.25	0.33
TransPac 47N	0.21±0.18	0.18±0.16	0.06	0.14	0.000	0.20	0.24	0.54	0.09
SLC 86	0.59±0.37	0.89±0.61	0.12	0.17	0.000	0.43	0.69	1.19	0.11
Biowatt 87-1	0.31±0.15	0.30±0.16	0.07	0.24	0.000	0.11	0.21	0.51	0.14
Biowatt 87-2	0.20±0.16	0.17±0.16	0.03	0.15	0.000	0.03	0.22	0.34	0.27
GSP	1.69±1.11	1.95±1.16	0.22	0.25	0.000	0.25	0.22	0.66	0.05
T E W	0.14±0.09	0.17±0.12	0.08	0.26	0.000	0.02	0.18	0.38	0.52
SLC 87	0.77±0.48	0.98±0.57	0.24	0.18	0.000	0.33	0.34	0.72	0.13
Biowatt 87-3	0.18±0.12	0.20±0.15	0.08	0.19	0.000	0.05	0.24	0.46	0.34
AVIRIS	1.26±0.51	1.11±0.50	0.03	0.09	0.000	0.25	0.00	0.31	0.45
Biowatt 874	0.36±0.09	0.40±0.12	0.15	0.17	0.000	0.10	0.23	0.55	0.23
Solars 17	0.28±0.17	0.32±0.21	0.06	0.20	0.000	0.07	0.19	0.49	0.36
Solars 19	0.26±0.23	0.28±0.23	0.09	0.17	0.000	0.22	0.21	0.55	0.28
CaBS 11	0.36±0.24	0.52±0.36	0.03	0.19	0.000	0.32	0.41	0.98	0.24
CaBS 12	0.55±0.51	0.77±0.70	0.12	0.22	0.000	0.38	0.36	0.96	0.21
Icecolors	0.64±0.41	0.68±0.49	0.13	0.03	0.000	0.25	0.40	0.73	0.14
MLML 91	0.91±0.66	0.92±0.69	0.18	0.10	0.000	0.28	0.20	0.61	0.11
BOFS	0.63±0.38	0.56±0.35	0.03	0.08	0.000	0.13	0.39	0.59	0.22
Moss Landing	3.65±4.28	3.65±5.10	0.01	0.25	0.000	0.19	0.01	0.23	0.32
EqPac Spring	0.18±0.07	0.23±0.08	0.11	0.28	0.000	0.03	0.30	0.56	0.32
optical Closure	2.58±2.07	2.46±2.09	0.05	0.03	0.000	0.24	0.01	0.36	0.48
EqPac Fall	0.20±0.09	0.27±0.11	0.12	0.24	0.000	0.08	0.30	0.63	0.35
MOCE 1	1.41±0.82	1.58±0.94	0.20	0.15	0.000	0.25	0.22	0.56	0.23
MOCE 2	1.00±1.08	0.82±0.79	0.63	0.09	0.000	0.10	0.06	0.26	0.22
IronEx 1	0.41±0.15	0.61±0.20	0.26	0.00	0.000	0.06	0.30	1.01	0.25
Arabesque 1	0.35±0.30	0.61±0.49	0.24	0.14	0.052	0.34	0.31	1.08	0.44
MOCE 3	0.13±0.08	0.16±0.08	0.05	0.12	0.004	0.08	0.20	0.37	0.82
Mill Creek	16.0±5.68	21.4±7.73	0.23	0.03	0.010	0.15	0.02	0.60	0.46
Snug Harbor	0.48±0.11	0.71±0.14	0.12	0.19	0.009	0.19	0.08	0.40	0.74
Turbid 5	21.8±7.05	18.5±7.76	0.11	0.02	0.015	0.35	0.01	0.39	0.21
MOCE 4	0.11±0.09	0.13±0.09	0.03	0.03	0.000	0.06	0.19	0.37	0.79
TOTAL	0.77±2.48	0.82±2.56	0.16	0.16	0.002	0.16	0.26	0.56	0.3

Table 2. Total chlorophyll a (TCHLA) and total accessory pigment concentrations by cruise. Also listed are ratios of various diagnostic accessory pigments to TCHLA (A = TCHLA, c = chl c, b = chl b, Ph a = phaeophytin a + phaeophorbide a, Fuco = fucoxanthin, Hex = 19'hexanoyloxyfucoxanthin, PSC = photosynthetic carotenoids, and PPC = photoprotective carotenoids).

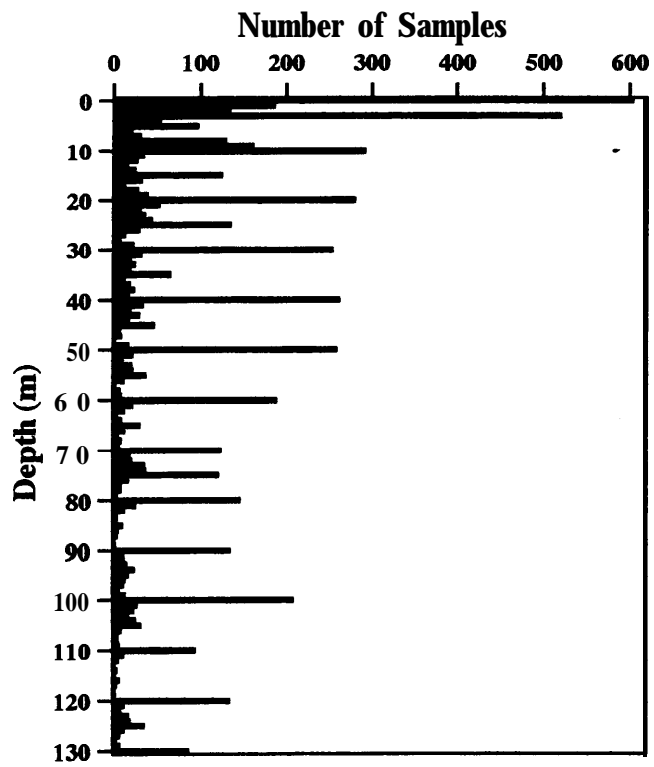


Fig 1.

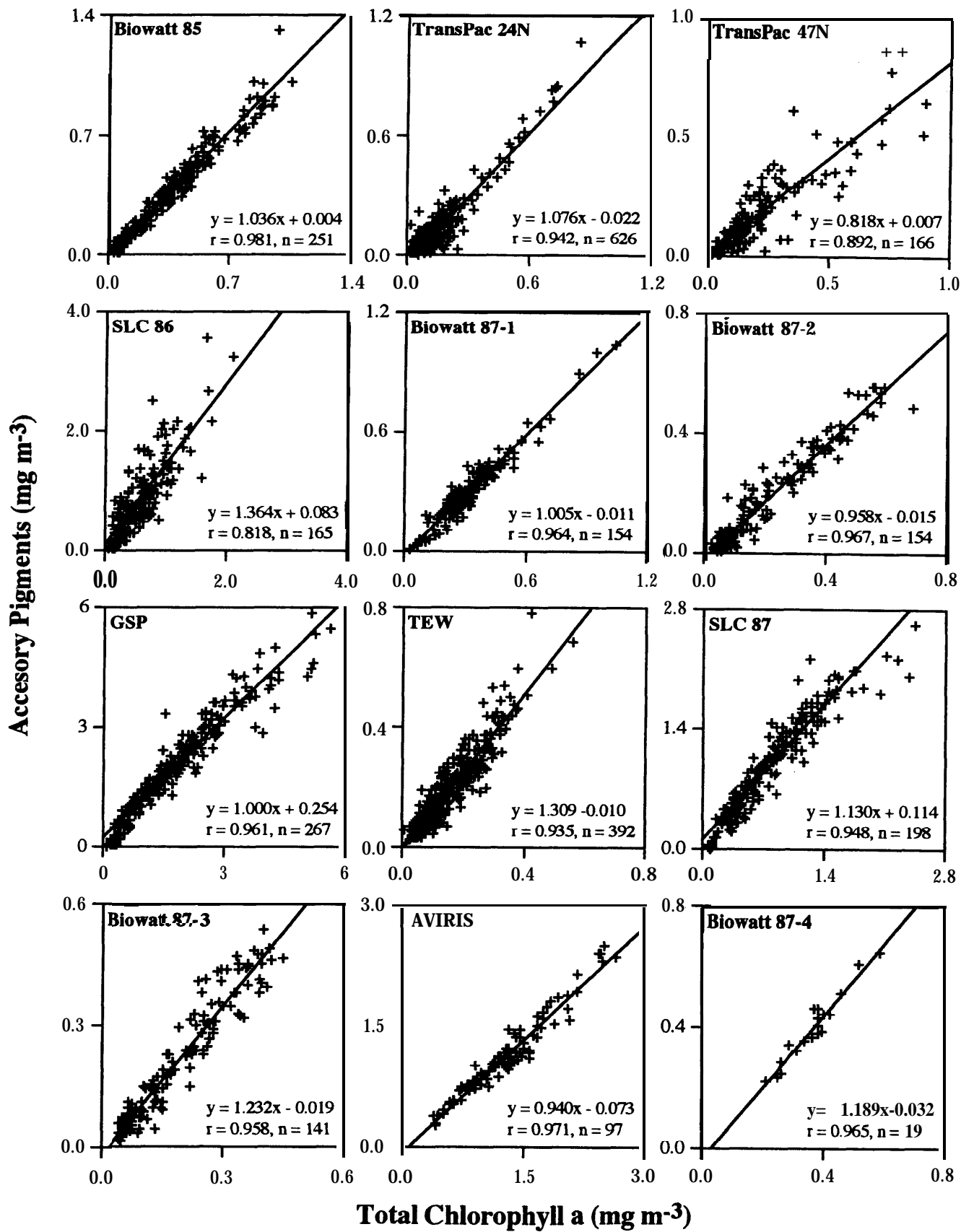


Fig 2.

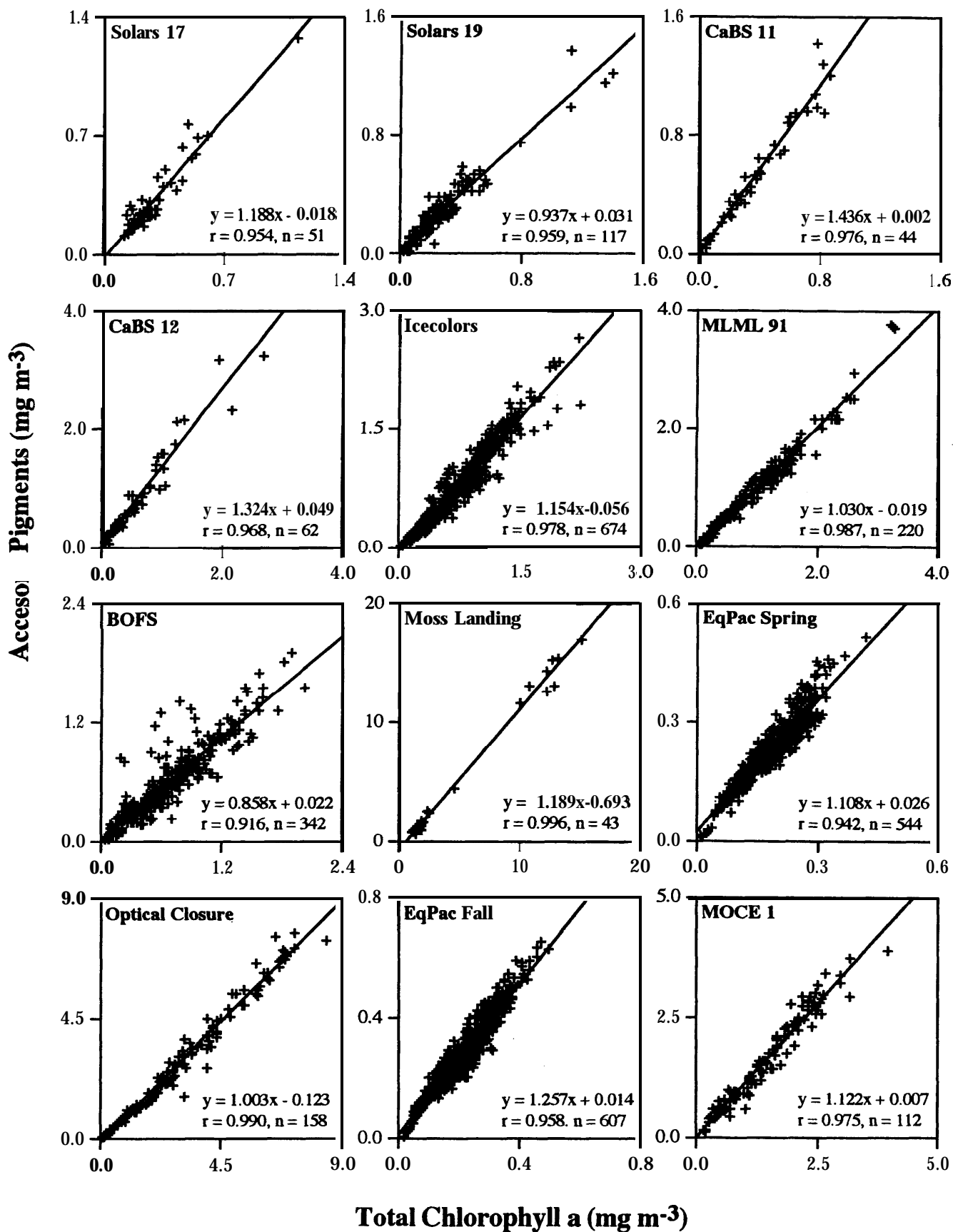
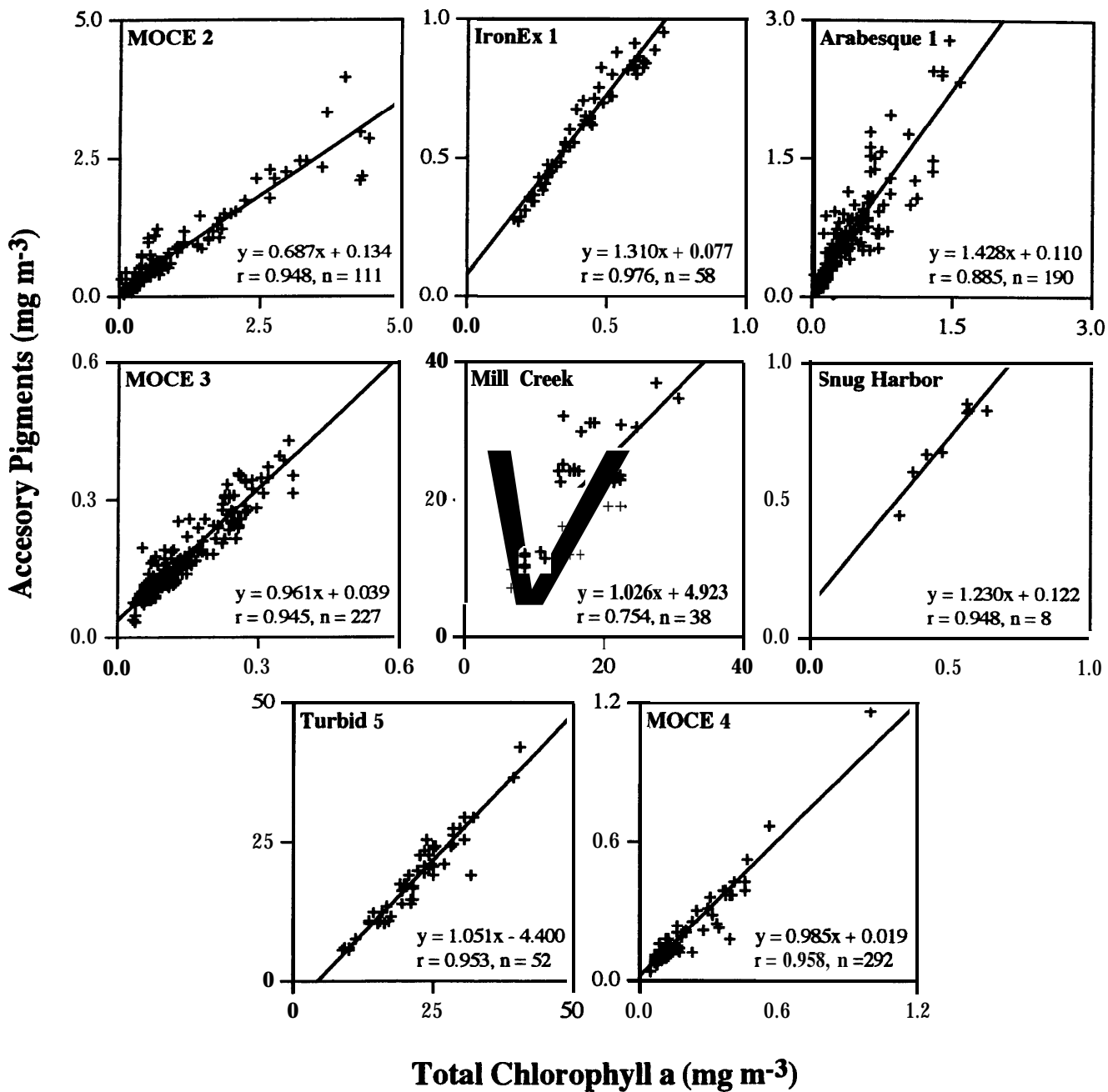


Fig. 2. (Cont)



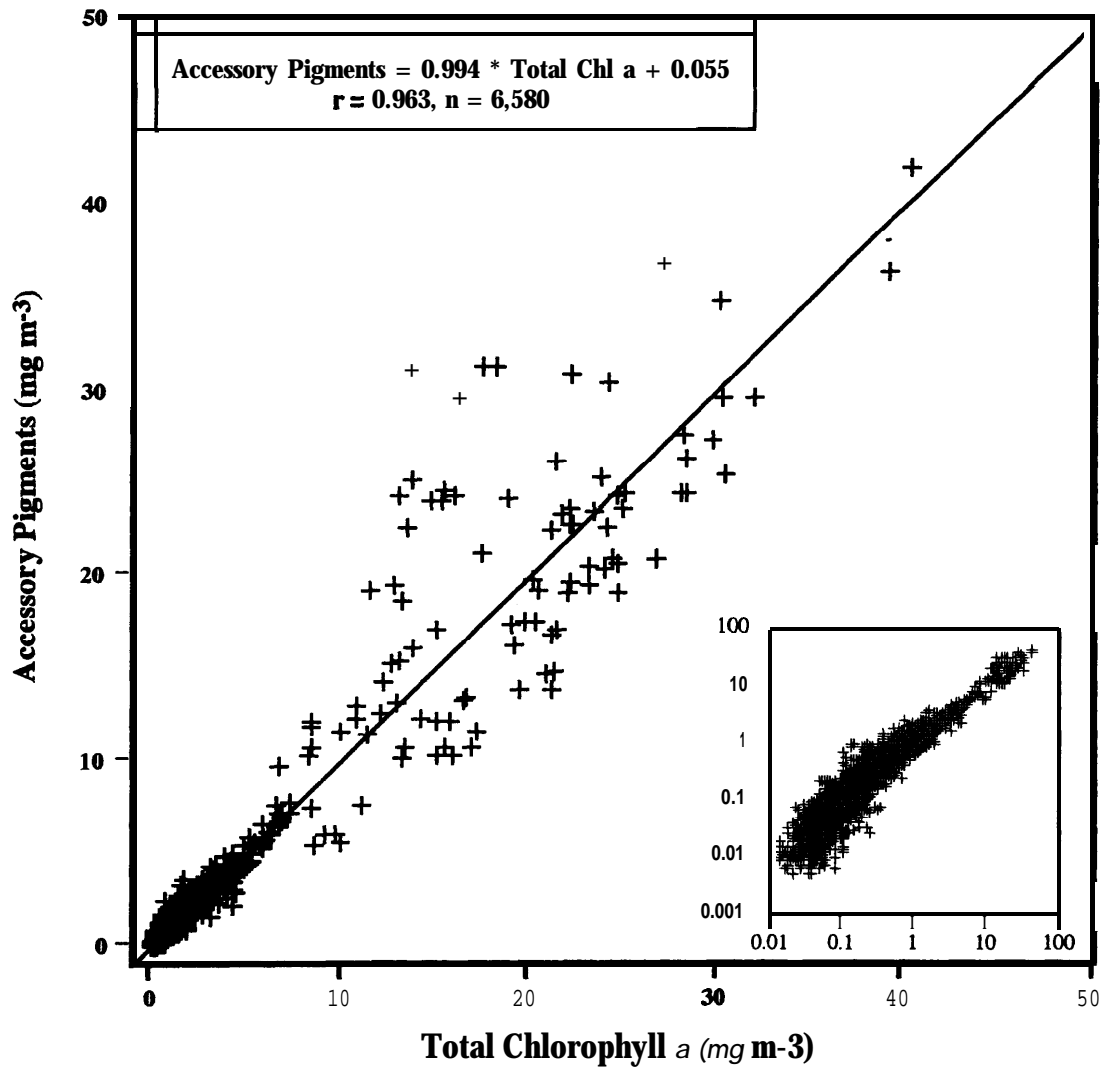


Fig. 3.

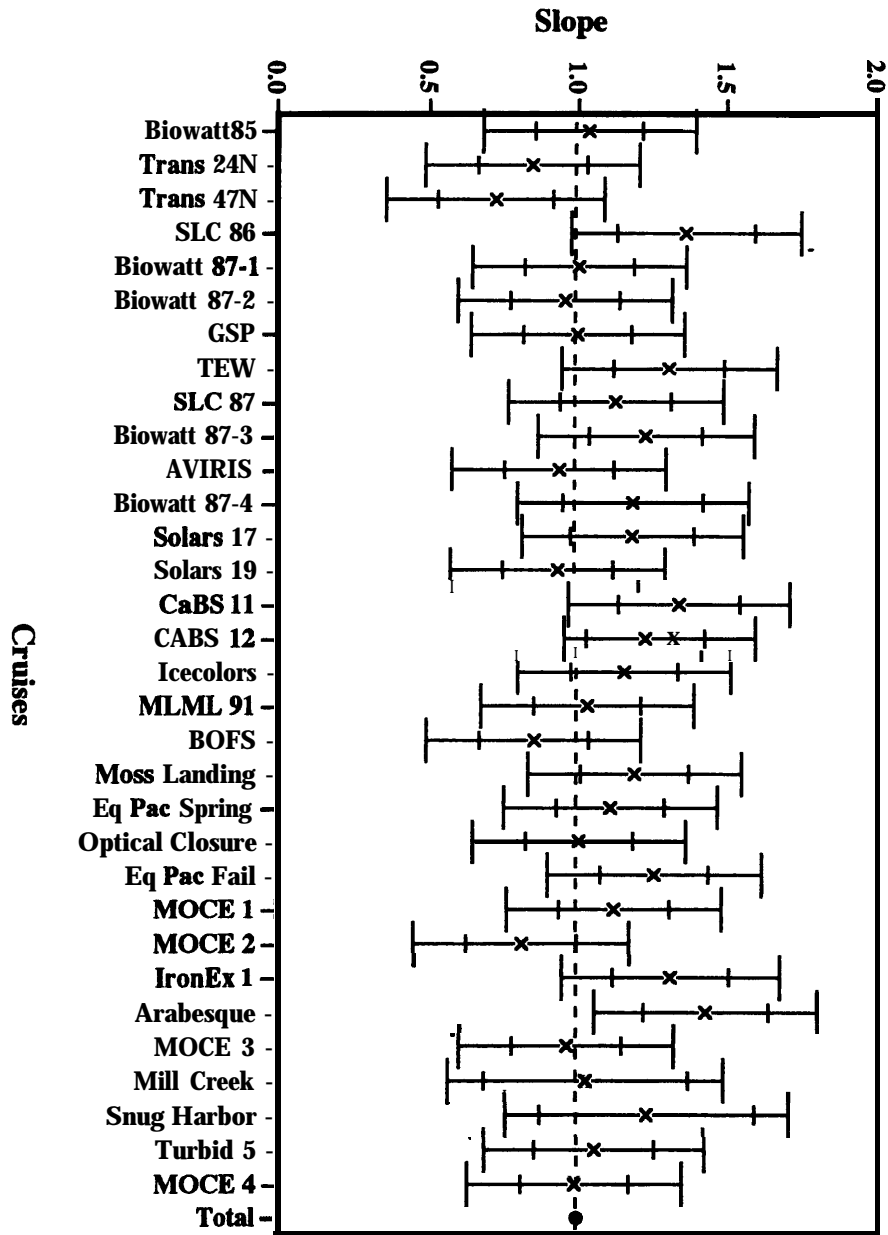


Fig. 4.

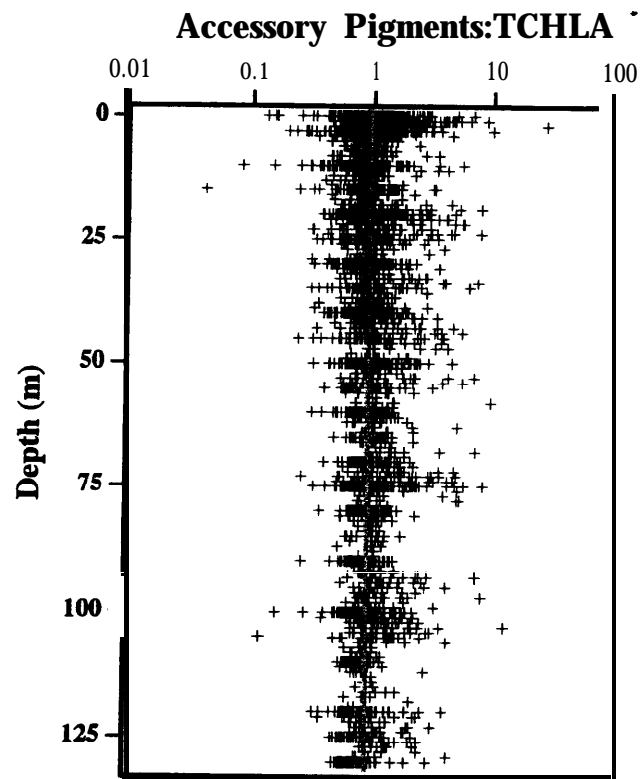


Fig. 5.